

**Moisture Content Monitoring using a Nuclear Moisture Gauge
and Preliminary Findings at Alabama Highway 5**

by

Dylan T. Jones

A thesis submitted to the Graduate Faculty of
Auburn University
in partial fulfillment of the
requirements for the Degree of
Master of Science

Auburn, Alabama
May 6, 2017

Keywords: expansive clay, nuclear moisture gauge, pavement

Copyright 2017 by Dylan T. Jones

Approved by

J. Brian Anderson, Ph.D., P.E., Chair, Associate Professor of Civil Engineering
David Timm, Ph.D., P.E., Brasfield & Gorrie Professor of Civil Engineering
Jack Montgomery, Ph.D., Assistant Professor of Civil Engineering

ABSTRACT

Expansive soils cause damage to lightly loaded foundations and structures across the world. Alabama Highway 5 was built directly on an expansive clay soil. In past years it has experienced tremendous amounts of damage due to the shrinking and swelling of the clay subgrade. Several remediation strategies were utilized in an effort to increase the life of the pavement surface. These strategies include efforts to increase drainage both beneath the pavement and beneath the shoulder, lime columns, vertical moisture barriers, and paved shoulders. In addition, each remediation strategy was instrumented with a variety of sensors to monitor pavement distress and soil behavior. To provide a way to quickly measure in-situ water contents with depth, access holes were installed at AL-5 for a nuclear moisture gauge. Preliminary findings indicate that at the time of publication, the pavement sections are performing well with the exception of the vertical barriers. Continued monitoring will help determine the effectiveness of each remediation strategy.

ACKNOWLEDGMENTS

I would like to thank the Alabama Department of Transportation for funding this research project and for their continued support. I would also like to thank my committee chair, Dr. J. Brian Anderson, for his support over the past two years. In addition, I would like to thank the other members on my committee, Dr. Jack Montgomery and Dr. David Timm. I would also like to thank Dan Jackson for his tremendous help throughout the project and always being there to bounce ideas off of. I would also like to thank the following people for their help on making this project a success: Elizabeth Stallings, Jeremy Herman, Lester Lee, Pavlo Voitenko, Justin McLaughlin, Jonathan Hogan, Matt Barr, and Andy Weldon. Finally I would like to thank my family and fiancé for their encouragement and support over the past two years.

TABLE OF CONTENTS

Abstract	ii
Acknowledgments.....	iii
Table of Contents	iv
List of Tables	ix
List of Figures	x
List of Abbreviations and Symbols.....	xvi
Chapter 1: Introduction	1
1.1 Background	1
1.2 Objective	3
1.3 Scope	3
Chapter 2: Background and Literature Review	4
2.1 Unsaturated Soils	4
2.1.1 Four Phase System.....	4
2.1.2 State Variables & Constitutive Relationships.....	5
2.1.3 Soil-Water Characteristic Curve	8
2.1.4 Active Zone.....	11

2.3 Neutron Moisture Gauge.....	12
2.3.1 General Theory	12
2.3.2 Hydroprobe Components.....	14
2.3.3 Calibration of Neutron Moisture Gauge	15
2.3.3 Access Tubes	18
2.3.4 Prior use in research.....	19
2.3 Remediation Strategies	22
2.3.1 Vertical Barriers.....	23
2.3.2 Lime Columns.....	24
2.3.3 Edge Drains.....	28
2.3.4 Deep Mix Columns	29
2.3.5 Paved Shoulders.....	30
Chapter 3: Research Setting.....	32
3.1 Site Description.....	32
3.2 Soil Characterization.....	34
3.3 Climate	36
3.4 Traffic Data.....	36
Chapter 4: Previous Research	38
4.1 Site Investigation and Lab Work	38
4.2 Instrumentation	41

4.2.1 Moisture Sensors.....	42
4.2.2 Suction Sensors.....	43
4.2.3 Piezometers.....	44
4.2.4 Asphalt Strain Gauges.....	45
4.2.5 Data Acquisition System and Weather Station.....	47
4.2.6 Installation Summary.....	48
4.3 IRI Data.....	50
Chapter 5: Construction of Test Sections.....	53
5.1 Sand Blanket – Test Section 1.....	53
5.2 Vertical Barriers – Test Section 2.....	60
5.3 Lime Columns – Test Section 3.....	71
5.4 Paved Shoulders – Test Section 4.....	80
5.5 Edge Drains – Test Section 5.....	82
5.6 Deep Mixed Columns – Test Section 7.....	84
5.7 Control Sections.....	90
Chapter 6: Soil Moisture Gauge.....	91
6.1 Troxler 4301 Depth Moisture Gauge.....	91
6.2 Access Holes.....	92
6.2.1 Access Tubes.....	92
6.2.2 Installation Process.....	93

6.3 Calibration.....	97
6.3.1 Effects of PVC	98
6.4 Monitoring Program.....	100
Chapter 7: Preliminary Results & Discussion	102
7.1 Construction of Test Sections	102
7.2 Hydroprobe	103
7.2.1 Field Calibration Results.....	103
7.2.2 Baseline Readings	104
7.3 Preliminary Findings.....	106
7.3.1 IRI Survey	106
7.3.2 Weather Data	110
7.3.3 Control	112
7.3.4 Sand Blanket – Test Section 1	116
7.3.5 Vertical Barriers – Test Section 2.....	120
7.3.6 Lime Columns – Test Section 3.....	124
7.3.7 Paved Shoulders – Test Section 4.....	128
7.3.8 Edge Drains – Test Section 6.....	132
7.3.9 Trees.....	136
7.3.10 Summary of Sensor Data	138
7.4 Website	139

Chapter 8: summary, Conclusions, & reccomendations	141
8.1 Summary	141
8.2 Conclusions.....	141
8.3 Recommendations.....	142
References.....	144
Appendix A: Boring Logs.....	150
Appendix B: Technical Data Sheet for Moisture Barrier	151
Appendix C: Troxler 4301 Calibration Sheet	152
Appendix D: Website Macro Codes	153

LIST OF TABLES

Table 1: Test Sections.....	32
Table 2: Soil Properties from USDA Soil Survey (after Harris 1998)	36
Table 3: Summary of AL-5 Laboratory Data (Stallings 2016).....	40
Table 4: Sensor Survivability (Jackson 2016)	49
Table 5: Baseline Readings for Hydroprobe (Volumetric Moisture Content (%)).....	105
Table 6: Baseline Hydroprobe Readings- Paved Shoulder.....	105

LIST OF FIGURES

Figure 1: Distresses Pavement at AL-5 (Herman 2015).....	2
Figure 2: Longitudinal Cracking at AL-5 (Herman 2015).....	2
Figure 3: Unsaturated Soil Element (Fredlund et al. 2012).....	5
Figure 4: Constitutive Surfaces for Unsaturated Soils (Fredlund and Rahardjo 1993).....	8
Figure 5: Illustration of McQueen and Miller’s (1974) Conceptual Model for General Behavior of the SWCC (Lu and Likos 2004).....	9
Figure 6: Representative SWCCs for Sand, Silt, and Clay (Lu and Likos 2004).....	10
Figure 7: Hysteresis in SWCC (Fredlund et al. 2012).....	11
Figure 8: Water Content Profiles in the Active Zone (Nelson and Miller 1992).....	12
Figure 9: Thermalized Neutrons (Troxler 2006).....	14
Figure 10: Neutron Moisture Gauge in Working Position (IAEA 2002).....	15
Figure 11: Typical Field Calibration Curve (Troxler 2006).....	16
Figure 12: Test Container Neutron Counts for various annular space fills (Bishop and Porro 1997).....	21
Figure 13: Moisture Ratio by Volume in function of count ratio (diameter is indicated on the curves) (Abeele 1978).....	22
Figure 14: Typical Injection System (Hayward Baker 2010).....	27
Figure 15: Typical Edge Drain Schematic (Chen et al. 2012).....	28

Figure 16: Schematic of Deep Mix Columns for the Stabilization of Expansive Soils (Madhyannapu 2007)	30
Figure 17: Longitudinal Crack Formation (Zornberg and Gupta 2009)	31
Figure 18: Project Test Sections (After Google Earth).....	33
Figure 19: Soil Survey of Perry County, AL (Harris 1998)	35
Figure 20: Boring Locations (After Google Earth).....	39
Figure 21: Decagon Devices GS1 Moisture Content Sensor (Jackson 2016)	42
Figure 22: GS1 Calibration Curve (after Jackson 2016) Orange Points indicate new calibration points.....	43
Figure 23: Decagon Devices MPS5 Suction Sensor (Jackson 2016)	44
Figure 24: Geokon 4500S Vibrating Wire Piezometer (Jackson 2016)	45
Figure 25: CTL ASG-152 Asphalt Strain Gauge (Jackson 2016)	46
Figure 26: Geocomp Asphalt Strain Gauge (Jackson 2016).....	46
Figure 27: Strain Gauge Layout.....	47
Figure 28: Data Acquisition System (Jackson 2016).....	47
Figure 29: Campbell Scientific WTX520 Weather Sensor (Jackson 2016)	48
Figure 30: Pavement Profiles (Sayers and Karamihas 1998)	50
Figure 31: Inertial Profiler Schematic (Sayers and Karamihas 1998)	50
Figure 32: IRI Survey – North Bound Lane – 05/31/2014	51
Figure 33: IRI Survey – South Bound Lane – 05/31/2014	51
Figure 34: IRI Survey – North Bound Lane – 11/15/2014	52
Figure 35: IRI Survey – South Bound Lane – 11/15/2014	52
Figure 36: Sand Blanket Cross Section (ALDOT 2015)	54

Figure 37: North Bound Lane- Edge Drain and Sand Blanket	55
Figure 38: North Bound Lane – Application of Sand Blanket	56
Figure 39: North Bound Lane – Placement of Tack Coat on Granular Base	57
Figure 40: Rainwater flowing out of Sand Blanket	58
Figure 41: Completed Sand Blanket Test Section	59
Figure 42: Vertical Barriers Cross Section (ALDOT 2015).....	60
Figure 43: Trench Cave-in – Vertical Barriers	62
Figure 44: Vertical Barrier Trench	63
Figure 45: Backfilling of Vertical Barriers.....	64
Figure 46: Sand Backfill of Vertical Barriers	65
Figure 47: Paving over Vertical Barrier Trench	66
Figure 48: Leveling Asphalt over Vertical Barriers	67
Figure 49: Leveling of Pavement over Vertical Barriers.....	68
Figure 50: Cracks along shoulder above Vertical Barriers.....	69
Figure 51: Rutting Observed above Vertical Barriers	70
Figure 52: Asphalt Spalling above Vertical Barriers.....	70
Figure 53: Geosynthetic protruding through base course of asphalt	71
Figure 54: Lime Columns Cross Section (ALDOT 2015).....	72
Figure 55: Lime Columns Plan View Detail (ALDOT 2015)	72
Figure 56: Drill Used for Lime Column Installation	73
Figure 57: Auger used for Lime Column Installation.....	74
Figure 58: Lime Column before Asphalt Patching.....	75
Figure 59: Pouring Asphalt into Lime Column Holes	76

Figure 60: Compacting asphalt in Lime Column.....	77
Figure 61: Lime Columns patched with Asphalt	78
Figure 62: Lime Columns Reflected Through Base Course and Holding Water	79
Figure 63: Hole in Asphalt above Lime Column.....	79
Figure 64: Paved Shoulder Cross Section (ALDOT 2015)	80
Figure 65: After paving of Paved Shoulders.....	81
Figure 66: Paved Shoulder prior to Leveling Course	82
Figure 67: Edge Drain Cross-Section at AL-5 (ALDOT Plans).....	83
Figure 68: Edge Drains after Backfilling with Stone.....	83
Figure 69: Deep Mixed Columns Cross Section (ALDOT 2015)	84
Figure 70: Deep Mixed Columns Plan View (ALDOT 2015).....	85
Figure 71: Deep Mix Column Drill Rig.....	86
Figure 72: Deep Mix Column Batch Plant	87
Figure 73: Drill Bit used for Deep Mix Column Installation.....	88
Figure 74: Extracted Column of Soil from Deep Mix Column	89
Figure 75: Clumps of soil showing lack of cement mixing	90
Figure 76: Troxler Model 4301 Depth Moisture Gauge.....	92
Figure 77: Auger and Bit used for Installation	94
Figure 78: ATV Drill Rig used for Hydroprobe Installation	95
Figure 79: Bottom End Cap of Access Tube	96
Figure 80: Waterproof Manhole Cover before grouted in place.....	96
Figure 81: Cross section of completed access hole	97
Figure 82: 55-Gallon Barrel Water Test Setup.....	99

Figure 83: Calibration Correction for PVC	100
Figure 84: Hydroprobe Stand.....	101
Figure 85: IRI Survey – North Bound Lane – 11/15/2016.....	102
Figure 86: IRI Survey – South Bound Lane – 11/15/2016.....	103
Figure 87: Field Calibration Results.....	104
Figure 88: Baseline Hydroprobe Readings – Paved Shoulder.....	106
Figure 89: IRI Survey – North Bound Lane – 3/3/2017	107
Figure 90: IRI Survey – South Bound Lane – 3/3/2017	107
Figure 91: Longitudinal Crack in Vertical Barrier Test Section.....	108
Figure 92: North Bound Lane-Outside Wheel Path.....	109
Figure 93: South Bound Lane – Outside Wheel Path.....	109
Figure 94: Average IRI Values over Time	110
Figure 95: Temperature Data at AL-5	111
Figure 96: Rainfall Data at AL-5.....	111
Figure 97: Strain with Time - Control	112
Figure 98: Moisture Content with Time – Control.....	114
Figure 99: Matric Suction with Time – Control (A&B shown with different scales for clarity)	115
Figure 100: Pore Pressure with Time - Control.....	116
Figure 101: Strain with Time – Sand Blanket	117
Figure 102: Moisture Content with Time – Sand Blanket.....	118
Figure 103: Matric Suction with Time – Sand Blanket	119
Figure 104: Pore Pressure with Time – Sand Blanket.....	120
Figure 105: Strain with Time – Vertical Barriers	121

Figure 106: Moisture Content with Time – Vertical Barriers.....	122
Figure 107: Matric Suction with Time – Vertical Barriers (A&B shown with different scales for clarity).....	123
Figure 108: Pore Pressure with Time – Vertical Barriers.....	124
Figure 109: Strain with Time – Lime Columns	125
Figure 110: Moisture Content with Time – Lime Columns	126
Figure 111: Matric Suction with Time – Lime Columns.....	127
Figure 112: Pore Pressure with Time – Lime Columns.....	128
Figure 113: Strain with Time – Paved Shoulders	129
Figure 114: Moisture Content with Time – Paved Shoulders	130
Figure 115: Matric Suction with Time – Paved Shoulders (A&B shown with different scales for clarity).....	131
Figure 116: Pore Pressure with Time – Paved Shoulders.....	132
Figure 117: Strain with Time – Edge Drains	133
Figure 118: Moisture Content with Time – Edge Drains	134
Figure 119: Matric Suction with Time – Edge Drains (A&B shown with different scales for clarity).....	135
Figure 120: Pore Pressure with Time – Edge Drains.....	136
Figure 121: Moisture Content with Time – Trees	137
Figure 122: Matric Suction with Time – Trees.....	138
Figure 123: AL-5 Website Home Screen.....	139
Figure 124: Website Page – Lime Columns	140

LIST OF ABBREVIATIONS AND SYMBOLS

AADT	Average Annual Daily Traffic
AADTT	Average Annual Daily Truck Traffic
AL	Alabama
AL-5	Alabama Highway 5
ALDOT	Alabama Department of Transportation
a_m	Coefficient of Compressibility with respect to Change in Matric Suction
a_t	Coefficient of Compressibility with respect to Change in Net Normal Stress
b_m	Coefficient of Water Content Change with respect to Change in Matric Suction
b_t	Coefficient of Water Content Change with respect to Change in Net Normal Stress
CL	Centerline of Pavement
cpm	Counts per minute
CR	Count Ratio
de	Incremental Change in Void Ratio
DSM	Deep Soil Mixing
$d(u_a - u_w)$	Incremental Change in Matric Suction
$d(\sigma_{mean} - u_a)$	Incremental Change in Net Normal Stress
ft	feet
IAEA	International Atomic Energy Agency
in	Inches

IRI	International Roughness Index
kPa	Kilopascals
LL	Liquid Limit
LSPI	Lime Slurry Pressure Injection
MP	Mile Point
N	Count rate in soil (cpm)
N _s	Count rate in standard material (cpm)
pcf	Pounds per Cubic Foot
PI	Plasticity Index
Ppm	parts per million
psf	Pounds Per Square Foot
PVC	Polyvinyl chloride
SWCC	Soil Water Characteristic Curve
TS	Test Section
u_a	Pore Air Pressure
$(u_a - u_w)$	Matric Suction
USCS	Unified Soil Classification System
USDA	United States Department of Agriculture
u_w	Pore Water Pressure
VWC	Volumetric Water Content
w	Gravimetric Water Content
θ	Volumetric Water Content
ρ_d	Dry Density

ρ_w	Density of Water
σ	Total Normal Stress
σ_{mean}	Average Normal Stress
$(\sigma - u_a)$	Net Normal Stress

CHAPTER 1: INTRODUCTION

1.1 Background

After a road is constructed, it is important that the road be maintained to ensure a safe riding surface for travelers. In some areas across the country, the ability to effectively maintain the roads has been compromised due to expansive clay soils. Expansive clay soils exist throughout the United States and around the world. In 1981 it was estimated that the damage caused by these expansive soils was around \$9 billion annually (Jones 1981). Due primarily to fluctuating moisture contents in the expansive soils, large amounts of volume change can occur. These volume changes can greatly affect lightly loaded structures and foundations, including roadways.

It is easy to see the effects of these expansive clay soils on farm-to-market roads in portions of southern and western Alabama. Farm-to-market roads were established in Alabama by the “Farm to Market Act” of 1943 which allotted one cent of the state gasoline tax to be used for the construction of county roads and bridges (ARBA 2017). In many cases, these roads were constructed directly on the existing subgrade. This combined with large amounts of truck traffic causes a significant amount of distress to the pavement surface as the subgrade shrinks and swells. This distress is especially evident along Alabama Highway 5 (AL-5) where rutting, longitudinal cracks, and patching are prevalent along much of the road. To maintain a safe riding surface, resurfacing of the road is necessary on an almost annual basis. Pictures of this distress is shown in Figure 1 and Figure 2.



Figure 1: Distresses Pavement at AL-5 (Herman 2015)



Figure 2: Longitudinal Cracking at AL-5 (Herman 2015)

Due to the unsustainable resurfacing projects required to maintain AL-5, the Alabama Department of Transportation (ALDOT) sponsored a research project along a section of AL-5. In this section, various in-situ remediation techniques were implemented in an effort to prolong the life of the pavement and reduce the resurfacing interval. These remediation techniques aimed to improve the volumetric stability of the subgrade by controlling the seasonal moisture

fluctuations. It is important to note that it was not possible to close and detour AL-5, thus methods investigated focused on being able to keep AL-5 open to traffic. To monitor the remediation techniques, an array of sensors were installed to monitor long term soil conditions and pavement distress.

1.2 Objective

This effort is a part of the overall project to determine the causes of distress at AL-5, and investigate remediation strategies for expansive clays under roadways. The objectives of this investigation were as follows:

- Document the construction of the remediation strategies used at AL-5.
- Develop efficient methods of installing access holes for monitoring moisture content fluctuations with a nuclear moisture gauge.
- Develop a method for real time monitoring of the sensors installed at AL-5.

1.3 Scope

To accomplish these objectives, numerous pictures were taken during the construction of the remediation strategies. Also, challenges and obstacles were recorded as they developed. In addition, access holes for a nuclear moisture gauge were installed along AL-5. Finally, a website was developed to publish daily readings from the numerous sensors previously installed at AL-5.

CHAPTER 2: BACKGROUND AND LITERATURE REVIEW

The shrink-swell nature of expansive soils are primarily associated with changes in water content in unsaturated soils. For this reason, a general discussion on the mechanics of unsaturated soils is provided below. This will help to show why fluctuating moisture contents are so important to expansive soils. In addition, the theory behind the nuclear moisture gauge is discussed to provide relevant background information. Finally, a literature review of is provided to present the ideology behind the chosen remediation strategies implemented at AL-5.

2.1 Unsaturated Soils

It has become custom to define soils as a three phase system comprised of air, water, and soil particles. This idea allows for the analysis of many geotechnical problems by making key assumptions. These assumptions being that a soil is either completely saturated, no air in the voids, or completely dry, no water in the voids. While this traditional approach is appropriate for a variety of geotechnical problems, in reality, completely dry soils are rarely encountered. Rather, soils mainly exist in an unsaturated state somewhere between these two extremes. Because shrink-swell behavior is closely associated with unsaturated soils, it is important to understand the general principles of unsaturated soil mechanics.

2.1.1 Four Phase System

To better characterize the physical nature of an unsaturated soil for stress analysis, the soil is described as a four phase system. In addition to the traditional three phase system, air, water, and soil particles, a fourth phase commonly known as the contractile skin is used to describe the air-water interface. (Fredlund and Morgenstern 1977)

This contractile skin can be thought of as a thin membrane which forms a barrier between the air and water phases. Changes in the stress state of the contractile skin can cause changes in water content, volume, and shear strength. When a soil is subjected to drying, the contractile skin acts like a rubber membrane which pulls soil particles together subsequently causing a decrease in volume. (Fredlund et al. 2012) A diagram of a soil element with the four phases labeled is shown in Figure 3.

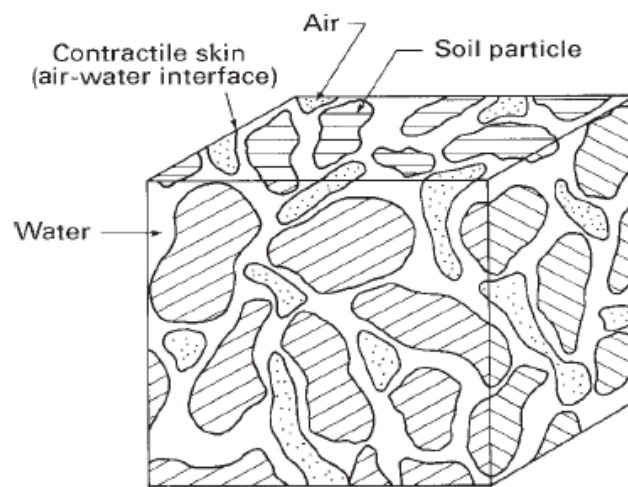


Figure 3: Unsaturated Soil Element (Fredlund et al. 2012)

2.1.2 State Variables & Constitutive Relationships

By definition a state variable is a “non-material variable required for the characterization of a system”. (Fredlund and Rahardjo 1993) A state variable can be a stress state variable used to characterize a stress condition or a deformation state variable which is used to characterize the deviation from an initial state. It is important to emphasize that both types of state variables are independent of the physical properties of a soil. These state variables can be used to create empirical single-valued equations called constitutive relationships. (Fredlund and Rahardjo 1993)

The mechanical behavior of a saturated soil can be described solely by the state of the effective stress on the soil. Because of this, changes in volume and shear strength are controlled only by changes in the effective stress. This concept is well studied and accepted for saturated soils.

Describing the behavior of an unsaturated soil is more complex due to the addition of the fourth phase. Due to the success of the effective stress concept in saturated soil mechanics, it has been attempted to use a single-valued effective stress for unsaturated soils but has proven difficult at best (Fredlund and Rahardjo 1993). While numerous effective stress equations for unsaturated soils have been developed (Croney et al. 1958, Bishop 1959, Aitchison 1961, Jennings 1961), they all incorporate a soil parameter making them constitutive relationships rather than stress state descriptions (Fredlund and Rahardjo 1993). Fredlund and Rahardjo (1993) suggest that a more appropriate way to describe the behavior of unsaturated soils is to use two independent stress state variables.

Based on multi-phase continuum mechanics, Fredlund and Morgenstern (1977) concluded that a combination of two independent stress variables can be used to describe the stress state of an unsaturated soil. There are three combinations of stress state variables, but the one most widely accepted is the combination of net normal stress ($\sigma - u_a$) and matric suction ($u_a - u_w$). These stress state variables were experimentally tested by Fredlund (1973) and used to develop constitutive equations describing the volume change and shear strength behavior of unsaturated soils. This is of particular interest as it describes the volume change responsible for the shrink-swell nature under pavements.

To describe the volume change behavior of unsaturated soils, two deformation state variables are required to create constitutive relationships. The two deformation state variables

commonly used to describe volume change are void ratio, e , and gravimetric water content, w .

When combined with the stress state variables mentioned above, the two constitutive relationships shown in Equations 1 and 2 from Fredlund and Rahardjo (1993) are formed.

$$de = a_t d(\sigma_{mean} - u_a) + a_m d(u_a - u_w) \quad (1)$$

$$dw = b_t d(\sigma_{mean} - u_a) + b_m d(u_a - u_w) \quad (2)$$

Where de = incremental change in void ratio

dw = incremental change in water content (gravimetric)

$d(\sigma_{mean} - u_a)$ = incremental change in net normal stress

$d(u_a - u_w)$ = incremental change in matric suction

a_t = coefficient of compressibility with respect to change in net normal stress

a_m = coefficient of compressibility with respect to change in matric suction

b_t = coefficient of water content change with respect to change in net normal stress

b_m = coefficient of water content change with respect to change in matric suction

$$\sigma_{mean} = \frac{\sigma_1 + \sigma_2 + \sigma_3}{3}$$

u_a = pore air pressure

u_w = pore water pressure

Because the constitutive relationships incorporate two stress state variables, visually, the plot of these equations must take on a three dimensional shape. Figure 4 shows a representation of this three dimensional mesh for each deformation state variable. These plots show that the void ratio and water content are affected by the change in both matric suction and net normal stress. With that said, it is appropriate to assume that under a pavement the net normal stress does not change and the change in void ratio is controlled solely by the matric suction.

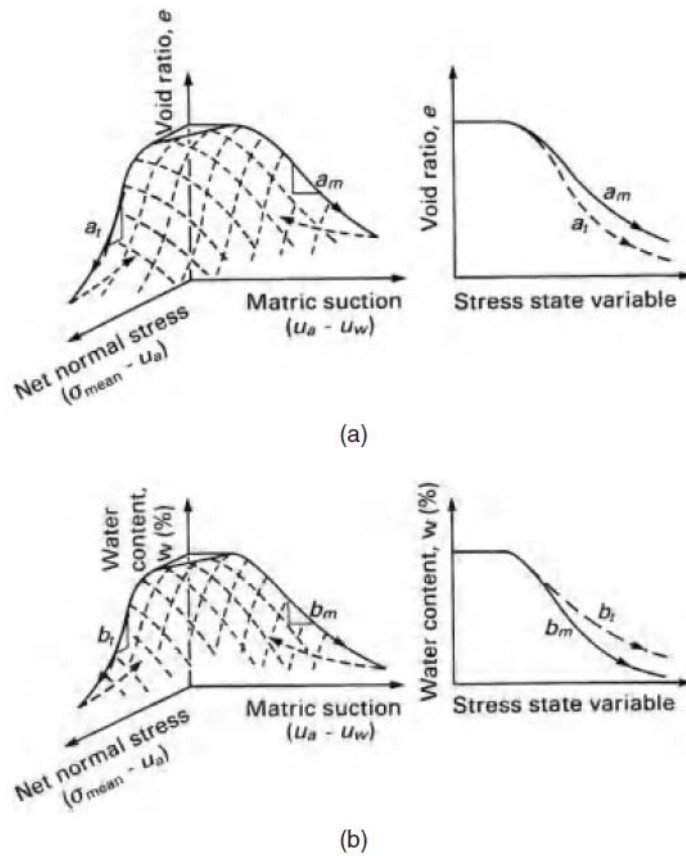


Figure 4: Constitutive Surfaces for Unsaturated Soils (Fredlund and Rahardjo 1993)

2.1.3 Soil-Water Characteristic Curve

As shown above, the state of the matric suction has a large role in the shrink-swell nature of an unsaturated soil when the net normal stress is constant. A soil water characteristic curve (SWCC) defines the constitutive relationship between water content and matric suction. As the water content rises the matric suction decreases and as water content decreases matric suction increases. This general trend is shown conceptually in Figure 5.

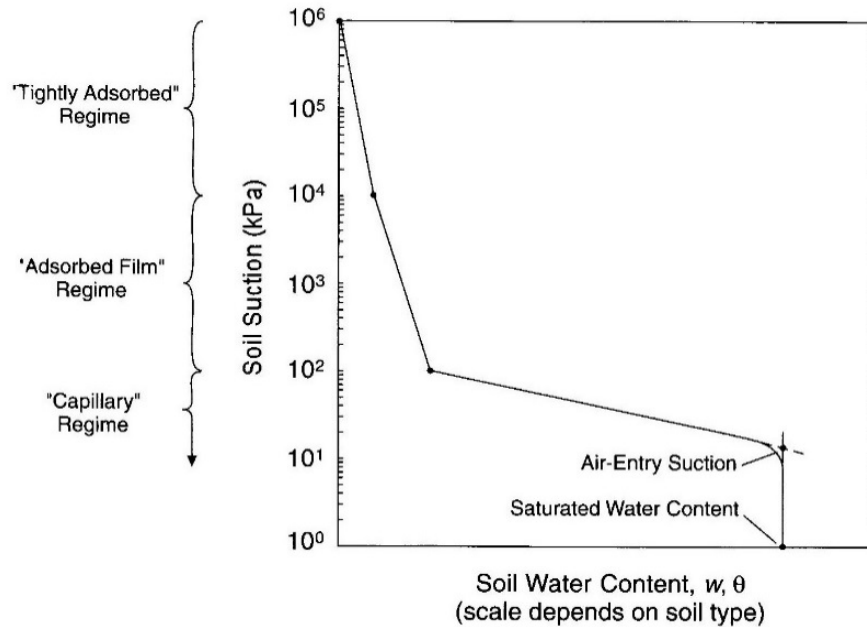


Figure 5: Illustration of McQueen and Miller's (1974) Conceptual Model for General Behavior of the SWCC (Lu and Likos 2004)

As shown in Figure 5, the state of suction can be divided into three different parts. These regions are defined by the way in which water is held in the soil. In the capillary regime, the water is held in the pores primarily by capillarity. In the adsorbed film regime, the water is held in the soil by surface forces such as electric field polarization, van der Waals forces, and exchangeable cation hydration. Finally, in the tightly absorbed regime, water is held by molecular forces including hydrogen bonds. (Lu and Likos 2004)

Fredlund and Rahardjo (1993) defines the air entry value as “the matric suction value that must be exceeded before air recedes into the soil pores.” In a general sense, the air entry value or (air entry suction) defines the point in which the soil transitions from saturated to unsaturated. This point is largely controlled by the largest pore size in a soil matrix (Fredlund and Rahardjo 1993).

The shape of a SWCC is dependent on the properties of the soil including pore size distribution, density, organic content, percent clay, and mineralogy (Lu and Likos 2004). Of

these, the distribution of pore sizes is one of the most important properties that influences the shape of the SWCC (Lu and Likos 2004). This is evident in Figure 6, which shows the SWCCs for a sand, silt, and clay. It is also important to note that there is hysteresis in the SWCC associated with wetting and drying as shown in Figure 7.

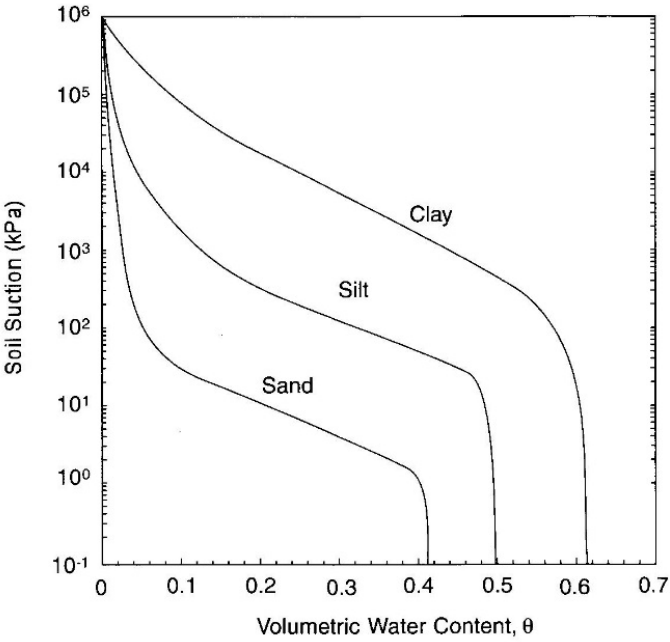


Figure 6: Representative SWCCs for Sand, Silt, and Clay (Lu and Likos 2004)

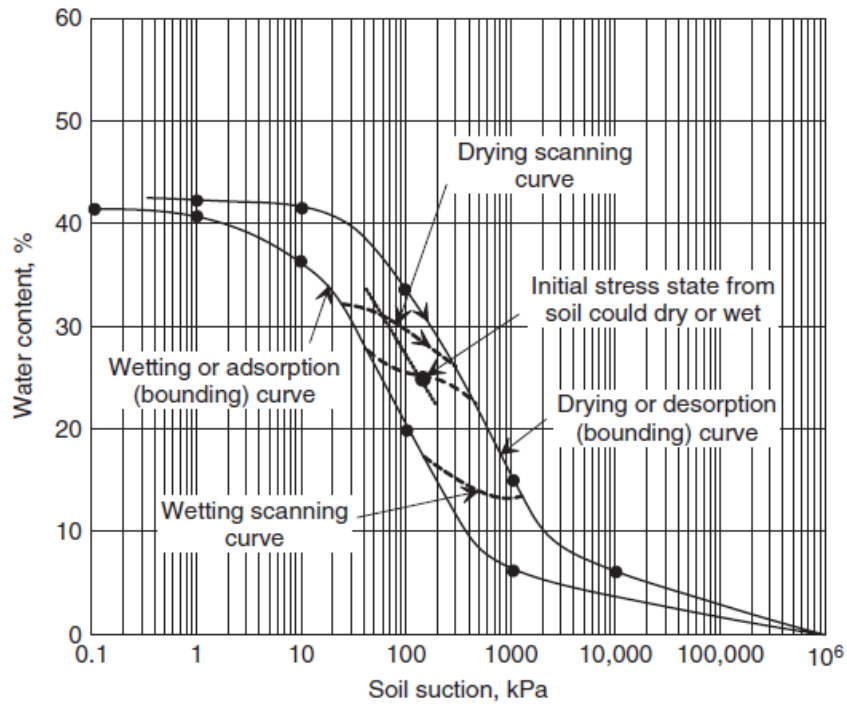


Figure 7: Hysteresis in SWCC (Fredlund et al. 2012)

2.1.4 Active Zone

As discussed, the shrink-swell behavior of expansive unsaturated clays is largely influenced by the changes in matric suction and ultimately the water content. These fluctuations in water content are influenced by environmental factors, such as vegetation and stress, as well as climatic factors including rainfall and temperature variations. The region of soil below ground level that experiences these fluctuations has been given the term “active zone” (Nelson and Miller 1992). A depiction of the active zone is shown in Figure 8.

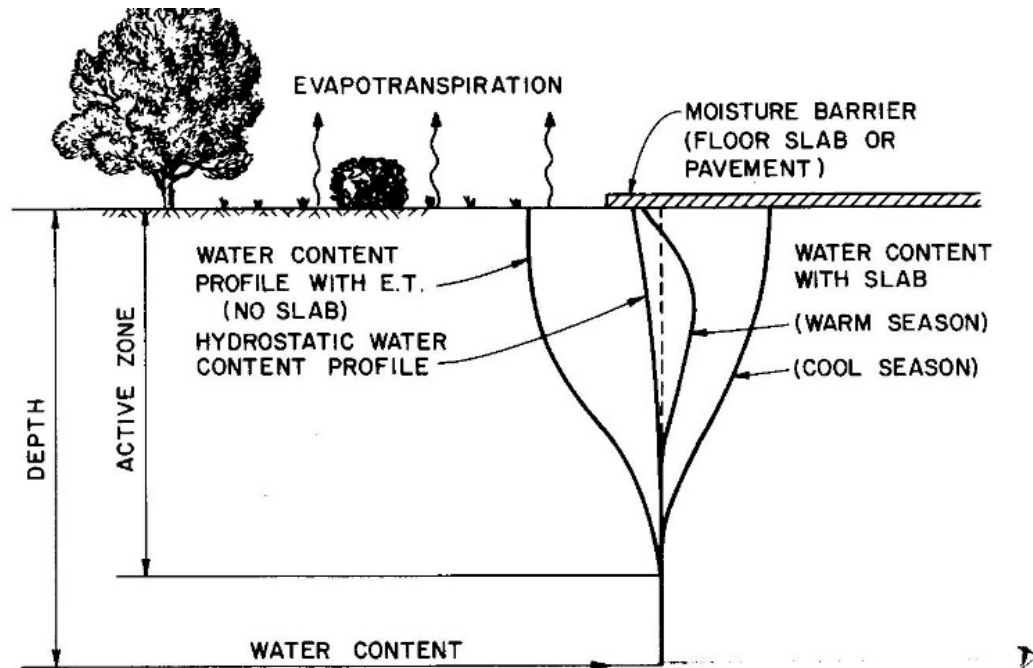


Figure 8: Water Content Profiles in the Active Zone (Nelson and Miller 1992)

2.3 Neutron Moisture Gauge

Due to the importance of water content on the shrink-swell behavior of expansive soils, it is helpful to be able to determine the in-situ water contents of a soil. By monitoring the water content with depth, the depth of the active zone can be determined. Also, knowing the seasonal fluctuations in water content helps to determine if a soil will exhibit shrink-swell behavior. Various methods exist to determine the in-situ water content of a soil. The neutron moisture gauge or “hydroprobe” allows for repeated measurements of volumetric water content to be taken at various depths quickly and effectively.

2.3.1 General Theory

In the simplest sense, a hydroprobe emits fast neutrons from a radioactive source and counts the number of slow or thermalized neutrons that return. The count of slow neutrons that return can be correlated to a volumetric moisture content. This works because the flux of slow neutrons is mainly associated with the hydrogen content of the surrounding material (IAEA

1970). In this case, the surrounding material is soil and the main source of hydrogen atoms are those in water. Therefore, the count of slowed neutrons would be higher in a soil with higher water content versus one with a lower water content.

The energy at which a neutron is emitted varies between 0 and 11 MeV, depending on the source, but on average is around 4.5MeV (IAEA 1970). In order for a slowed or thermalized neutron to be detected the energy must be reduced to approximately 1 eV or less (IAEA 1970). The process in which the emitted fast neutrons interact with nuclei of the surrounding soil is complex and can be classified into two categories, absorption and scattering. The method in which the fast neutron is slowed depends greatly on the makeup of the surrounding soil. Absorption is a process in which a neutron is absorbed by a surrounding nucleus, creating an unstable compound nucleus. Neutrons are generally only slowed by this method when they have initial energies of 10 eV or greater. For this reason, neutrons slowed by absorption are rarely significant to neutron moisture gauges. (IAEA 1970)

Of more importance to hydroprobes are those neutrons slowed by scattering. In this process, neutrons collide with surrounding nuclei and transfer some or all of its kinetic energy without becoming absorbed (IAEA 1970). Scattering can either be considered elastic or inelastic, with the latter having little significance to neutron moisture gauges. Elastic scattering occurs when a neutron transfers part of its energy to a surrounding nucleus and in turn is slowed. During this process the direction of the neutron is also changed. (IAEA 1970) An idealized visualization of this process is shown in Figure 9.

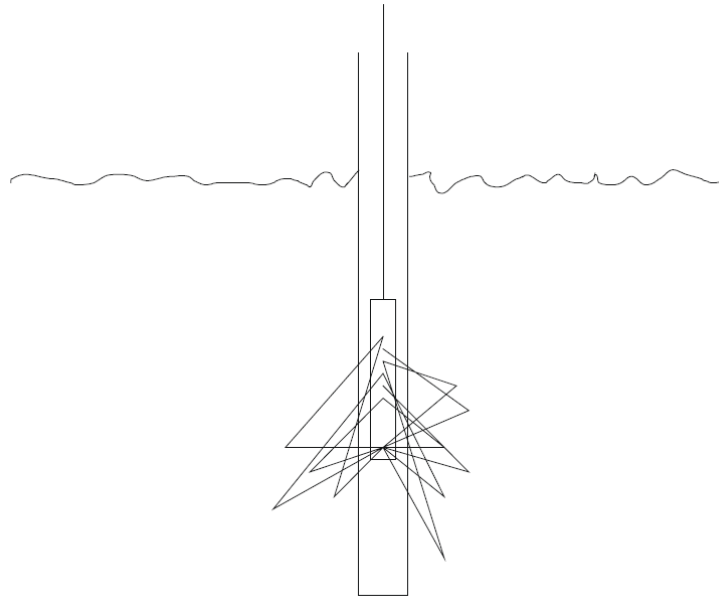


Figure 9: Thermalized Neutrons (Troxler 2006)

It is important to note that while hydrogen is the most predominant element involved in the slowing of neutrons, other elements can slow neutrons as well. Because of this, in order to get accurate readings of water content, the hydroprobe must be calibrated to specific soils. Also, because volumetric water content is recorded, changes in the bulk specific density of the soil can result in skewed readings. However, it can be assumed that the specific density of the subgrade beneath a road is constant.

2.3.2 Hydroprobe Components

A hydroprobe has three main components: the probe, the shield, and the electronic counting system. A typical hydroprobe is shown in Figure 10. The probe contains the radioactive source, a slow neutron detector, and a pre-amplifier. Once the slow neutrons are detected, the signal is amplified and sent to the electronic counting system at the surface. The source of the neutrons vary depending on the manufacture but typically consist of an alpha-particle emitter such as americium or radium and a fine powder of beryllium (IAEA 2002). As

the alpha particles bombard the beryllium, the reaction shown in Equation 3 occurs emitting the fast neutron.



The shield stores the probe when the gauge is not being used. It is generally made of lead and materials containing hydrogen as these materials block gamma radiation and fast neutrons which can be hazardous. (IAEA 2002) The electronic counting system also varies based on the manufacture. However, they all contain an amplifier, a high-voltage source, a counter, a timer, a power source, and a microprocessor. When the electronic counting system receives a signal from the detector, the microprocessor counts the raw signals and converts it to a counts per minute (cpm). The microprocessor then uses factory or user defined calibration equations to convert cpm to a volumetric water content. (IAEA 2002)

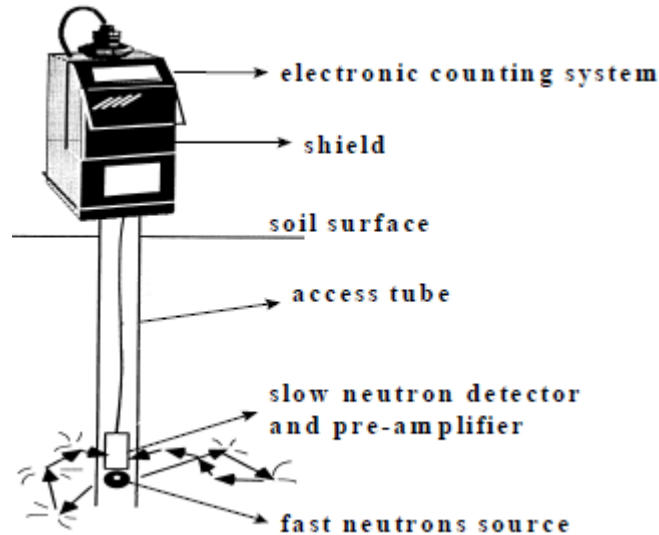


Figure 10: Neutron Moisture Gauge in Working Position (IAEA 2002)

2.3.3 Calibration of Neutron Moisture Gauge

As mentioned previously, in order to get accurate readings of water content, the moisture gauge must be calibrated to specific soils. In addition, the material and dimensions of the access tube can alter the readings. Laboratory calibrations, field calibrations, and theoretical models are

all methods used to calibrate the moisture gauge. In all methods a calibration is used to quantify the relationship between the cpm of slow neutrons and the volumetric water content of the soil. To avoid error associated with electronic drift, temperature changes, and other factors that affect the probe, the cpm of slow neutrons is converted to a count ratio (IAEA 2002). The count ratio is defined by Equation 4 (IAEA 2002).

$$CR = \frac{N}{N_s} \quad (4)$$

Where: CR = Count Ratio

N = Count rate in soil (cpm)

N_s = Count rate in standard material (cpm)

The count rate in a standard material is typically given the name “standard count”. In many cases the standard material is contained within the shield. Water can also be used as a standard material. It is recommended that the stability of the neutron moisture gauge be checked by taking readings in the standard prior to taking readings in the soil. (IAEA 2002) Using the count ratio, a calibration curve can then be created for various soils. An example of a calibration curve is shown in Figure 11.

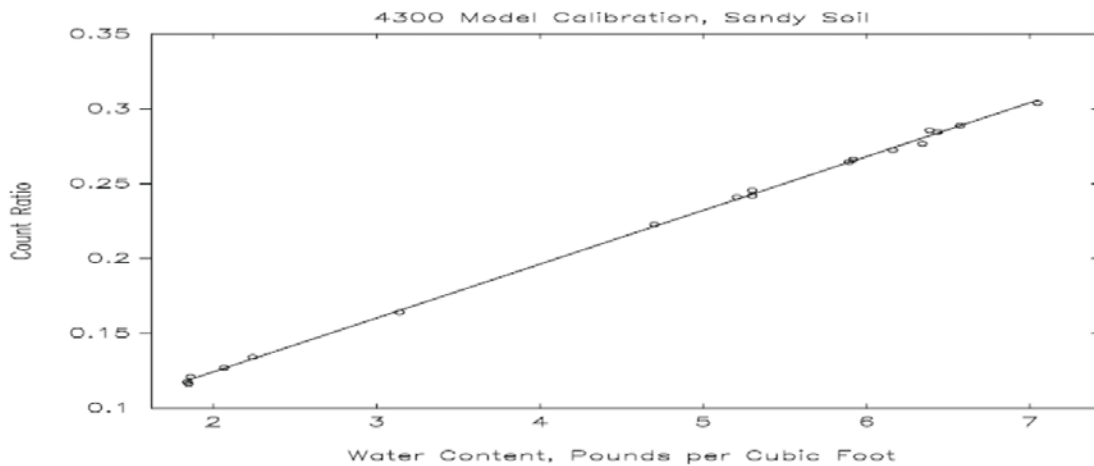


Figure 11: Typical Field Calibration Curve (Troxler 2006)

The calibration curve relates the count ratio to the volumetric water content of a specific soil and generally has a linear relationship. Both the slope and the intercept of this equation vary depending on soil type as well as the type of probe. (IAEA 2002) The slope can be associated with the sensitivity of the probe. In general, a flatter slope equates to a more sensitive probe. While the intercept has no theoretical significance, it is related to the hydrogen content. A dry soil that has a high hydrogen content will have a higher intercept. (IAEA 2002)

To create a field calibration curve, samples must be taken while the access hole is installed. Once the access hole is installed, readings are taken with the nuclear moisture probe at depths representative of the soil samples. The soil samples must then be tested in the lab for in-situ moisture content. Because the hydroprobe relates count ratio to volumetric water content, gravimetric water contents do not suffice. Either the specific gravity of the soil must be known or undisturbed soil samples must be taken during installation of the access hole. While this method is the simplest, it is difficult to get accurate calibrations for various reasons. First in order to develop a full calibration curve, samples must be taken at a wide range of water contents. This is challenging as the in-situ water content can take weeks to months to change significant amounts depending on soil type and environmental factors. Also, in order to obtain samples at different water contents, numerous access holes must be installed in similar soils which can be both time consuming and cost prohibitive.

Another calibration method primarily used by the manufacturer is completed in the laboratory. This method requires large soil samples which are used to fill drums typically 31-47 inches in diameter and 31-47 inches tall. (IAEA 2002) An access tube is placed in the center of the drum and readings are taken. Because this calibration method is completed in the laboratory, density and moisture content can be controlled making it easier to establish a full calibration

curve. This method has its disadvantages as well. One problem is that it can be challenging to obtain large enough soil samples to fill a drum. Also, the soil must be placed in the drum at the same density as in the field. Finally, if trying to measure water contents in the field with a stratified soil profile, each soil type must be collected to ensure proper calibrations.

The hydroprobe can also be calibrated using finite element theoretical models based on neutron-diffusion theory. This method is quite complex and requires that the elemental composition of the soil be known. (Li and Ren 2010) If the elemental composition of a soil is known, Li and Ren (2010) showed that a calibration relationship for expansive soils could be accurately estimated using a neutron diffusion model.

2.3.3 Access Tubes

Access tubes are installed in the ground to provide a conduit to lower the probe down. Various types and sizes of access tubes can be used. Ideally, access tubes made of aluminum are preferred because it is transparent to neutrons and will not corrode. Other materials can be used including steel, iron, and polyvinyl chloride (PVC) to name a few. Steel and iron are not ideal as they absorb neutrons and lower the sensitivity of the probe to water content. The sensitivity of the probe is also reduced when using PVC pipe because PVC contains chlorine which can absorb thermalized neutrons. While these materials alter the reading of the hydroprobe, they can be used if properly calibrated.

The diameter and wall thickness of the access tube can also effect the readings. Because an air gap between the probe and the wall reduces sensitivity, the inside diameter of the access tube should be only slightly larger than the probe diameter. Likewise, the thicker the wall of the tube the less sensitive the probe becomes. (IAEA 2002) In any case, it is important that the inside of the access tube stays dry. To ensure the tube stays dry, it is recommended to place a rubber

stopper at the bottom of the pipe before installation so that water cannot migrate into the pipe (IAEA 1970).

The installation of the access tube is just as important as the material it is made of. To obtain accurate readings the access tube should be installed in a manner that ensures the access tube is in good contact with the surrounding soil. This can be an extremely difficult task in stony, heavy-swelling, and layered soils (IAEA 2002). One method is to drill a hole with an auger slightly larger in diameter than that of the tube. The tube can then be pushed into place. If using aluminum or steel access tubes, it is possible to push the pipe in the ground without first drilling a hole. The soil retained in the pipe can then be augered out.

2.3.4 Prior use in research

Access tubes made of PVC pipe provide a good alternative when cost and availability are constraints. Also, as previous mentioned, installing access tubes can be a challenging task when using PVC. For this reason, the following discussion will help to understand the challenges associated with installing and using PVC pipe as an access tube. The following literature helped rationalize using PVC pipe as an access tube.

Research conducted by Bishop and Porro (1997) showed that differences in water content could be distinguished when using PVC as an access tube. This research also showed that an access tube could be installed using sand or bentonite to fill the annular space between the access tube and the soil. In this study, Bishop and Porro (1997) used a Boart Longyear Co. CPN 503DR hydroprobe with a 50-mCi AM-Be source. Nine test containers were constructed to test the effects of the PVC pipe and varying annular fill materials on hydroprobe readings. The soil used in this research was a crushed basalt. (Bishop and Porro 1997)

When a different material other than the existing soil is used to fill the annular space around the access tube, Bishop and Porro (1997) state that it is “impossible to determine the moisture content of either material from a single reading.” This is because the soil and the fill have different moisture holding capacities (Bishop and Porro 1997). However, relative changes in water content of the soil can still be achieved as shown in Figure 12. This graph shows that when a dry sand is used to fill the annular space between the soil and the access tube, changes in water content of the surrounding soil can be detected. It also shows, in every case, that the hydroprobe is capable of detecting changes in water content through the PVC pipe and annular materials (Bishop and Porro 1997). Additionally, Kramer et al. (1990) showed that the hydroprobe was able to detect changes in moisture content when the access tube was installed using grout to fill the annular space between the tube and the soil.

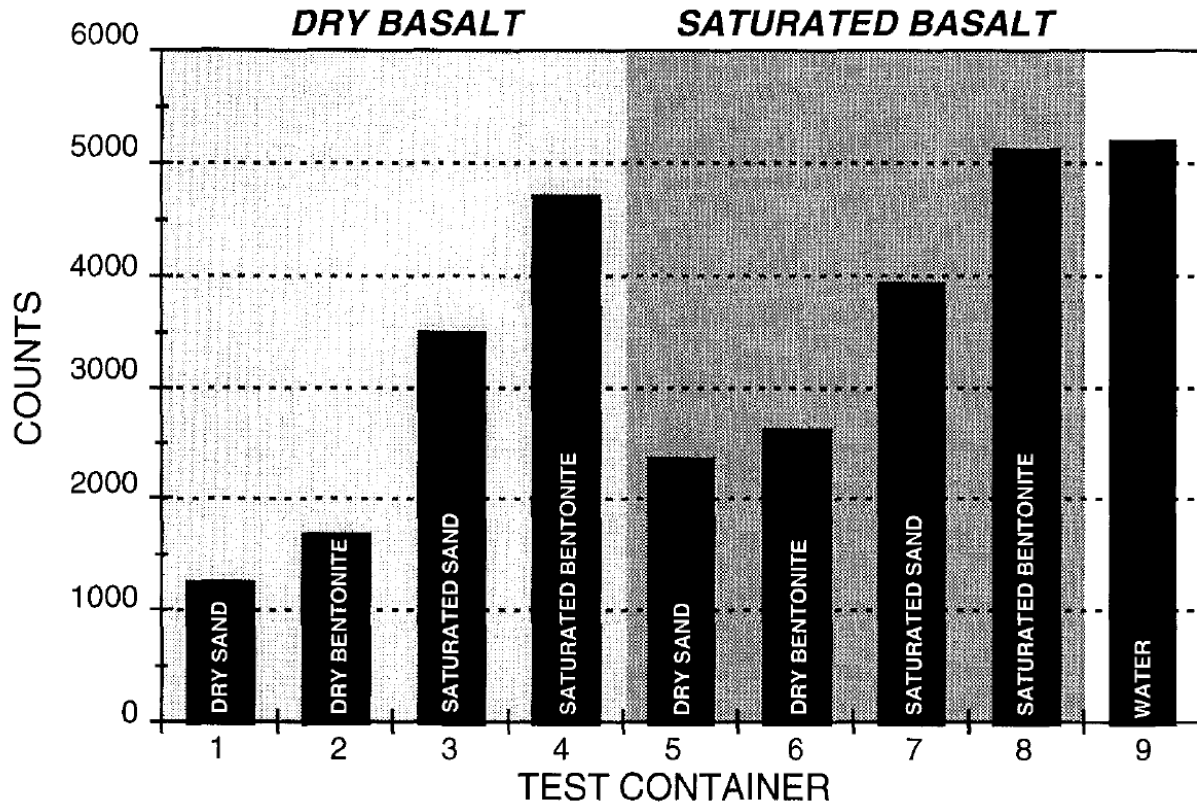


Figure 12: Test Container Neutron Counts for various annular space fills (Bishop and Porro 1997)

Abeele (1978) studied the influence of using various diameter steel, PVC, and aluminum access tubes. Readings in the different access tubes were compared to results obtained in uncased holes with corresponding diameters (Abeele 1978). The experiment was run using disturbed Bandelier tuff and a Troxler Electronic Labs, Inc. (Model 1255SN835) hydroprobe. The calibration curves created for each access tube configuration are shown in Figure 13.

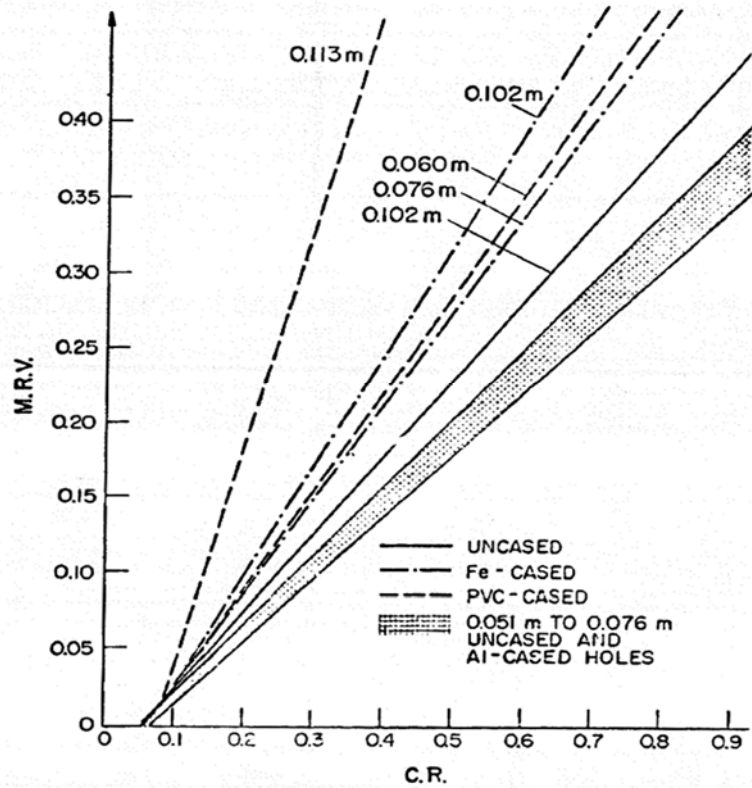


Figure 13: Moisture Ratio by Volume in function of count ratio (diameter is indicated on the curves) (Abeele 1978)

As shown in Figure 13: Moisture Ratio by Volume in function of count ratio (diameter is indicated on the curves) (Abeele 1978), the results from the aluminum access tubes are very similar to that of an uncased hole with corresponding diameters (Abeele 1978). This is expected as aluminum is mostly transparent to fast neutrons. From Figure 13, the deviation of the PVC and steel access tubes from the uncased holes is evident. Although the sensitivity of the hydroprobe is decreased when using PVC access tubes, Abeele (1978) showed that water fluctuations in the soil can still be detected and a calibration curve can be determined.

2.3 Remediation Strategies

An extensive literature review was conducted by Herman (2015) to identify and develop the various solutions encountered in technical literature for the stabilization of expansive

subgrades. His findings are presented here for completeness and to present the ideology behind the chosen remediation strategies implemented at AL-5. From his findings, the use of vertical barriers, lime columns, edge drains, deep mix columns, and paved shoulders were recommended to ALDOT and will be discussed in detail below. The use of a sand blanket was also desired by ALDOT, however, no literature on this remediation strategy could be found.

2.3.1 Vertical Barriers

Using vertical barriers is a mechanistic strategy used to minimize subgrade moisture fluctuations. By minimizing moisture fluctuations, the shrink-swell behavior of the subgrade is reduced preventing pavement damage. Vertical moisture barriers are typically composed of geomembrane sheets, geotextile coated fabrics, or fabric-sheeted laminates (Steinberg, 1998). They are installed in narrow trenches dug longitudinally along both edges of a pavement. Picornell and Lytton (1986) note that the depth of a vertical barrier should extend to the maximum shrinkage crack fabric depth, which is usually located beneath each pavement edge. Extending the barriers to a sufficient depth is important for their successful performance. Steinberg (1998) reports a case study in North Dakota in which vertical barriers installed to 4-foot depths performed poorly, and suggests that the subgrade would have been stabilized if the barrier depth had been doubled. Nelson and Miller (1992) note that it is generally not practical to install vertical moisture barriers through the entire depth of the active zone, but rather they recommend a depth of one-half to two-thirds the active zone. Vertical barriers should also extend beyond vegetative roots and be durable enough to resist root penetration.

After placement, each trench is backfilled (preferably with a relatively impermeable material), compacted, and capped. The barriers effectively seal the edges of the pavement and minimize moisture fluctuations directly beneath it. Vertical barriers greatly increase the time it

takes for seepage to occur under the pavement by increasing the required length of travel for the flow of water. Furthermore, the capillary mechanics of the subgrade cause the moisture to distribute upward more evenly, reducing differential heave. The barriers also aid in the development and stabilization of the state of suction directly beneath the pavement. According to Evans and McManus (1999), “This stable suction will be the equilibrium suction that exists in the deeper foundation soils”.

The use of vertical moisture barriers has proven successful on several projects in Texas. In the late 1970s, the first vertical moisture barriers were installed to 8-foot depths on IH-410 and IH-37 in San Antonio, Texas. Initial moisture sensor readings indicated lower water content variations inside the barrier-enclosed areas of IH-410 (Steinberg 1980). Observations in 1985 and 1987 indicated that the barriers had reduced roughness and cracking along both highways as well as minimized subgrade moisture content fluctuations (Steinberg 1985; Nelson and Miller 1992). Additionally, Steinberg (1989, 1992) summarized the installation and performance of nineteen vertical moisture barriers installed along various Texas pavements. He concluded that the barriers generally minimized moisture fluctuations beneath the subgrades and reduced long term roughness and cracking.

2.3.2 Lime Columns

Lime is the most frequently used chemical stabilizer for expansive subgrades (Petry and Little 2002). Lime is a term that generally denotes quicklime (CaO) or hydrated lime (Ca(OH)_2). Quicklime is produced by exposing high purity limestone to strong heat, and hydrated lime is produced by mixing quicklime with enough water to form a white powder. Lime stabilizes a soil by replacing monovalent cations (cations with a +1 charge, such as Na^+ , Li^+ , and K^+), which are commonly present in clays, with divalent calcium (Ca^{+2}) cations. This causes a significant

reduction in the size of the diffused water layer surrounding individual clay particles, which in turn reduces the capacity of a clay to adsorb water. Furthermore, the cation replacement results in the flocculation and agglomeration of clay particles, increasing clay shear strength and workability (Little 1995). Lime further stabilizes a soil by reacting pozzolanically with the silica and aluminum present in the soil to form a cementitious glue that bonds the soil particles together.

Lime stabilizers may be mixed and compacted into the upper few inches or feet of a subgrade, applied through drill-holes, or injected as a slurry. Generally, the success of lime-stabilization is dependent upon adding the correct amount of lime, properly compacting and curing the lime-soil mix, and pulverizing the lime to a proper degree. Failure to fulfill any one of these requirements can result in poor performance. Additional considerations must be made regarding temperature, since lime-soil reactions are temperature dependent (Little 1995).

Of particular concern when considering lime-soil stabilization is the possibility of high concentrations of soluble sulfates in the soil. Performing lime stabilization in clays containing high concentrations of salts with soluble sulfates (such as sodium sulfate (Na_2SO_4) and gypsum ($\text{CaSO}_4 \cdot 2\text{H}_2\text{O}$)) will trigger the formation of ettringite, a reaction product comprised of calcium, alumina, water, and sulfate (Little 1995). The formation of ettringite diminishes the lime meant to react with the soil and forms a material which contains expansive characteristics itself. Expansion caused by ettringite formation is known as lime-induced sulfate heave. Lime-induced sulfate heave may be greater than the heave of the untreated expansive clay (Mitchell 1986). Soils containing above 1,000 ppm of soluble sulfates have been reported to react with lime to form ettringite (Little and Nair 2009). Therefore, expansive subgrades should be tested for sulfates prior to performing lime-soil stabilization. Test procedures range from simple in-situ

electromagnetometer tests to more complex laboratory tests involving small soil samples and centrifuges. Little and Nair (2009) provide a recommended practice manual for testing and stabilizing sulfate-rich subgrades.

Lime may also be applied through the drill-hole technique. When the drill-hole technique is utilized, holes are drilled through the subgrade to depths of 2.5 to 4 ft at four to five-foot centers (Nelson and Miller 1992). Dry or slurry lime is then placed in the holes. If dry lime is placed, water is added to increase mobility. The pavement is then constructed. Very little research exists reporting the success of the drill-hole technique. According to Nelson and Miller (1992):

Results of the drill-hole technique are erratic, and the authors do not encourage its use. One factor that limits the effectiveness of the method is the inability to uniformly distribute the lime in the soil mass. Also, the diffusion process is very slow unless the soil has an extensive network of fissures.

The lime slurry pressure injection (LSPI) method was developed to provide a better alternative to the drill-hole technique (Nelson and Miller 1992). The LSPI method consists of pumping lime slurry into a subgrade using an injection vehicle equipped with injection pipes. Injections are made at 12 to 18-inch intervals to a total depth extending through the active zone. At each interval, slurry is pumped until refusal or until a target pressure is achieved. Injection depths can range from three to ten feet, and are typically spaced at five-foot grid patterns (Little 1995). Figure 14 illustrates a typical injection vehicle.



Figure 14: Typical Injection System (Hayward Baker 2010)

LSPI is more likely to successfully stabilize a subgrade if the subgrade exhibits a relatively deep dry crack fabric. Upon injection, lime slurry takes the path of least resistance along crack and fissure walls within the subgrade. Upon infiltrating the cracks, the lime encapsulates and seals off large portions of clay, reducing the capacity for capillary and seepage phenomenon. This in turn greatly reduces the potential for volumetric changes within the subgrade. Furthermore, high injection pressures can cause hydraulic fracturing within the subgrade, creating new planes of slurry infiltration. It must be emphasized that the slurry does not diffuse homogeneously “through” the bulk soil; rather, it travels along the available cracks and fissures (Snethen 1979). Therefore, if the subgrade does not exhibit a relatively deep dry crack fabric, the injection process will be performed with less confidence. The success of the procedure will be dependent upon the occurrence of hydraulic fracturing, which may be difficult

to achieve and/or identify during construction. If hydraulic fracturing does not occur, the injection process may encounter refusal without a sufficient diffusion of the lime.

2.3.3 Edge Drains

Edge drains are subsurface drainage systems that have been utilized to stabilize expansive subgrades. The drains are installed in shallow trenches dug longitudinally along the edges of the pavement. A perforated pipe and a clean permeable backfill are placed in the trench. These materials are typically wrapped in a geotextile, which functions as a filter to allow water to pass through while retaining soil particles. The trench is topped with embankment fill and pavement materials. Care must be taken not to crush the pipes during backfilling and compacting operations, and construction must be performed carefully to avoid clogging. Flackenstein and Allen (2007) give an extensive overview of best construction practices for edge drains. Figure 15 shows a typical schematic of an edge drain system.

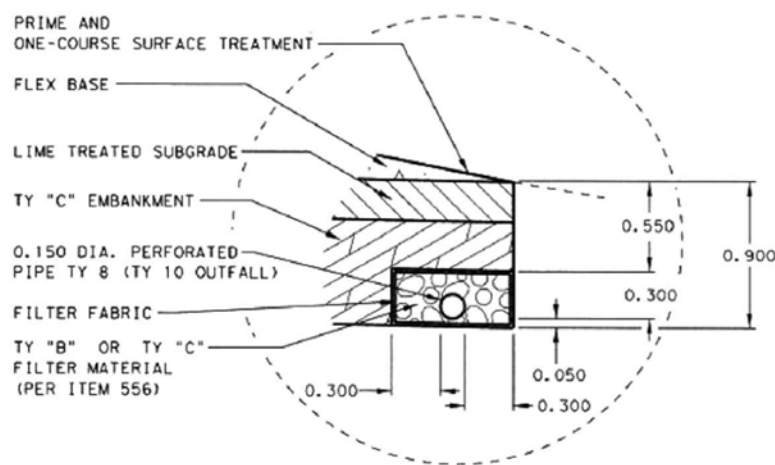


Figure 15: Typical Edge Drain Schematic (Chen et al. 2012)

Chen et al. (2012) cited the success and cost efficiency of edge drains in preventing heave damage along US-59 and SH-114 in the Atlanta (Texas) and Fort Worth districts, respectively. The installation of edge drains along US-59 resulted in excellent pavement performance for 10

years. The installation of edge drains along SH-114 resulted in excellent pavement performance for 5 years. Both roads have continued to perform well as of 2012. Regarding the edge drain installed along SH-114, Chen et al. (2012) state the following: “The District reported that water from the edge drain can be heard (even on a dry day) as it is discharged into the culvert”.

2.3.4 Deep Mix Columns

The use of deep soil mixing (DSM) technology is usually reserved for strengthening very soft clays and/or soils with high organic contents. Studies performed by Madhyannapu et al. (2007, 2009, 2010) were the first to evaluate the utilization of DSM technology for stabilizing expansive soils. Two 15 by 40-foot test sections, located in the median of Interstate 820 near Fort Worth, Texas, were selected for the placement of DSM columns. Both test sections (one containing 44 DSM columns and the other containing 65 DSM columns) were installed at different grid patterns. The columns were augured to ten-foot depths at two-foot diameters, and the center-to-center spacing was one meter. A geogrid was laid over the columns and tied to rods that were anchored into the columns. The geogrid was installed to facilitate stress transfer throughout the columns. 1.2 feet of fill was then dumped onto the geogrid and compacted using a vibratory tamper. Figure 16 shows a schematic of the final DSM design. The test sections were monitored for two years, and movements in and around the columns were found to be negligible.

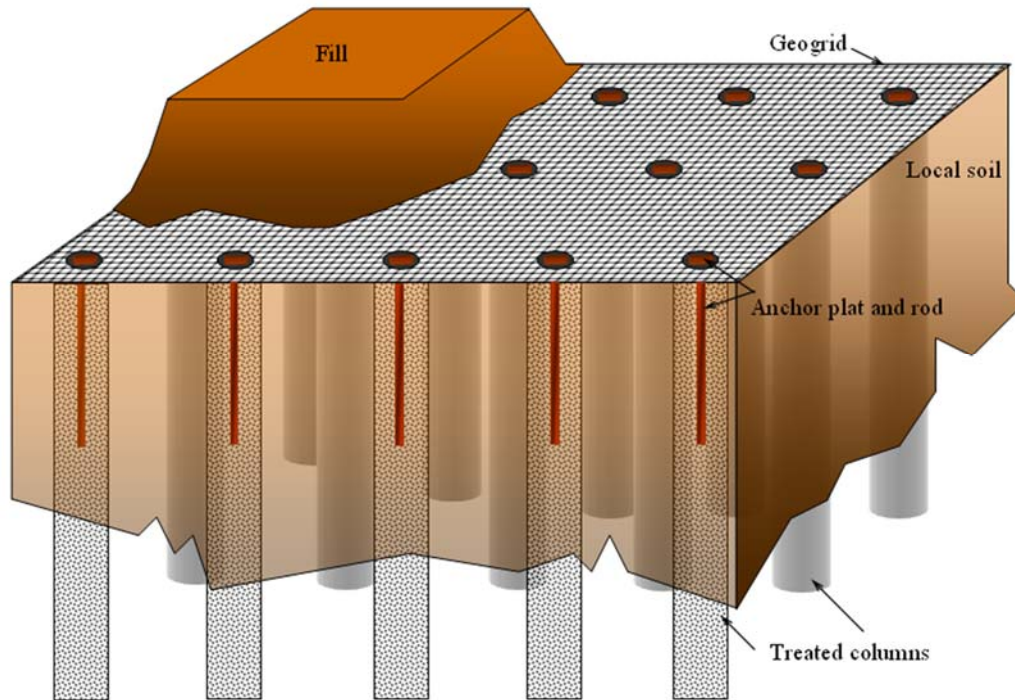


Figure 16: Schematic of Deep Mix Columns for the Stabilization of Expansive Soils (Madhyannapu 2007)

2.3.5 Paved Shoulders

A common distress mechanism associated with roadways built on expansive clay soils is the development of longitudinal cracks near the edge of the pavement. These longitudinal cracks are the result of differential moisture fluctuations beneath the pavement. During the summer months and dry season, the moisture content in the vicinity of the shoulders decreases and the soil shrinks. Just the opposite occurs during the wet season, as the moisture content increases and the soil expands. However, the moisture content near the center line of the roadway is not as affected by seasonal changes and remains at a more constant moisture content. This differential changes in water content between the edge of pavement and center line create differential settlement and thus cracking along the edge of the pavement (Zornberg and Gupta 2009). This mechanism is illustrated in Figure 17.

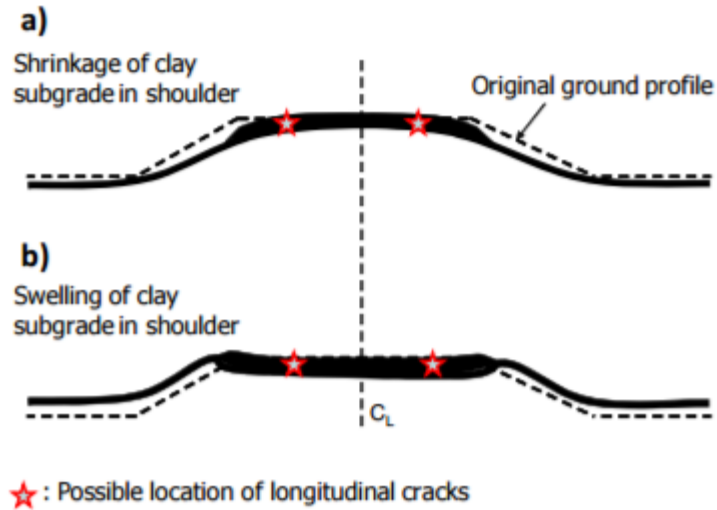


Figure 17: Longitudinal Crack Formation (Zornberg and Gupta 2009)

By widening the paved shoulders, the location of the longitudinal cracks in theory will be moved out of the travel lane and into the shoulder. A study conducted by Lytton et al. (2005) used rigorous modeling to determine the deformations that occur in a pavement due to moisture diffusion and ultimately changes in suction. In the study, Lytton et al. (2005) was able to show that the addition of both 4 foot and 8 foot wide shoulders significantly reduced the vertical displacements in the outside wheel path due to cyclic wetting and drying.

CHAPTER 3: RESEARCH SETTING

3.1 Site Description

The research site is located approximately 20 miles west of Selma, AL in Perry County. The site consists of a 4-mile section of Alabama State Highway 5 between mile points 50.85 and 54.85. The 4-mile section is relatively flat and runs through both wooded and farm lands. The site is divided into eight sections as shown in Figure 18. The mile points for each test section as well as the remediation technique used is shown in Table 1.

Table 1: Test Sections

Test Section	Remediation Technique	Milepost
1	Sand Blanket	50.85 - 51.35
2	Vertical Moisture Barriers	51.35 - 51.85
3	Lime Columns	51.85 - 52.35
4	6' Paved Shoulders	52.35 - 52.85
5	Edge Drains	52.85 - 53.35
6	Control	53.35 - 53.85
7	Deep Mixing - Canceled	53.85 - 54.35
8	Control	54.35 - 54.85

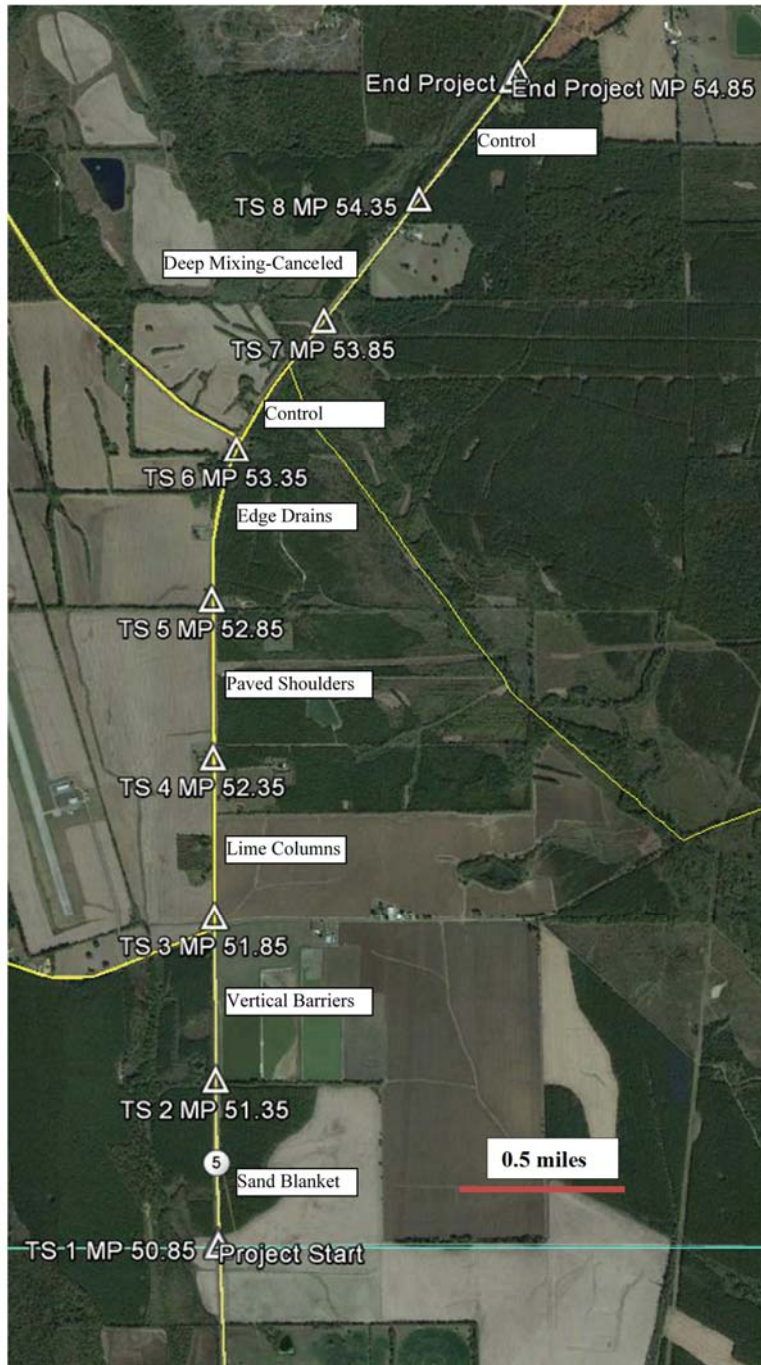


Figure 18: Project Test Sections (After Google Earth)

It was originally intended that each test section receive a different remediation technique. However, during the initial site exploration a thinner clay layer in Test Section 8 was discovered. For this reason, Test Section 8 serves as an additional control section. As noted in Figure 18, the construction of the deep mix columns was cancelled after initial trials were deemed unsuccessful

and impractical. It should also be noted that due to construction constraints, the sand blanket was only constructed in the middle of the half mile long section. Therefore, the first and last 500 feet of Test Section 1 as well as Test Sections 6, 7, and 8 were used as control sections. The construction of the test sections and final wearing course was completed in August of 2016.

3.2 Soil Characterization

Initially a “farm-to-market” route, AL-5 was constructed directly on the native subgrade and built from local materials. A soil survey of Perry County, AL was conducted in 1998 by the United States Department of Agriculture (USDA). The map of this survey with the research site circled is shown in Figure 19. As shown in the map, the general soil type in the research site is Vaiden-Okolona-Sucarnoochee. These soils are classified as poorly to moderately well drained, brown to olive gray clayey soils. The parent material is generally the underlying Mooreville Chalk Foundation, however, some areas near the creek contain clayey alluvium (Harris 1998). This soil type is categorized as poorly suited for urban uses due to its slow permeability and moderate to very high shrink-swell potential. (Harris 1998) A summary of the soil properties is provided in Table 2.

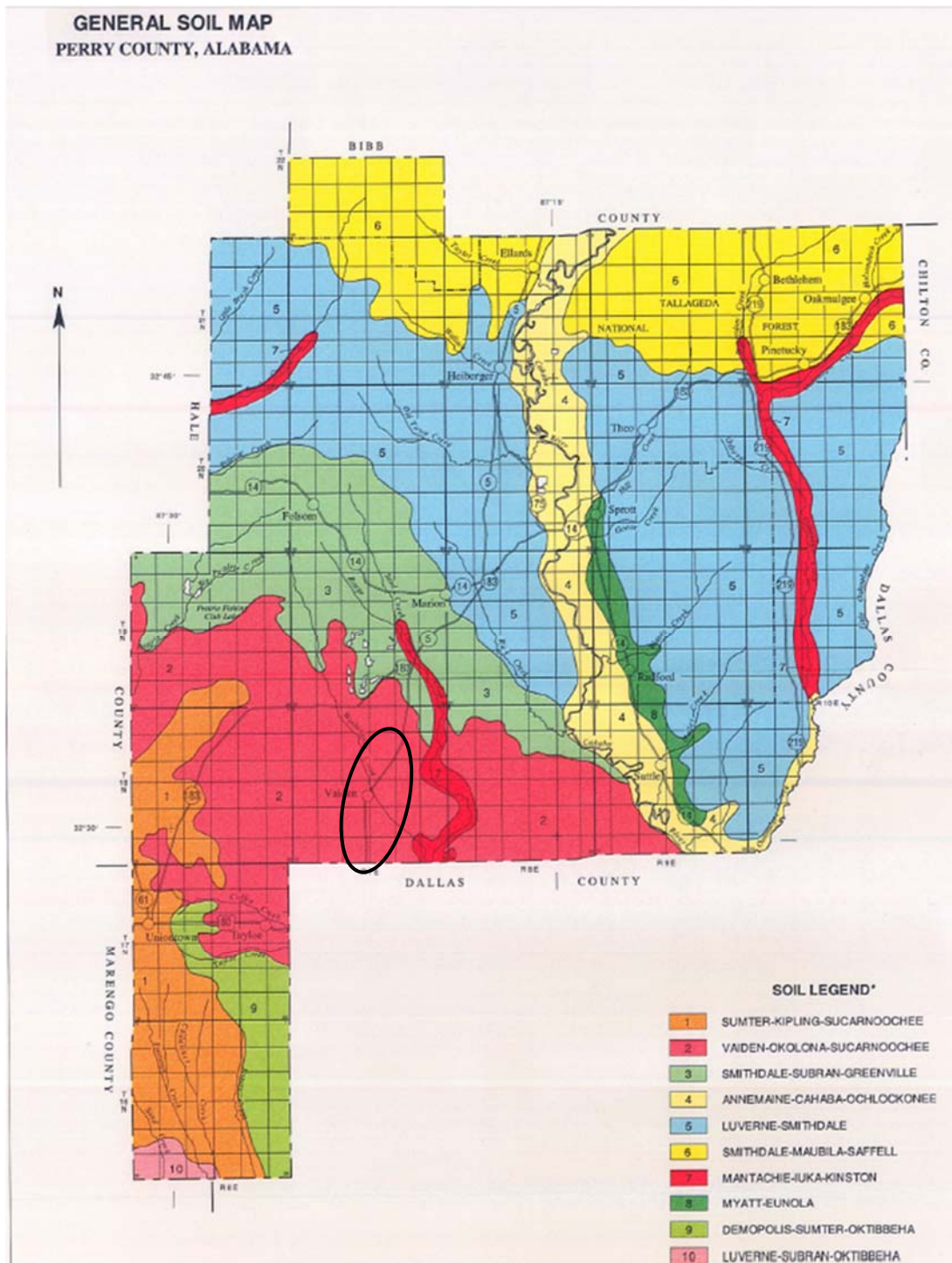


Figure 19: Soil Survey of Perry County, AL (Harris 1998)

Table 2: Soil Properties from USDA Soil Survey (after Harris 1998)

Type	Depth (in)	USCS Classification	% Passing 200	LL	PI	Permeability (in/hr)	Shrink-Swell potential
Okolona Silty Clay Loam	0-6	CL, CH	85-98	46-55	25-32	<0.06	High
	6-60	CH, MH	90-98	60-90	29-65	<0.06	Very High
Vaiden Clay	0-5	MH, CH	90-100	50-60	20-30	0.06-0.2	High
	5-21	CH, MH	85-100	50-90	30-50	<0.06	Very High
	21-60	CH	85-100	50-90	30-52	<0.06	Very High
Kipling Clay Loam	0-5	CL	85-95	30-45	15-25	0.06-0.2	Moderate
	5-65	CH, CL	85-95	38-70	22-45	0.06-0.2	High
	65-80	CH, CL	75-95	48-80	26-50	<0.06	Very High
Sucarnoochee Clay	0-16	CL, CH, MH	85-95	40-65	15-35	0.06-0.2	High
	16-54	MH, CH, CL	85-98	45-70	20-40	<0.06	High
	54-60	CH, MH	85-98	50-80	25-45	<0.06	High

3.3 Climate

The climate at the research site is heavily influenced by moist tropical air originating in the Gulf of Mexico. Summers are long and hot while winters are cool and fairly short. During the summer in Perry County the average temperature is 79 degrees with an average daily maximum of 90 degrees. During winter months, the average temperature is 46 degrees with a daily minimum average of 34 degrees. Precipitation is generally heavy throughout the year, however during construction of the test sections an unusually long drought occurred. The total annual precipitation is roughly 54 inches with the majority falling between April and October. (Harris 1998)

3.4 Traffic Data

Traffic data from 2014 was collected from ALDOT's traffic database. A traffic counting station located within the project bounds at mile point 51.21 reported an average annual daily traffic (AADT) of 1120 vehicles. Of these vehicles, 40 percent were reported as truck traffic or

class 5 vehicles and above. This percentage equates to an average annual daily truck traffic (AADTT) of 448 trucks. (ALDOT 2016)

CHAPTER 4: PREVIOUS RESEARCH

4.1 Site Investigation and Lab Work

An extensive site investigation program was conducted by Herman (2015) including site reconnaissance and a subsurface investigation. In total 17 borings were drilled approximately a ¼ of a mile apart throughout the project. A map of the boring locations is shown in Figure 20. Continuous soil samples were obtained using thin-wall Shelby tubes. The soils encountered during this investigation were consistent with the soil types from the USDA soil survey (Herman 2015). Boring logs from this investigation can be found in Appendix A.

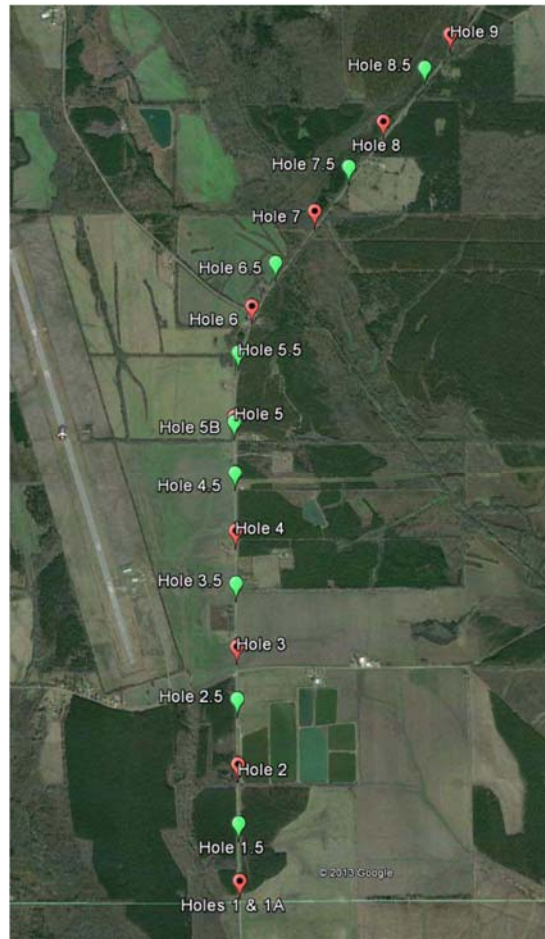


Figure 20: Boring Locations (After Google Earth)

Stallings (2016) conducted a broad laboratory analysis of the soil samples taken from the project site. Various tests were conducted on the samples including soil classification tests such as grain size analysis, Atterberg limits and specific gravity tests. One-dimensional swell tests were also performed. Finally soil-water characteristic curves were created for the soils. At the time of writing this paper, tests to determine the drying side of the soil-water characteristic curves are underway by Stallings. From the laboratory tests, it was concluded that the subgrade soils at AL-5 is expansive and more than likely a cause of the pavement distress (Stallings 2016). A summary of the laboratory data can be found in Table 3. Stallings (2016) also studied the impact of trees near the road. It was concluded, that trees within 60 feet of the edge of pavement

have the potential to induce large amounts of suction within the subgrade of the pavement. Specifics about the site investigation and laboratory analysis can be found in detail in prior papers (Herman 2015, Stallings 2016).

Table 3: Summary of AL-5 Laboratory Data (Stallings 2016)

Borehole	Depth (ft)	LL	PI	%<#200 Sieve	Water Content (%)	Dry Density (pcf)	Specific Gravity	Swell Pressure (psf)
B-1A	1.5	70	46					
B-1A	3.5	88	58					
B-1A	5.5	110	83					
B-1A	7.5	79	50					
B-1A	9.5	103	74					
B-1.5A	1.5	97	68					
B-1.5A	3.5	66	42	98	37.0	84.0	2.75	736.0
B-1.5A	7.5	91	66					
B-1.5A	9.5	85	61	98	32.9	87.5	2.62	1301.0
B-2A	3.0	83	52					
B-2A	5.0	73	48					
B-2A	7.0	86	59					
B-2A	9.0	95	68					
B-2.5A	1.5	70	46					
B-2.5A	3.5	84	58	93	31.9	90.1	2.75	927.0
B-2.5A	5.5	79	47					
B-2.5A	7.5			98	29.2	92.4	2.72	1560.0
B-3A	1.5	93	67					
B-3A	3.5	65	41					
B-3A	7.5	74	49					
B-3.5A	1.3	68	40	99	38.6	82.5	2.70	1035.0
B-3.5A	3.3	87	59					
B-3.5A	5.3	84	57					
B-3.5A	7.3			97	41.5	77.7	2.74	1073.0
B-4A	1.8	72	47					
B-4A	5.8	93	70					
B-4.5A	1.2	68	40	97	38.8	81.5	2.72	1082.0
B-4.5A	5.2	97	69					
B-4.5A	7.2			96	33.3	84.4	2.73	
B-5A	1.5	50	26					
B-5A	7.5	91	68					
B-5.5A	1.0	86	60	96	39.6	81.0	2.75	871.0
B-5.5A	7.0	88	61	96	33.3	87.7	2.70	1393.0

Borehole	Depth (ft)	LL	PI	%<#200 Sieve	Water Content (%)	Dry Density (pcf)	Specific Gravity	Swell Pressure (psf)
B-Tree C	3.0			94	39.6	79.3		622.0
B-Tree C	7.0			94	32.2	89.8		1374.0
B-6A	1.5	97	73					
B-6A	7.5	80	50					
B-6.5A	1.5						2.69	
B-6.5A	3.5	71	47	60	28.2	90.2		509.0
B-6.5A	5.5	57	39					
B-6.5A	7.5	50	35					
B-6.5A	8.8			45				
B-7A	3.5	57	40					
B-7A	5.5	58	38					
B-7A	7.5	63	42					
B-7.5A	5.0	67	49	81	29.2	93.9	2.72	608.0
B-7.5A	7.0	60	42	78	27.8	95.4	2.81	709.0
B-8A	5.0	64	48					
B-8A	7.0	50	34					
B-8.5A	1.0			90				
B-8.5A	3.0			78				

4.2 Instrumentation

To understand the behavior of the subgrade and evaluate the remediation techniques, each test section was instrumented with a variety of sensors. Data acquisition systems were installed to record data and connected via a cellular modem for remote monitoring. In total, 7 different stations were installed to monitor subgrade behavior. One station was installed in each remediation section as well as one control section. At each station, sensors were installed to measure soil moisture content, matric suction, pore water pressure, and asphalt strain. The seventh station was installed near a large tree at the north end of the project to monitor the effects of vegetation on matric suction and moisture content. A weather station was also installed at the project to monitor environmental conditions including temperature and precipitation. The selection process for determining appropriate sensors, as well as installation and calibration techniques are described in detail in previous publications. (Jackson 2016)

4.2.1 Moisture Sensors

The moisture content sensor installed throughout the project was the GS1 manufactured by Decagon Devices. The GS1 measures the volumetric water content (VWC) of the soil by measuring the dielectric permittivity of the soil and correlating it to VWC (Jackson 2016). The sensor is shown in Figure 21.

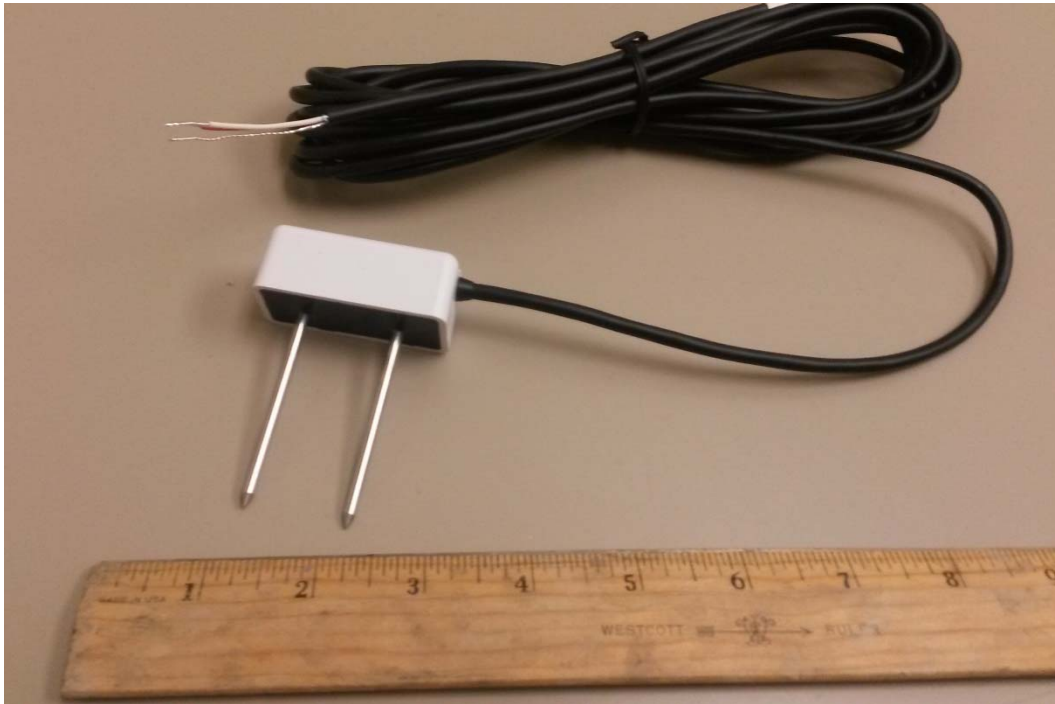


Figure 21: Decagon Devices GS1 Moisture Content Sensor (Jackson 2016)

Based on recommendations by Jackson (2016), the calibration of the GS1 sensor was refined by testing more points at the wetter end of the curve. The same procedure as outlined by Jackson (2016) was used. The additional points were plotted and are shown in orange on Figure 22. Also shown is the calibration curve developed by Jackson (2016). From this plot, the two wettest points fall outside of the curve. This is most likely because at this moisture content the soil is approaching complete saturation. This makes it very difficult to achieve the in-situ

density skewing the results. For this reason, it was decided that the curve developed by Jackson (2016) was accurate from the driest soil conditions up until the soil approached saturation.

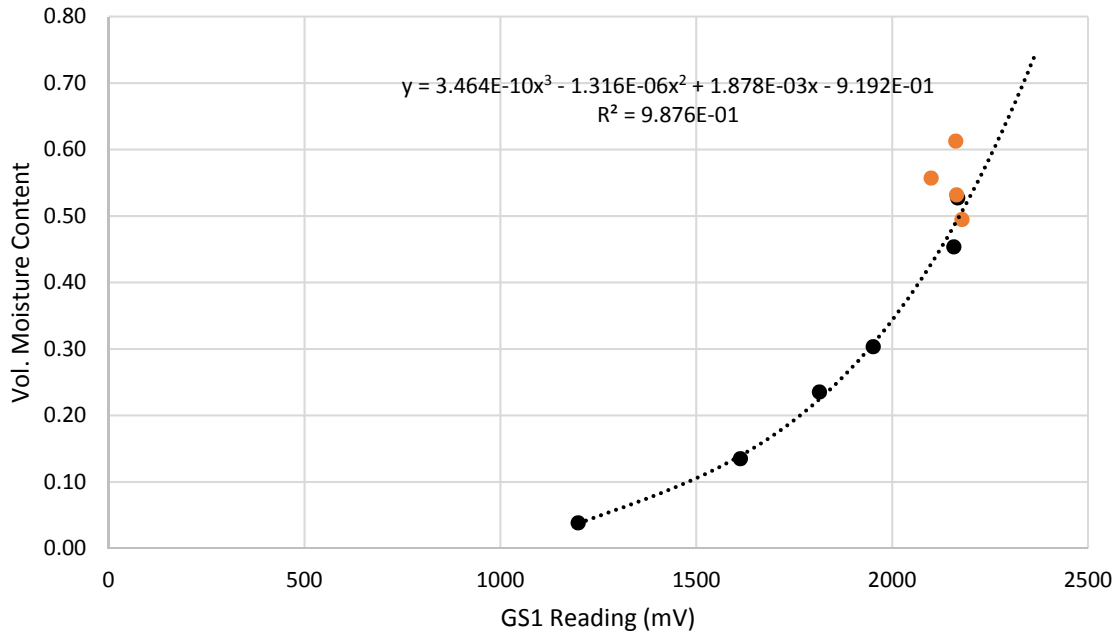


Figure 22: GS1 Calibration Curve (after Jackson 2016) Orange Points indicate new calibration points

4.2.2 Suction Sensors

To measure matric suction, the MPS6 from Decagon Devices was used. The sensor works by placing the ceramic disks in hydraulic contact with the soil. This allows the suction in the ceramic disks to equalize with the surrounding soil suction. The moisture content of the ceramic disk is then measured using a dielectric technique similar to that of the GS1. Finally, the moisture characteristic curve of the ceramic disk is used to correlate water content to matric suction. Factory calibrations were used for this device (Jackson 2016). A picture of this sensor is shown in Figure 23.



Figure 23: Decagon Devices MPS5 Suction Sensor (Jackson 2016)

4.2.3 Piezometers

Geokon 4500S vibrating wire piezometers were installed to measure positive pore pressures. The sensors were individually calibrated by Geokon. (Jackson 2016) A picture of this sensor is shown in Figure 24.



Figure 24: Geokon 4500S Vibrating Wire Piezometer (Jackson 2016)

4.2.4 Asphalt Strain Gauges

In an attempt to measure the level of pavement distress, asphalt strain gauges were installed in the pavement. Two types of asphalt strain gauges were used throughout the project. Due to time and availability constraints, the ASG-152 by CTL group was used in Test Section 1 to monitor the sand blanket. In all other sections less expensive asphalt strain gauges manufactured by CTL were used. The two strain gauges are shown in Figure 25 and Figure 26. Both gauges incorporate a full Wheatstone bridge circuit with four active 350 ohm strain gauges mounted on a 6/6 nylon rod. The gauges were calibrated by the manufacturer. (Jackson 2016)



Figure 25: CTL ASG-152 Asphalt Strain Gauge (Jackson 2016)



Figure 26: Geocomp Asphalt Strain Gauge (Jackson 2016)

The layout of the strain gauge arrays were the same except for the sand blanket Test Section. To better understand the strain gauge trends discussed later in this paper, diagrams of the strain gauge layout is shown in Figure 27: Strain Gauge Layout. A negative reading represents compression and a positive reading represents tension.

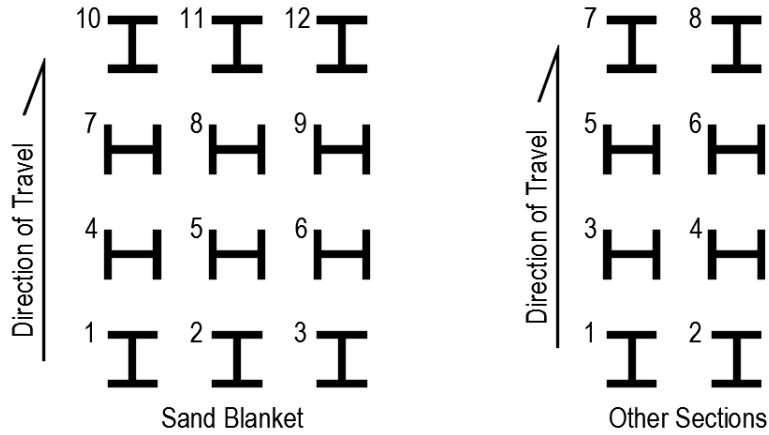


Figure 27: Strain Gauge Layout

4.2.5 Data Acquisition System and Weather Station

CR6 dataloggers manufactured by Campbell Scientific were installed to monitor the sensors at each test section. In addition, three AM16/32B multiplexers were used to connect all the sensors at each test section. Each station is powered by a BP12 battery. A solar panel was installed at each station along with a CH200 charging regulator to recharge the battery during daylight hours. The data acquisition system is shown in Figure 28.

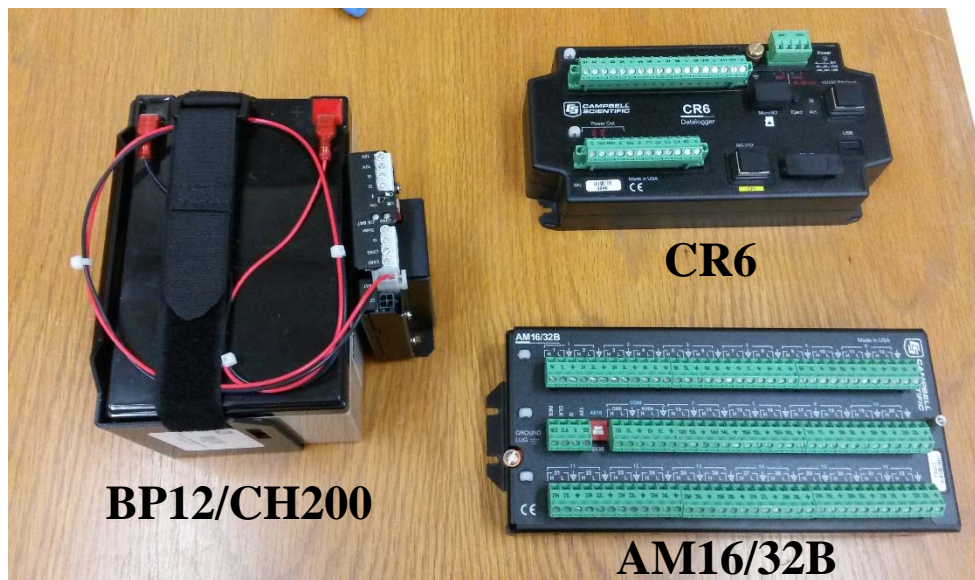


Figure 28: Data Acquisition System (Jackson 2016)

One Campbell Scientific WTX520 weather sensor was installed. The weather sensor is capable of measuring air temperature, barometric pressure, wind speed and direction, relative humidity, and precipitation. The weather sensor is shown Figure 29.



Figure 29: Campbell Scientific WTX520 Weather Sensor (Jackson 2016)

4.2.6 Installation Summary

The moisture sensors, suction sensors, and piezometers were installed in a 6” borehole. At each test section a set of downhole sensors were installed in the subgrade beneath the pavement and in the adjacent shoulder. In each borehole, four moisture sensors were installed in the side of the borehole at target depths of 10 feet, 7.5 feet, 5 feet, and 2.5 feet. Four suction sensors were also installed at these target depths in each hole. Two piezometers per hole were installed at target depths of 12 feet and 7.5 feet.

The asphalt strain gauges were installed in the pavement in all sections. The only exception to this was the sand blanket test section. In this section the asphalt strain gauges were

installed directly on the subgrade due to the method of construction. Twelve sensors were installed in the sand blanket test section. In the remaining test sections, only eight sensors were installed in order to minimize costs. Half of the sensors at each section were oriented with the direction of traffic (longitudinal) and the other half was oriented perpendicular to the direction of traffic (transverse). The installation process is well documented in prior publications (Jackson 2016). The survivability of the sensors was very good and is summarized in Table 4: Sensor Survivability (Jackson 2016).

Table 4: Sensor Survivability (Jackson 2016)

Test Section	Moisture			Suction		
	Surviving	Total	Percent Surviving	Surviving	Total	Percent Surviving
Control	8	8	100%	8	8	100%
Sand Blanket	8	8	100%	8	8	100%
Vertical Barriers	8	8	100%	6	8	75%
Lime Columns	8	8	100%	7	8	88%
Paved Shoulders	8	8	100%	6	8	75%
Edge Drains	8	8	100%	6	8	75%
Trees	4	4	100%	3	4	75%
Total	52	52	100%	44	52	85%
Test Section	Piezometer			ASG		
	Surviving	Total	Percent Surviving	Surviving	Total	Percent Surviving
Control	4	4	100%	7	8	88%
Sand Blanket	4	4	100%	11	12	92%
Vertical Barriers	4	4	100%	8	8	100%
Lime Columns	4	4	100%	6	8	75%
Paved Shoulders	4	4	100%	8	8	100%
Edge Drains	4	4	100%	7	8	88%
Trees	NA	NA	NA	NA	NA	NA
Total	24	24	100%	47	52	90%

4.3 IRI Data

To provide another way to monitor the effectiveness of the remediation strategies used at AL-5, international roughness index (IRI) surveys were conducted both prior to construction and after completion of the final wearing course. An IRI survey measures variations in a pavement surface by creating longitudinal profiles. An illustration of this concept is shown in Figure 30. An IRI surveys were conducted using an inertial profiler similar to the figure shown in Figure 31. The IRI surveys were performed by a technician from the National Center for Asphalt Technology.

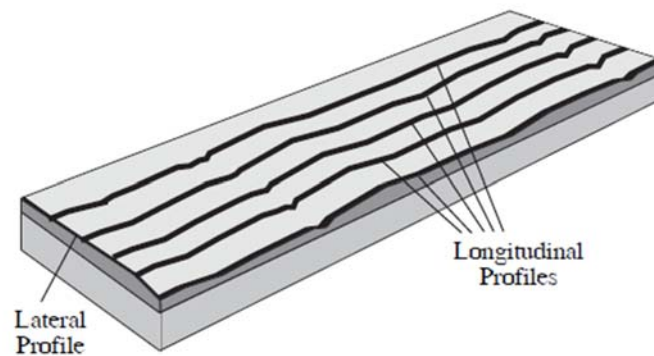


Figure 30: Pavement Profiles (Sayers and Karamihas 1998)

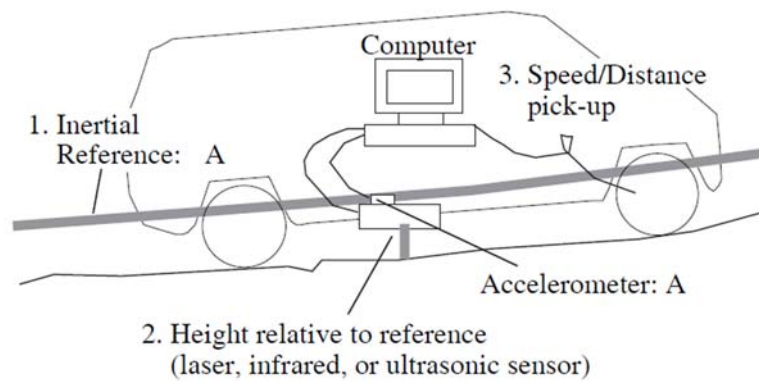


Figure 31: Inertial Profiler Schematic (Sayers and Karamihas 1998)

From two IRI surveys before construction, IRI values were shown to be well in excess of the failure threshold of 170 inches/mile defined by the FHWA (Herman 2015). The results of the IRI surveys dated May 31, 2014 and November 05, 2014 are shown in Figure 32 thru Figure 35.

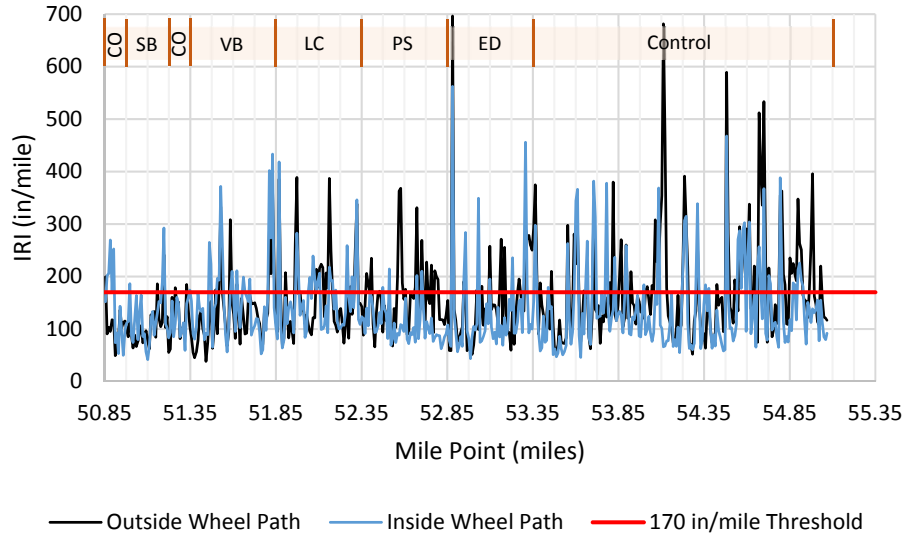


Figure 32: IRI Survey – North Bound Lane – 05/31/2014

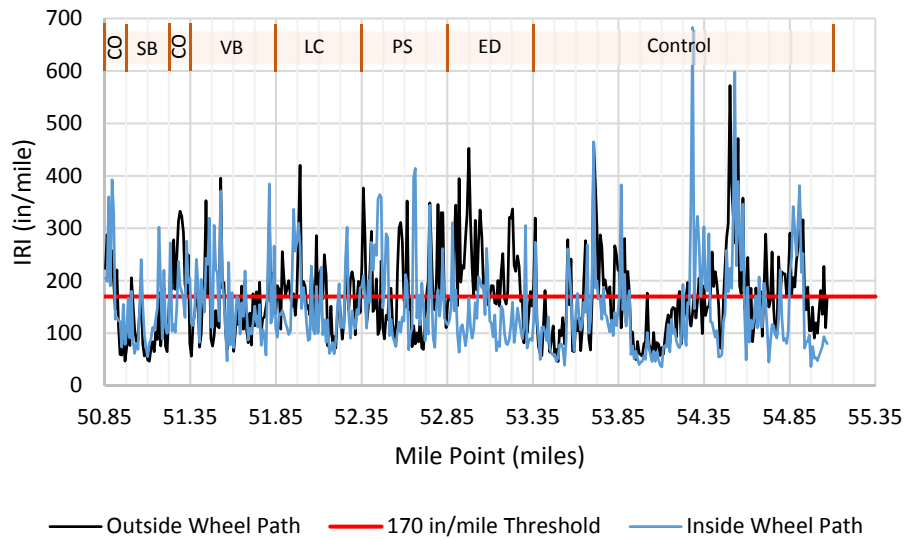


Figure 33: IRI Survey – South Bound Lane – 05/31/2014

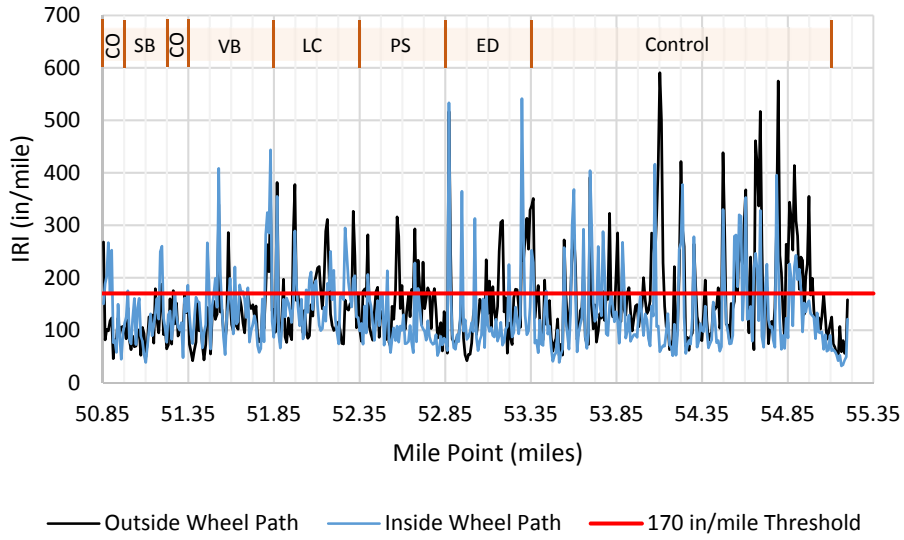


Figure 34: IRI Survey – North Bound Lane – 11/15/2014

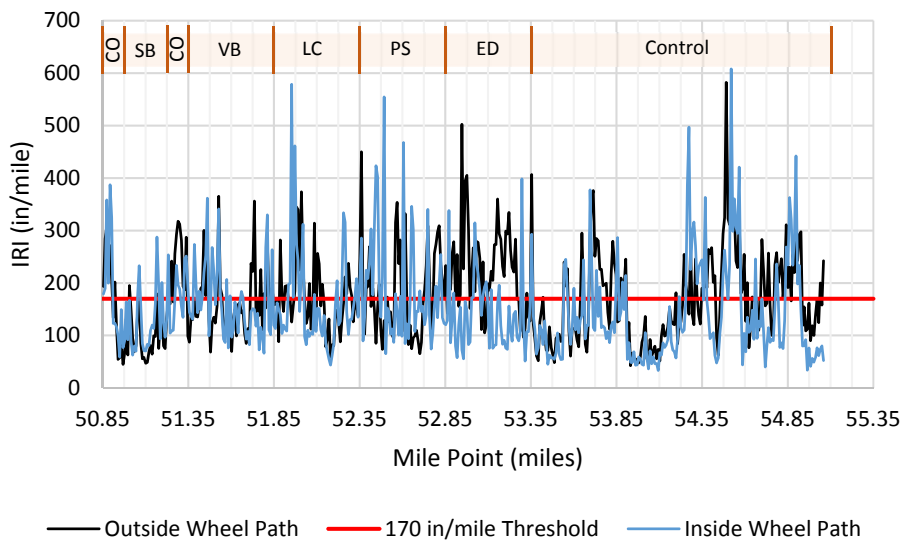


Figure 35: IRI Survey – South Bound Lane – 11/15/2014

CHAPTER 5: CONSTRUCTION OF TEST SECTIONS

Construction of the remediation strategies began in July of 2015. The general contractor on the project was Wiregrass Construction Company Inc. Project management was carried out by AECOM. This section details the construction process and the challenges that developed throughout the project. The construction of the test sections and final wearing course was completed in August of 2016.

5.1 Sand Blanket – Test Section 1

A sand blanket was used in Test Section 1. The general idea was to create a drainage layer beneath the pavement surface to keep the subgrade a more constant moisture content. The sand blanket also acts as a flexible barrier between the expansive clays and the pavement. This helps to minimize differential heave across the pavement which leads to cracking. A cross section of the sand blanket is shown in Figure 36. It is important to note that unlike the other Test Sections, the construction of the sand blanket required that the existing pavement be removed and replaced. Upon removal of the existing pavement, a geotextile was placed on the subgrade followed by 6 inches of sand. A 6 inch diameter perforated drainage pipe was placed on either side of the sand blanket layer underneath the shoulders as shown in Figure 36. This pipe was used to collect the water from the sand blanket and route it to the ditch line.

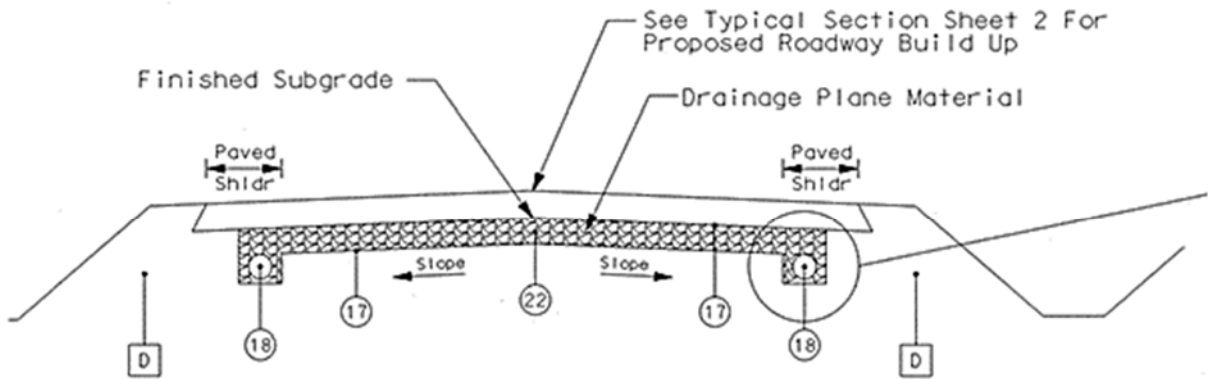


Figure 36: Sand Blanket Cross Section (ALDOT 2015)

Construction of the sand blanket began on 7/10/15 and the base course of asphalt was placed on 10/29/15. Since it was required that the road remain open to traffic, temporary traffic signals were installed and one lane was constructed at a time. A trench was first dug to install the drain along the edge of pavement. The trench was lined with a geotextile fabric and backfilled with the sand blanket material as shown in Figure 37. The installation of the 6 inch sand blanket layer is shown in Figure 38. Figure 39 shows the tack coat being applied to the granular base in the north bound lane. During the construction, water could be seen flowing out of the drain from the sand blanket following a rain as shown in Figure 40. Upon completion of both lanes, a final wearing course was paved as shown in Figure 41.

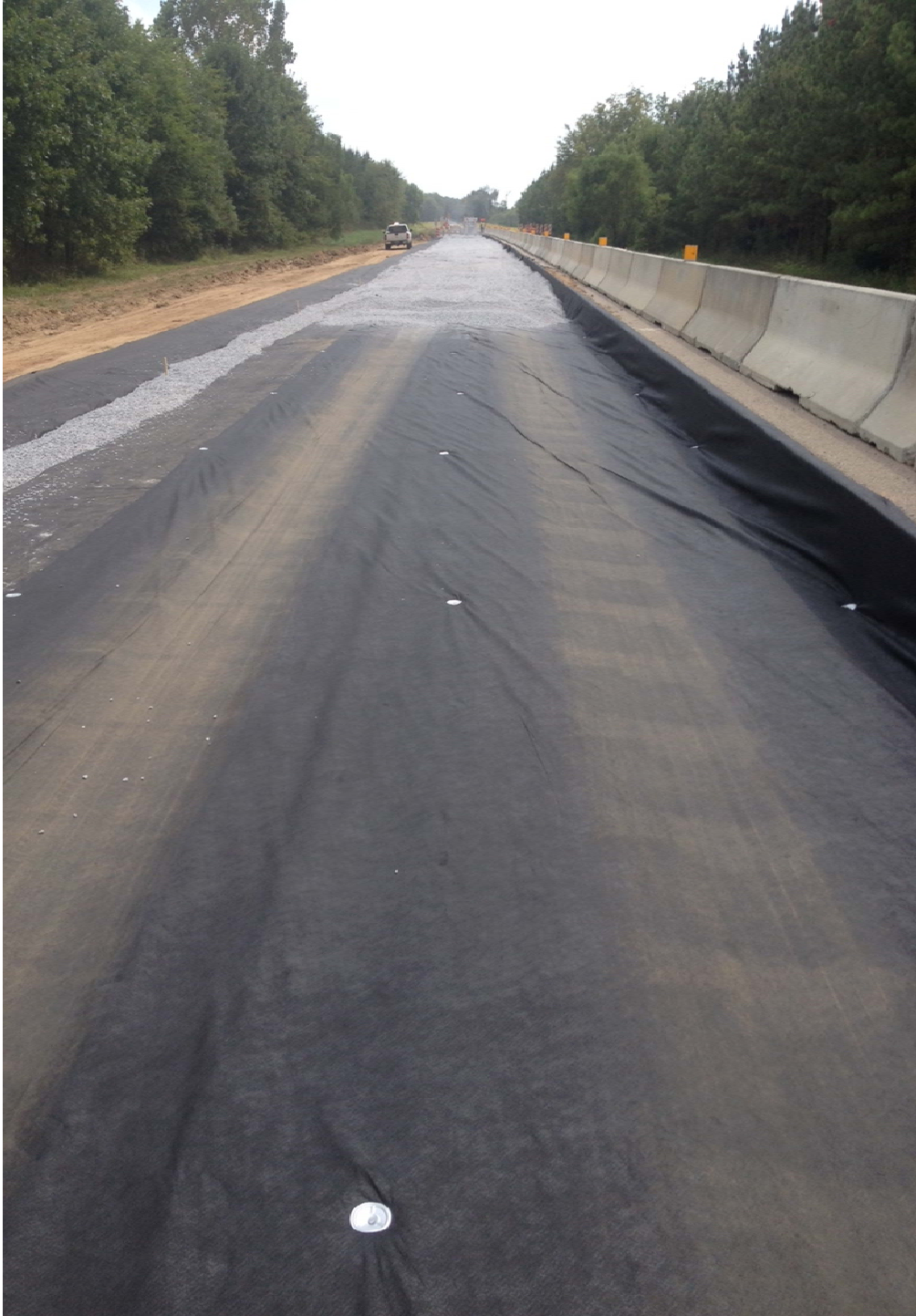


Figure 37: North Bound Lane- Edge Drain and Sand Blanket



Figure 38: North Bound Lane – Application of Sand Blanket



Figure 39: North Bound Lane – Placement of Tack Coat on Granular Base



Figure 40: Rainwater flowing out of Sand Blanket



Figure 41: Completed Sand Blanket Test Section

5.2 Vertical Barriers – Test Section 2

Vertical moisture barriers consist of sheets of impervious geosynthetic material which are placed in ditches along the edge of a pavement. The goal of the vertical barrier is to limit the lateral flow of water in and out of the subgrade. Nelson and Miller (1992) note that it is generally not practical to install vertical moisture barriers through the entire depth of the active zone, but rather they recommend a depth of one-half to two-thirds the active zone. Figure 42 shows the cross section of the vertical barrier test section. The plans required that a 12” wide channel be dug along the pavement and back filled with a filter sand after placement of the geosynthetic. For completeness, the technical data sheet for the geosynthetic used at AL-5 is shown in Appendix B.

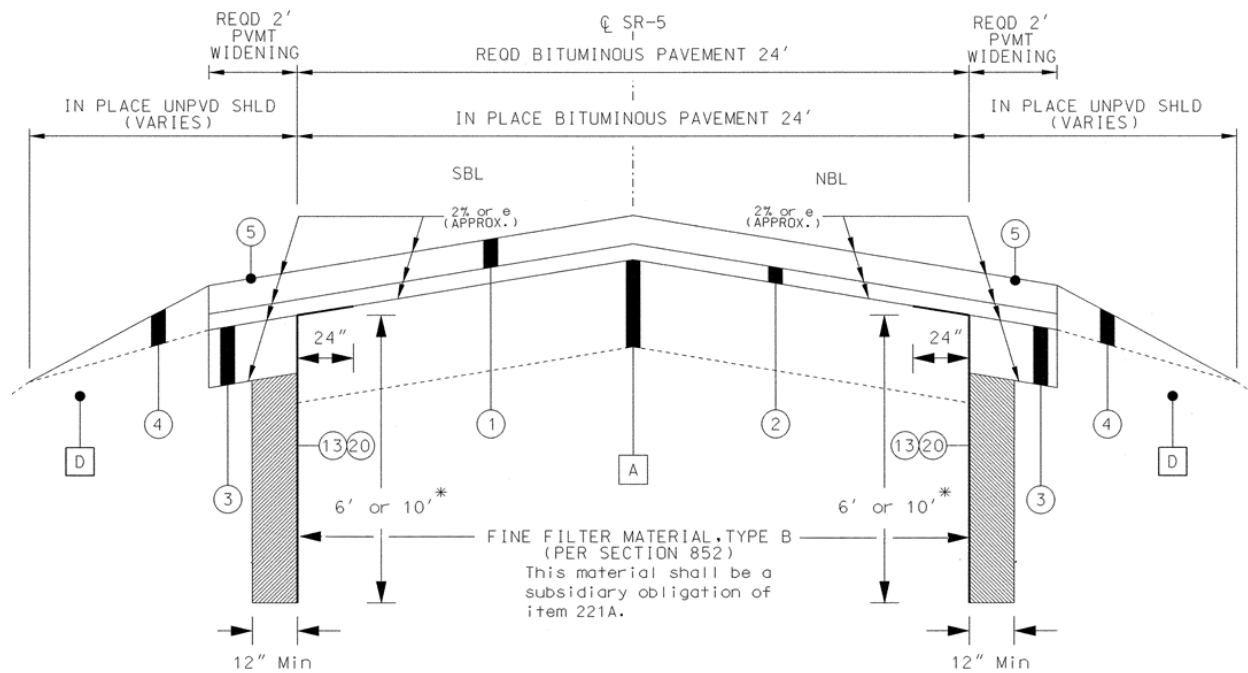


Figure 42: Vertical Barriers Cross Section (ALDOT 2015)

Construction of the vertical barriers began on 9/23/15 and was completed on 1/28/16. It was originally intended that 10 feet deep vertical barriers be installed along the southern half of the test section and 6 feet deep barriers on the northern half. Difficulties with opening a 10 feet

deep trench without the sidewalls collapsing resulted in the abandonment of the 10 feet deep vertical barriers. Instead, 6 feet deep barriers were placed along the entirety of the Test Section. An example of a collapse while attempting to dig the 10 feet trench is shown in Figure 43. An image of the open trench is shown in Figure 44. After excavation, the trench was lined and backfilled with a fine sand as shown in Figure 45 and Figure 46. A layer of asphalt was then paved directly over the sand as shown in Figure 47 and Figure 48.



Figure 43: Trench Cave-in – Vertical Barriers



Figure 44: Vertical Barrier Trench



Figure 45: Backfilling of Vertical Barriers



Figure 46: Sand Backfill of Vertical Barriers



Figure 47: Paving over Vertical Barrier Trench



Figure 48: Leveling Asphalt over Vertical Barriers

As shown in Figure 49, the geosynthetic was folded over on the top creating ripples and folds in the material. The leveling course of asphalt was then placed on top of this geosynthetic.



Figure 49: Leveling of Pavement over Vertical Barriers

After the base course of asphalt was placed on top of the vertical barrier test section, cracking, rutting, and spalling was observed directly above the vertical barriers. In some places, the geosynthetic protruded through the base course. Pictures of this can be seen in Figure 50 through Figure 53. Poor construction practice and compaction efforts were most likely to blame.



Figure 50: Cracks along shoulder above Vertical Barriers



Figure 51: Rutting Observed above Vertical Barriers



Figure 52: Asphalt Spalling above Vertical Barriers



Figure 53: Geosynthetic protruding through base course of asphalt

5.3 Lime Columns – Test Section 3

Lime columns were installed in Test Section 3 to chemically stabilize the subgrade. The lime was packed into 8 inch diameter drill-holes in the pavement surface as well as the shoulder. The hole was drilled to a depth of one foot below the adjacent ditch line. The cross section and layout of the lime columns is shown in Figure 54 and Figure 55, respectively.

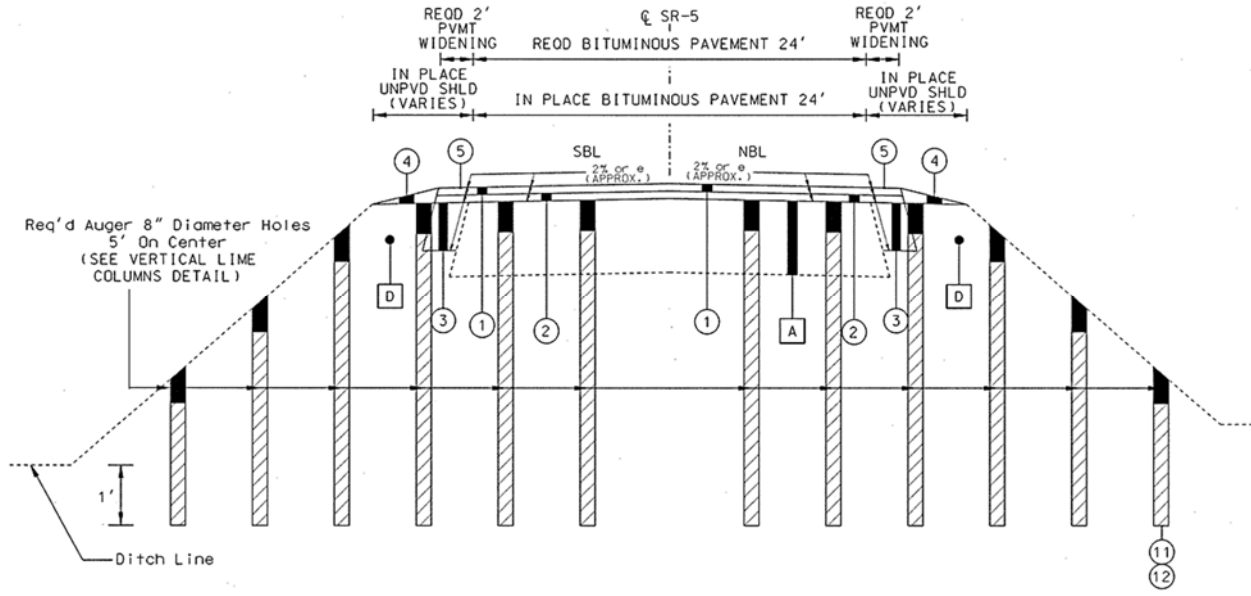


Figure 54: Lime Columns Cross Section (ALDOT 2015)

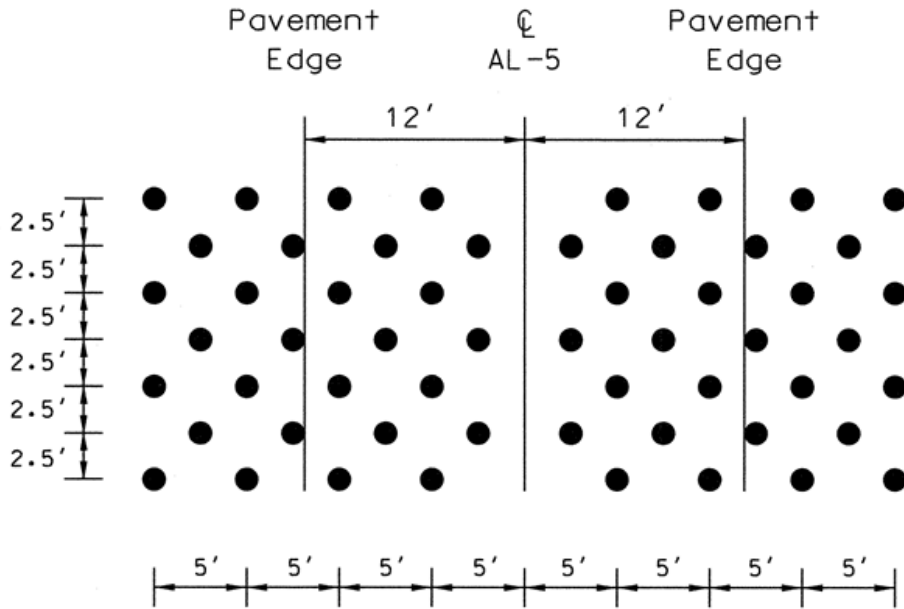


Figure 55: Lime Columns Plan View Detail (ALDOT 2015)

Construction of the lime column test section began 11/4/15 and was completed on 2/4/16. The installation of the lime columns turned out to be very quick and efficient due to the ability to mount an auger to a small track hoe as shown in Figure 56 and Figure 57. The lime columns were drilled and then dry packed with lime as shown in Figure 58. Each hole was then patched

with asphalt by pouring in hot asphalt from a bucket on a skid steer as shown in Figure 59. The asphalt was compacted and rolled as shown in Figure 60 and Figure 61.



Figure 56: Drill Used for Lime Column Installation



Figure 57: Auger used for Lime Column Installation



Figure 58: Lime Column before Asphalt Patching



Figure 59: Pouring Asphalt into Lime Column Holes



Figure 60: Compacting asphalt in Lime Column



Figure 61: Lime Columns patched with Asphalt

Depressions in the base course of the asphalt at the location of the lime columns as shown in Figure 62 were discovered. In one extreme case, a void reached the asphalt surface creating a hole in the pavement roughly a foot deep as shown in Figure 63. These depressions are most likely due to poor compaction of the asphalt cap at the top of the hole.



Figure 62: Lime Columns Reflected Through Base Course and Holding Water



Figure 63: Hole in Asphalt above Lime Column

5.4 Paved Shoulders – Test Section 4

During the initial field investigation, it was discovered that longitudinal cracks along the outside wheel path were common as shown in Chapter 3. It was proposed to use paved shoulders at Test Section 4 to remediate longitudinal cracks. In theory, by paving the shoulder the longitudinal crack would develop in the shoulder rather than in the outside wheel path. Six feet wide shoulders were paved on both sides of the road per the cross section shown in Figure 64. Construction of the paved shoulders began on 8/8/15 and was completed on 8/14/15. Two pictures taken following the paving of the paved shoulder is shown in Figure 65 and Figure 66.

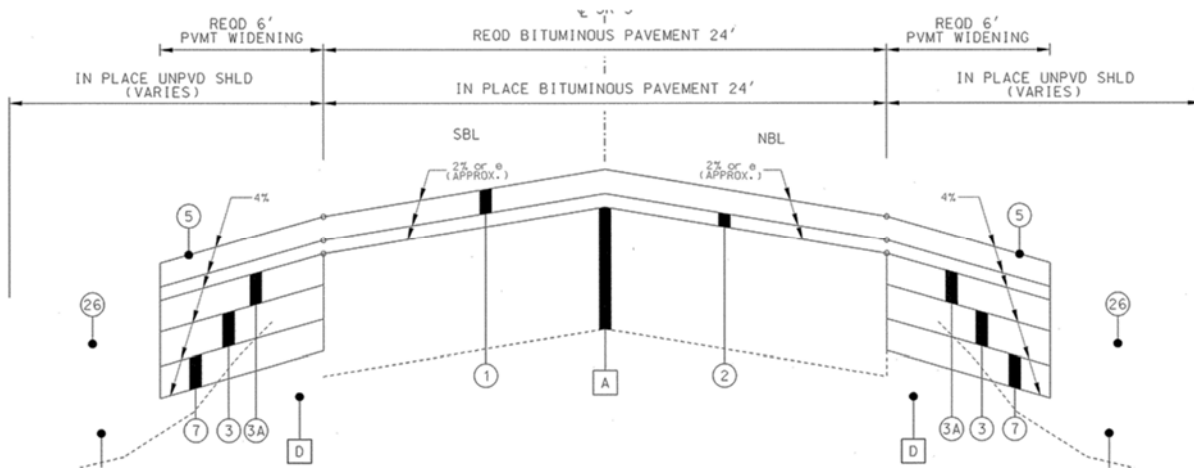


Figure 64: Paved Shoulder Cross Section (ALDOT 2015)



Figure 65: After paving of Paved Shoulders



Figure 66: Paved Shoulder prior to Leveling Course

5.5 Edge Drains – Test Section 5

Drains were installed along Test Section 5 at the edge of the pavement in an attempt to stabilize the moisture content of the subgrade. Figure 67 shows the edge drain cross-section used at AL-5. As shown, 4 inch diameter corrugated pipe was installed along the edge of the pavement in a 1 foot wide by 1 foot deep trench backfilled with #57 stone. A photo of the edge drains after being backfilled with #57 stone is shown in Figure 68. Construction of the edge drains began on 8/18/15 and was completed on 8/20/15.

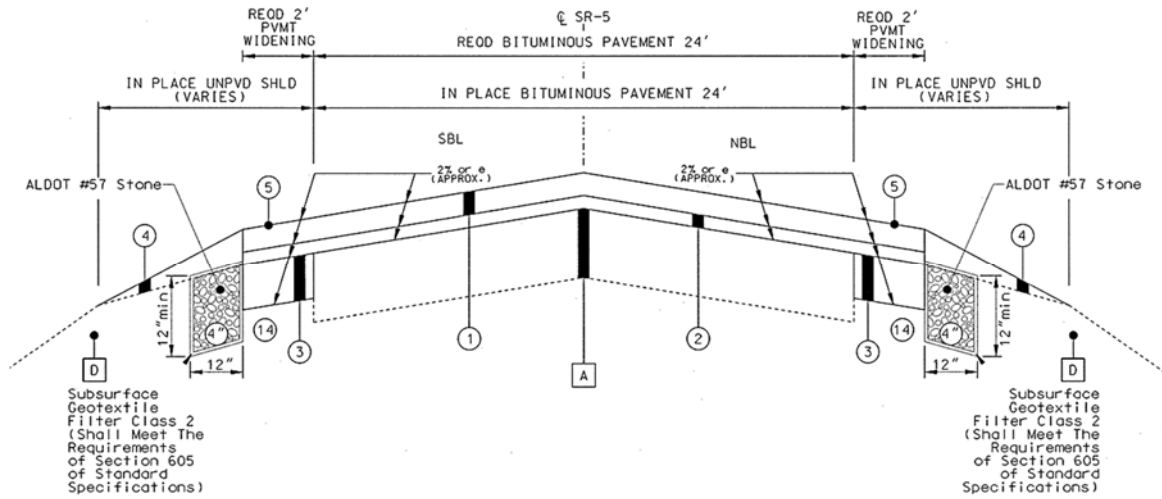


Figure 67: Edge Drain Cross-Section at AL-5 (ALDOT Plans)



Figure 68: Edge Drains after Backfilling with Stone

5.6 Deep Mixed Columns – Test Section 7

It was proposed that deep soil mixing be used in Test Section 7. This process involved mixing Portland cement with the existing soil in an effort to stabilize the expansive clay soils. The cross section and layout of the columns is shown in Figure 69 and Figure 70. As noted in the plans, the required diameter of the columns was 2 feet. The southern half of Test Section 7 was planned to have 6 feet deep columns and the northern half to have 15 feet deep columns.

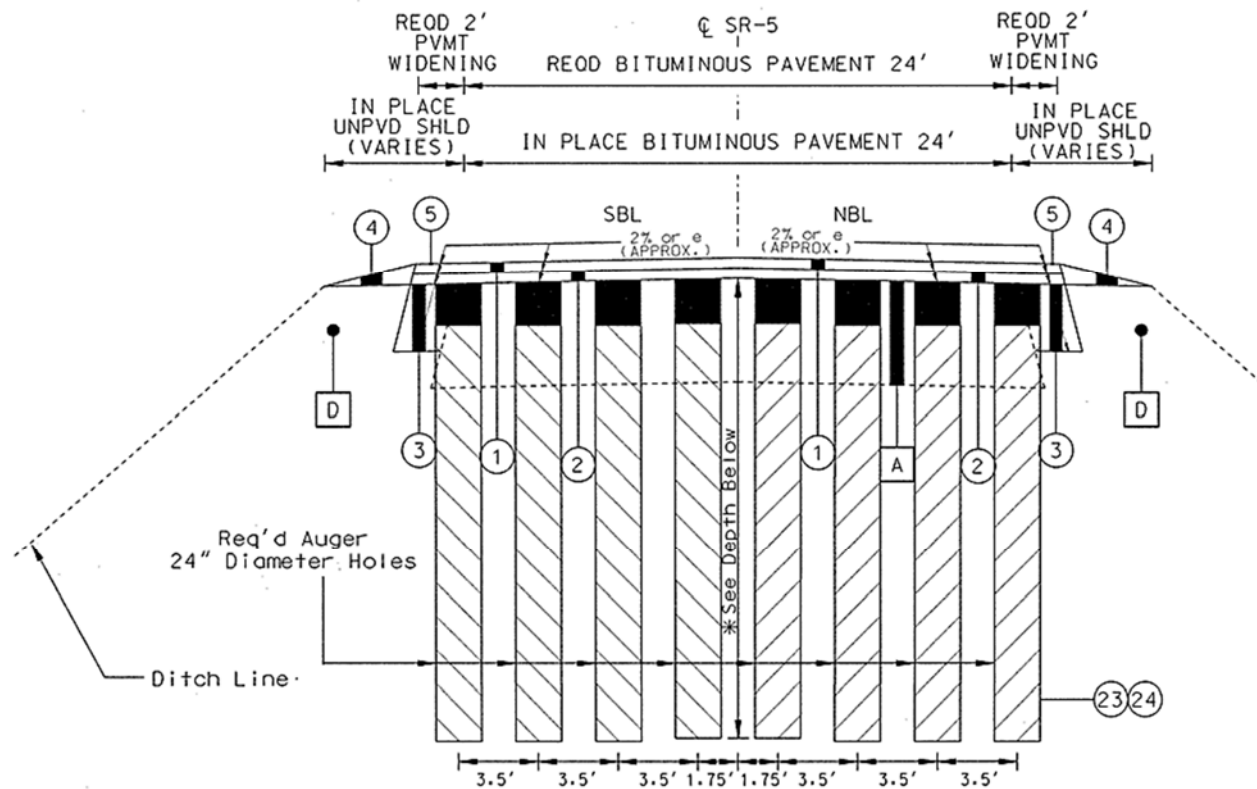


Figure 69: Deep Mixed Columns Cross Section (ALDOT 2015)

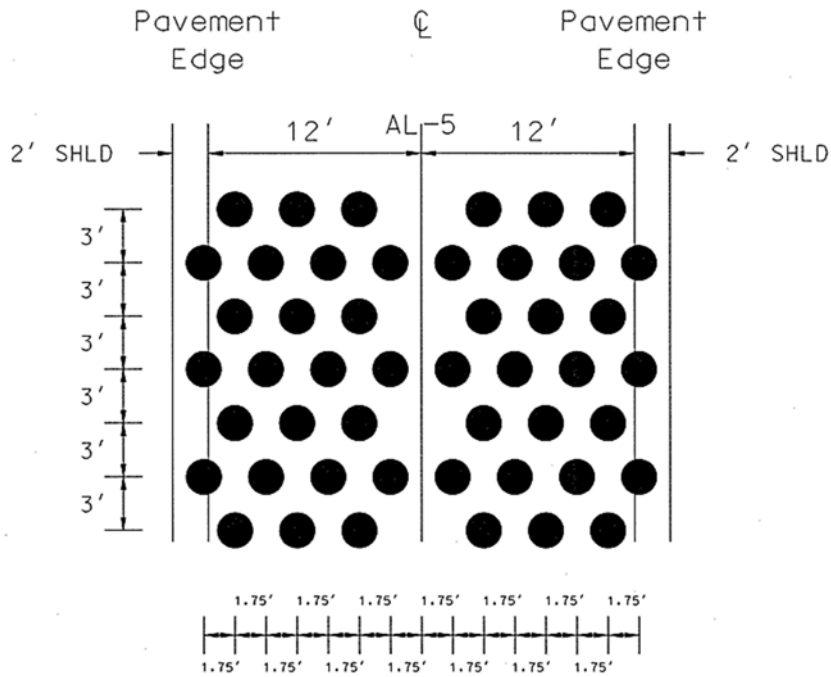


Figure 70: Deep Mixed Columns Plan View (ALDOT 2015)

A field validation program was completed on August 28, 2015. An image of the drill rig and batch plant used is shown in Figure 71 and Figure 72. During the installation of test columns, a variety of challenges and problems were discovered which ultimately led to the cancellation of the deep mixed column Test Section. For completeness, these challenges will be described in detail. First, due to the sheer size of the mix plant and drill rig, a substantial work platform had to be constructed adjacent to the road. As production of the deep columns continued, the platform would have to be moved and reconstructed causing extensive delays in the construction sequence.



Figure 71: Deep Mix Column Drill Rig



Figure 72: Deep Mix Column Batch Plant

In addition to this, the original intent was for the columns to be directly drilled through the pavement surface. However, the drill bit used, shown in Figure 73, was not capable of coring through the asphalt pavement. Therefore, a rectangular section of pavement was cut and the asphalt was removed so that the test columns could be installed. Due to the inability of the drill bit to penetrate the asphalt, the entirety of the asphalt pavement would have to be removed and replaced in sections as columns were installed. This was determined to be highly impractical and would cause delays and increase costs.



Figure 73: Drill Bit used for Deep Mix Column Installation

During the installation of the test columns, different cement dosage and slurry ratios were used. It was found that the method could not properly mix the cement slurry into the highly plastic clays at AL-5. As the drill was raised out of the hole a column of soil was extracted as well as shown in Figure 74. After breaking up this column of soil, it was discovered that the cement was not mixing into the soil. This can be seen in Figure 75. In this photo the gray color is the cement slurry mixture and the tan/brown is the in-situ soil. It was concluded by the contractor that the drill bit they were using was not appropriate for the type of soil at AL-5. For these reasons, deep mix columns were abandoned and Test Section 7 was used as another control section.



Figure 74: Extracted Column of Soil from Deep Mix Column



Figure 75: Clumps of soil showing lack of cement mixing

5.7 Control Sections

To evaluate the effectiveness of the various remediation strategies used at AL-5, control sections were included. In these sections, the only change to the existing road was widening the shoulder by 2 feet on either side. It should be noted that, a final leveling and wearing course of asphalt was paved over the entirety of the project including the control sections.

CHAPTER 6: SOIL MOISTURE GAUGE

In addition to the electronic moisture content sensors mentioned above, a nuclear moisture gauge was used to monitor the fluctuations in water contents at AL-5. Access holes were installed throughout the project at locations corresponding to the downhole sensors. By doing this, moisture fluctuations recorded by the nuclear gauge could be compared to the electronic sensors. Developing an effective access hole installation method will allow the moisture gauge to be used to determine the moisture fluctuations and depth of active zones under other roads experiencing distress caused by the shrink-swell nature of expansive soils.

6.1 Troxler 4301 Depth Moisture Gauge

A Troxler Model 4301 Depth Moisture Gauge was acquired by ALDOT for use at AL-5. The gauge is comprised of a shield, control unit, and a probe. This model uses a 1.5 inch diameter probe that contains a 10mCi americium-241:beryllium source. A helium-3 detector is also located in the probe. A picture of the gauge is shown in Figure 76. The gauge was supplied with a 10 foot cord which is used to lower the probe to desired depths for readings.

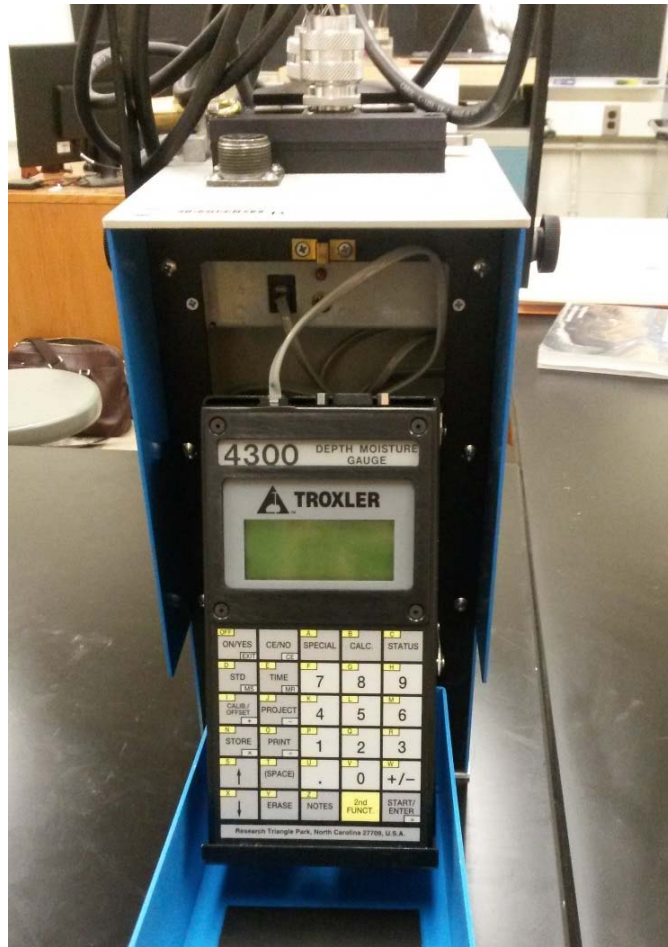


Figure 76: Troxler Model 4301 Depth Moisture Gauge

6.2 Access Holes

Fourteen access holes were installed throughout the project upon completion of the final paving surface in late August of 2016. Each access hole was placed approximately five feet away from the downhole sensors in both the road and shoulder. This provided a way to compare the moisture gauge readings to the electronic moisture sensors without interfering with any of the electronic sensors.

6.2.1 Access Tubes

According to factory recommendations, a 1.55 inch inside diameter aluminum pipe with an outside diameter of 1.63 inches should be used to provide best results (Troxler 2006).

However, due to high costs and limited availability of this specific pipe, a 1.5 inch nominal diameter PVC pipe was chosen for access tubes. The actual inside and outside diameters of the PVC pipe was 1.61 inches and 1.9 inches, respectively. This pipe is commonly stocked in 10 ft long sections. Also, based on research conducted by Stallings (2015), the active zone was not anticipated to be deeper than 10 feet. For these reasons, a 10 feet length was chosen for the access tubes.

6.2.2 Installation Process

Determining a method to install the PVC pipe in the ground proved to be a challenging task. Ideally, the outside of the PVC pipe should be in good contact with the soil to prevent skewed readings associated with air in the annular space between the pipe and soil. From the literature one recommendation was to push the access tube into the ground without first boring a hole. While this idea could potentially work for aluminum or steel pipes, the PVC pipe is not stiff enough to overcome buckling effects during pushing into the stiff clay.

Another option in the literature was to drill a bore hole the same diameter as the pipe and then push the pipe into place. This would provide good contact between the pipe and soil while allowing easy installation of the pipe. However, due to the small size of the PVC pipe, finding a set of augers with a 1.9 inch diameter was not possible. The smallest set of augers ALDOT was able to acquire were 2 inch in diameter with a 2-1/4 inch bit. A picture of the augers and bit is shown in Figure 77 for reference. This created a small annular void between the pipe and the soil which could affect the readings. As mentioned previously, Bishop and Porro (1997) were able to show that filling this annular void with sand made it possible to determine fluctuations in moisture content of the surrounding soil. Because of their findings, it was decided to fill the annular void with filter sand.



Figure 77: Auger and Bit used for Installation

Using the auger, a 10 feet 2 inch deep hole was drilled and the PVC pipe was lowered into place. An image of the drill rig is shown in Figure 78. To prevent water from infiltrating the access tube, the bottom of the PVC pipe was sealed with a rubber stopper and a PVC cap before lowering into place as shown in Figure 79. Under normal circumstances, it is recommended to leave the access tube sticking out above the ground two to three feet. However, for obvious reasons this was not possible due to traffic. Instead the top of the access tube was terminated inside a waterproof manhole flush with the road and ground surface as shown in Figure 80. The manhole cover was secured in place with a quick setting grout. An additional rubber stopper was used to seal the top of the tube within the manhole cover. A cross section of the completed access hole is shown in Figure 81.



Figure 78: ATV Drill Rig used for Hydroprobe Installation



Figure 79: Bottom End Cap of Access Tube



Figure 80: Waterproof Manhole Cover before grouted in place

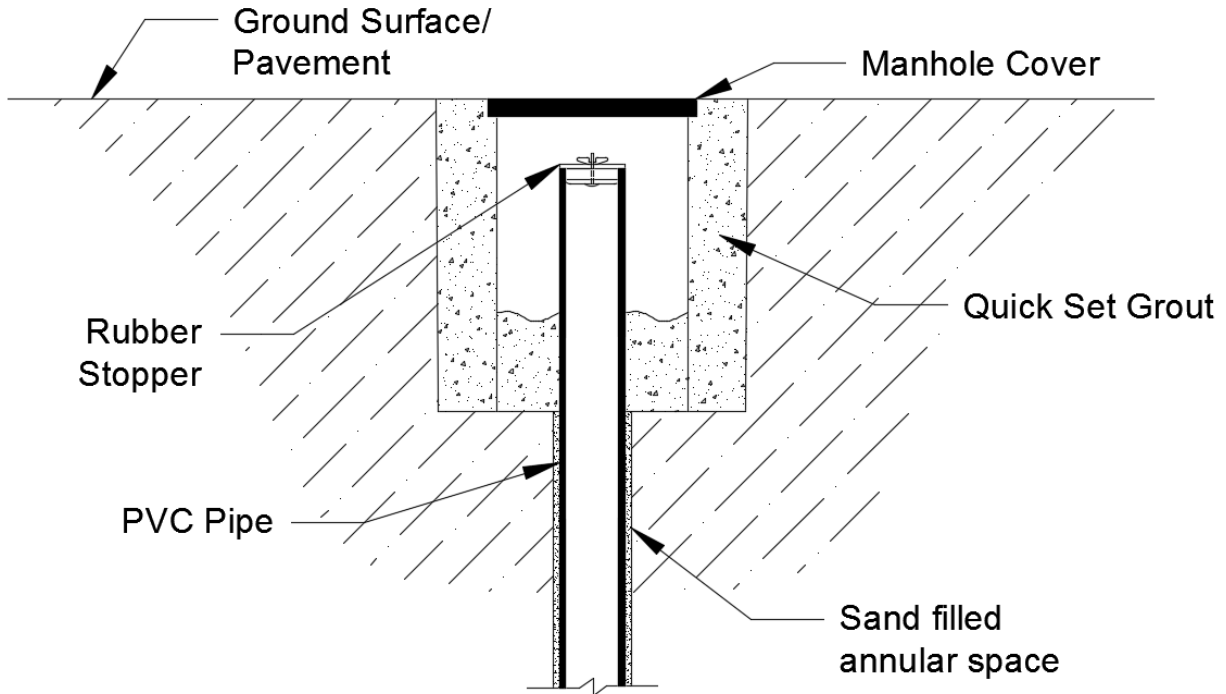


Figure 81: Cross section of completed access hole

6.3 Calibration

To determine both accurate and absolute moisture contents, the hydroprobe has to be calibrated for each different soil type. As recommended by Troxler (2006), a field calibration was attempted during installation of the access holes. The goal was to produce a calibration curve specific to soils encountered at AL-5. Upon completion of the drilling, the auger flight was extracted in one piece and laid on the ground. Soil samples were collected from the drill shavings in 2 foot increments and placed in sealed bags. Once the manhole cover was installed, readings were taken down the access hole with the hydroprobe at depths corresponding to the soil samples. Gravimetric moisture content tests were conducted in the lab on all soil samples and converted to volumetric moisture contents using Equation 5. A dry density (ρ_d) of 1.345 g/cm³ was used as determined by Stallings (2016).

$$\theta = w \left(\frac{\rho_d}{\rho_w} \right) \quad (5)$$

Where θ = volumetric moisture content expressed as a decimal

ρ_d = dry density (g/cm³)

ρ_w = density of water (g/cm³)

w = gravimetric moisture content expressed as a decimal

6.3.1 Effects of PVC

Due to the hydrogen and chlorine present in PVC pipe, the ability for the hydroprobe to determine fluctuations in the moisture content of the surrounding soil was in question.

According to Troxler (2006) PVC pipe can lower the gauge readings by at least fifteen percent.

To determine the effects of the PVC pipe on the gauge readings, Troxler (2006) recommended the following procedure. A section of PVC pipe was sealed at the bottom and positioned in the center of a 55-gallon barrel full of water. The probe was then lowered to the middle of the barrel and numerous readings were taken to obtain the average count. This average count was then compared to the corresponding point on the factory calibration curve. An image of this setup is shown in Figure 82.



Figure 82: 55-Gallon Barrel Water Test Setup

Prior to testing, the standard was determined to be 822 counts/min. In total 20 readings were taken with the probe in the center of the 55-gallon barrel full of water. The average count and count ratio was found to be 763 counts/min and .928, respectively. This count ratio was compared to standard #5 on the factory calibration sheet which is provide in Appendix C. The count ratio of standard #5 was 1.868. It was then determined that the PVC pipe resulted in a reduction of the counts by 50.3%. This was predicted due to the absorption of thermalized neutrons by the chlorine in the PVC pipe. The factory calibration points were reduced by 50.3% to create a new calibration based on the effects of the PVC pipe alone. The plot of the factory calibration as well as the calibration for the PVC pipe is shown in Figure 83. The equation for the linear trend line fit to the PVC calibration is shown in Equation 6.

$$\theta = 82.236(CR) - .9881 \quad (6)$$

Where θ = volumetric moisture content expressed as a decimal

CR = count ratio

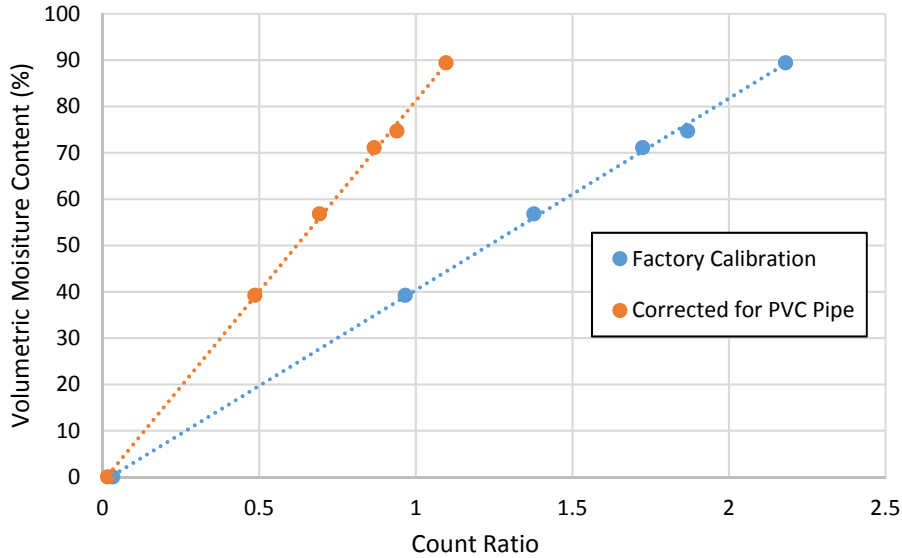


Figure 83: Calibration Correction for PVC

6.4 Monitoring Program

To ensure accurate readings, the standard count must be obtained daily. Typically, the standard count is taken with the moisture gauge sitting on top of the access tube extending out of the ground two to three feet. By doing this, the standard count obtained is consistent across all access holes. Due to the top of the access tube being below the ground surface this was not possible. The manufacture noted that it would be acceptable to place the hydroprobe on the ground to take readings as long as the standard count was taken on a surface that would not affect the standard count. To ensure consistency across the project, a stand was developed to allow the hydroprobe to sit roughly a foot above the ground surface or road. The stand was made of aluminum as it is a material which does not affect the hydroprobe reading. A photo of this stand in use is shown in Figure 84.



Figure 84: Hydroprobe Stand

To determine a moisture profile with depth, 6 readings were taken at 1.25 foot increments starting at a depth of 2.5 feet. By doing this, readings were taken at the approximate depths of the adjacent moisture sensors. To obtain more accurate results, two one minute readings were taken at each depth. The standard and count number were recorded for each reading. To determine relative moisture changes, a baseline reading was taken at each access tube and depth. Baseline readings were taken in the shoulder on March 7, 2017.

CHAPTER 7: PRELIMINARY RESULTS & DISCUSSION

7.1 Construction of Test Sections

After the construction was completed and before any rainfall events, another IRI survey was conducted to establish a baseline for future surveys to be measured against. This survey was completed on November 15, 2016 and the results are shown in Figure 85 and Figure 86. This survey shows that after construction was completed, the smoothness of the pavement was restored as the large majority of the road fell below the 170 inches/mile failure threshold. It should be noted that some spikes in the data exceed the failure threshold. This is most likely the result of poor construction practices.

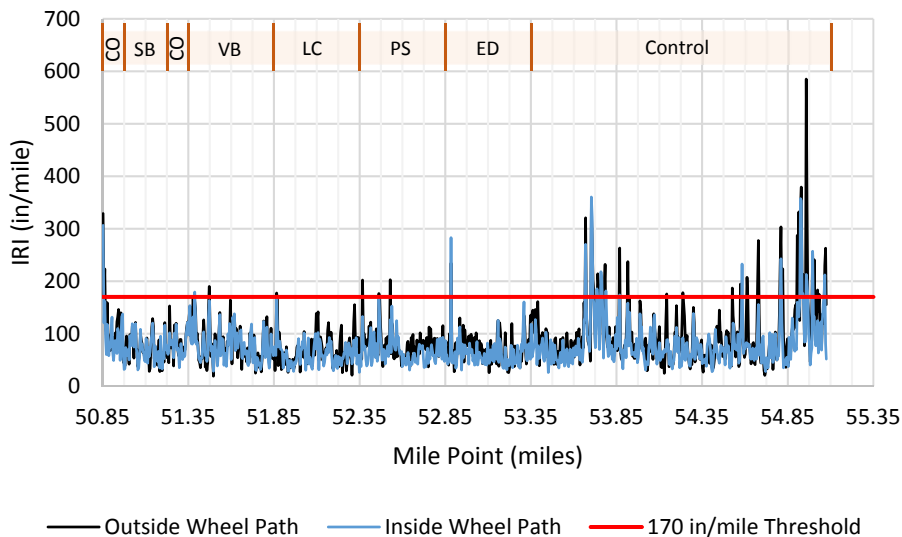


Figure 85: IRI Survey – North Bound Lane – 11/15/2016

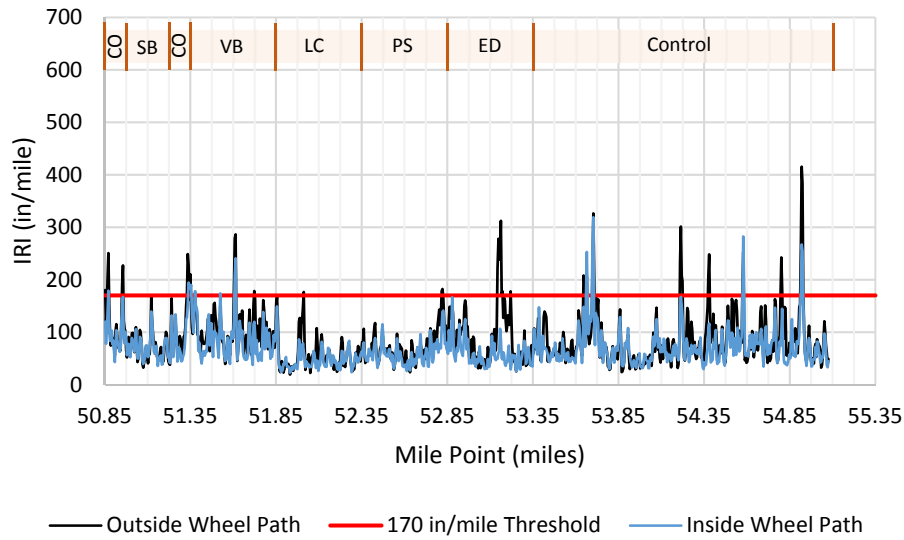


Figure 86: IRI Survey – South Bound Lane – 11/15/2016

7.2 Hydroprobe

7.2.1 Field Calibration Results

Unfortunately due to an electronic malfunction on the main board in the hydroprobe, the readings taken during installation of the access holes were most likely inaccurate. After comparing the hydroprobe readings to moisture contents from the drill shavings, this was proven to be the case. The plot of actual moisture content to counts from the hydroprobe readings, shown in Figure 87, was sporadic and a trend line could not be fit to the data with any confidence. Also shown in this plot is the factory calibration curve. Ideally, the field calibration curve would resemble the factory curve just shifted to the right due to the PVC pipe. Because the hydroprobe malfunction was unknown at the time of access hole installation, a field calibration curve was not able to be determined.

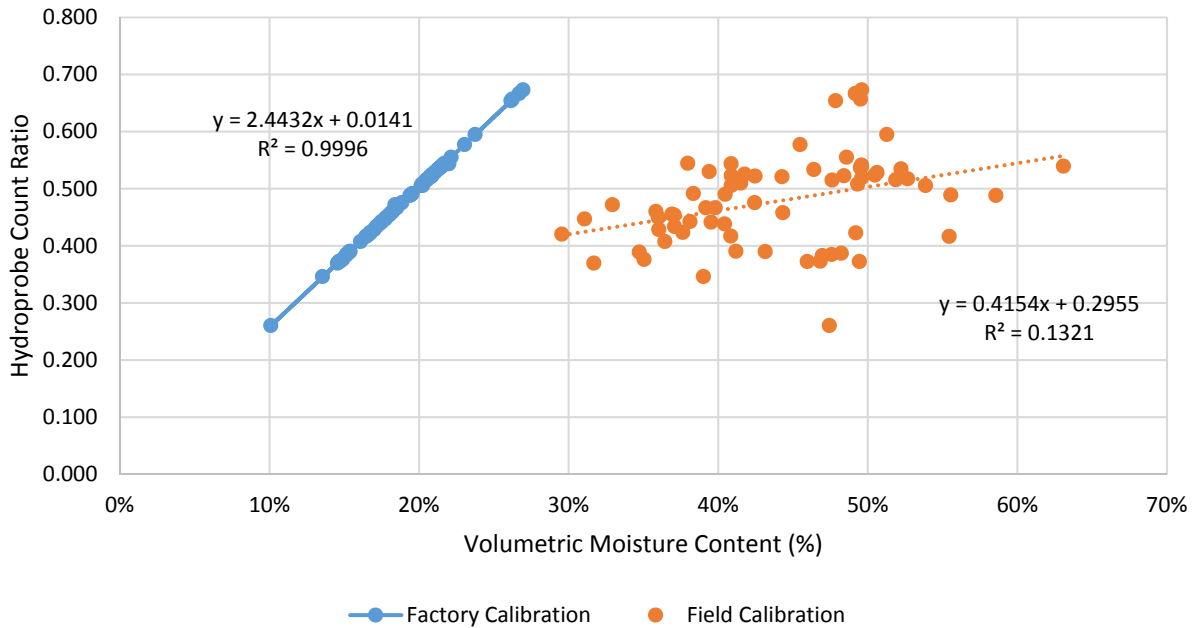


Figure 87: Field Calibration Results

Without a field calibration curve, absolute moisture contents cannot be measured in the fourteen access holes installed at AL-5. However, it is still possible to monitor relative fluctuations in moisture contents. This is just as valuable, because the depth of the active zone can still be determined. Also, seasonal variations in the moisture content will be recorded with both the hydroprobe and the electronic moisture content sensors. It will be possible to create a field calibration curve by correlating hydroprobe readings to absolute moisture contents from electronic moisture sensors. It should also be noted that due to variations in soil profiles along the site, each hole may require an individual calibration curve.

7.2.2 Baseline Readings

Once the electronic board on the hydroprobe was replaced by the manufacturer and determined to be working properly, baseline readings were taken at each access hole at AL-5. The readings were taken in the shoulder on March 6, 2017 and in the road on March 22, 2017. The data was corrected for the effects of the PVC pipe using Equation 6.

Table 5: Baseline Readings for Hydroprobe (Volumetric Moisture Content (%))

Depth	Control		Sand Blanket		Vertical Barriers		Lime Columns	
	Road	Shoulder	Road	Shoulder	Road	Shoulder	Road	Shoulder
2.5	45.65246	53.468	29.537	50.008	42.389	51.513	49.46805	56.778
3.75	57.95272	53.067	41.636	51.563	49.518	53.067	54.58898	54.922
5	60.21195	51.763	47.560	49.858	54.639	54.170	57.09923	52.616
6.25	54.38816	51.763	56.798	50.159	53.384	53.117	57.19964	56.226
7.5	51.92811	48.955	53.334	50.811	52.531	47.250	53.48446	55.524
8.75	55.24164	48.454	52.982	49.306	47.861	49.256	49.11662	54.872

Depth	Paved Shoulders		Edge Drains		Trees	
	Road	Shoulder	Road	Shoulder	Closest to Road	Closest to Tree
2.5	41.435	46.849	48.9158	49.858	47.250	52.515
3.75	56.196	50.911	53.63508	49.005	46.849	50.760
5	53.233	51.011	51.17503	49.407	44.843	49.256
6.25	53.133	49.507	52.22934	50.259	45.696	46.799
7.5	53.585	48.955	52.58077	48.153	44.843	47.601
8.75	51.526	47.651	54.03672	49.707	43.490	45.295

The baseline readings for the Paved Shoulder Test Section are shown in Table 5. For comparison, the readings from the moisture sensors are also shown in Table 6 and Figure 88.

Table 6: Baseline Hydroprobe Readings- Paved Shoulder

Depth	Hydroprobe		Moisture Sensor	
	Road	Shoulder	Road	Shoulder
2.5	41.43523	46.849	43.191	51.335
3.75	56.19554	50.911		
5	53.23344	51.011	50.780	50.028
6.25	53.13303	49.507		
7.5	53.58487	48.955	54.607	41.983
8.75	51.52646	47.651		
10			47.344	42.907

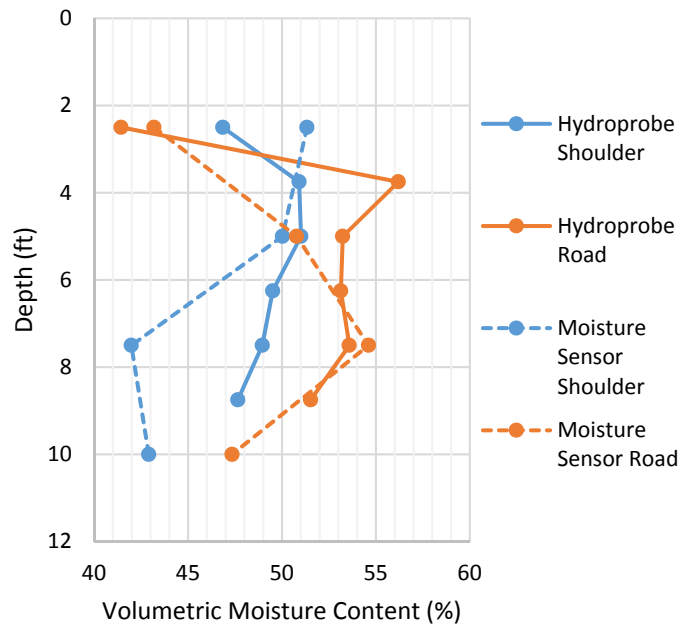


Figure 88: Baseline Hydroprobe Readings – Paved Shoulder

While the moisture profile is not an exact match of the moisture sensor, the readings are reasonably close using only the correction for the PVC pipe. This trend is seen across all the test sections. The variance can most likely be explained by not using a field calibration curve. With that said, relative moisture fluctuations can still be monitored. Also, due to the ability to take readings at more depths, the moisture profile from the hydroprobe has a better resolution than that of the moisture sensors. This will allow the depth of the active zone to be determined with more precision.

7.3 Preliminary Findings

7.3.1 IRI Survey

Another IRI survey was conducted on March 3, 2017 roughly 3.5 months after the baseline survey. The results of this survey are shown in Figure 89 and Figure 90. From this survey, it appears that not enough time has passed for any damage to start to accumulate.

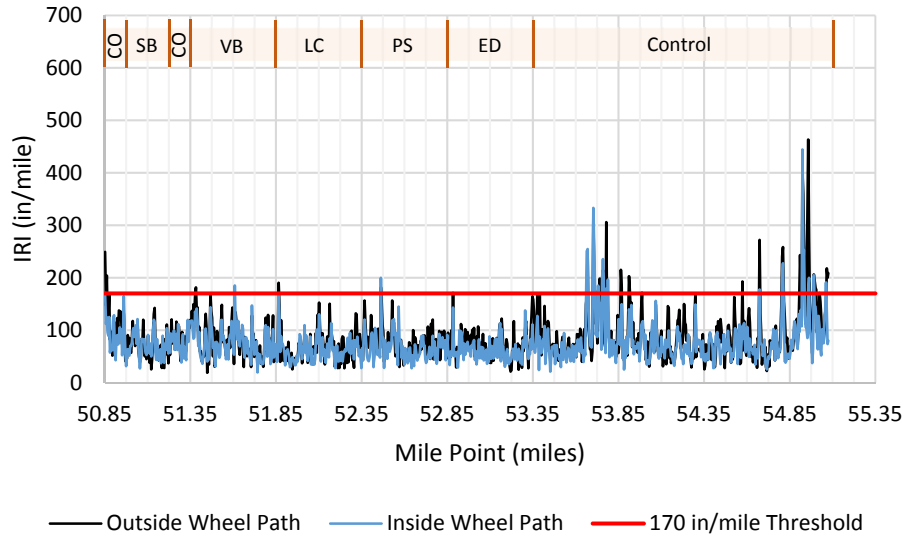


Figure 89: IRI Survey – North Bound Lane – 3/3/2017

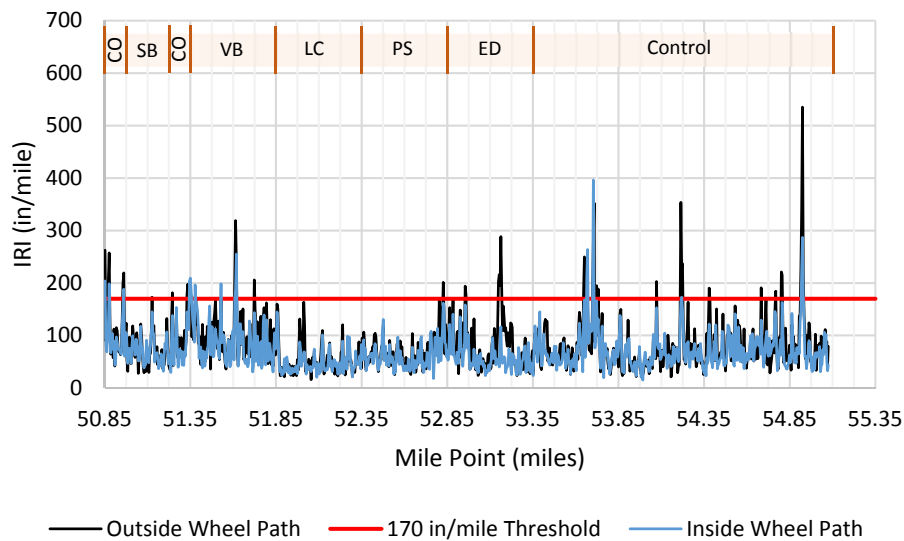


Figure 90: IRI Survey – South Bound Lane – 3/3/2017

With the exception to some spikes in the IRI in the south bound lane of the vertical barrier test section, the majority of the pavement where test sections were installed is still below the 170 in/mile threshold. In the control section at the northern end of the project, the IRI is already exceeding the failure threshold in many places. The spike in the IRI at mile point 53.725 can be attributed to the bridge at this location. Likewise, the large spike in IRI at mile point 54.9

can be attributed to the end of the project where the resurfacing of the pavement terminated. Finally, the large spike at 54.225 is possibly due to the presence of a large tree near the road at this location.

One trend that is shown in the results from this survey is that the IRI spikes above the threshold in the south bound lane of the vertical barrier section. These spikes are most likely associated with the large longitudinal crack that has developed due to the vertical barrier as shown in Figure 91. Another possible explanation is the presence of trees along the west side of the road also pictured in the in Figure 91.



Figure 91: Longitudinal Crack in Vertical Barrier Test Section

From a visual and smoothness standpoint, the entirety of the project did not appear to have been affected by the rainfall events. The road remains smooth with no signs of heaving due to the subgrade. With the exception of the vertical barriers test section, no cracking was observed throughout the project. To better visualize the progression of IRI values, the outside

wheel path for each lane from the November 16' and March 17' surveys were plotted together. These plots are shown in Figure 92 and Figure 93. The two surveys of the north bound lane show almost identical results. In the south bound lane, the survey conducted in March 17' shows that many of the spikes shown in the control section have gone away since the November 16' survey. However, the spikes near the bridge and end of project are still present.

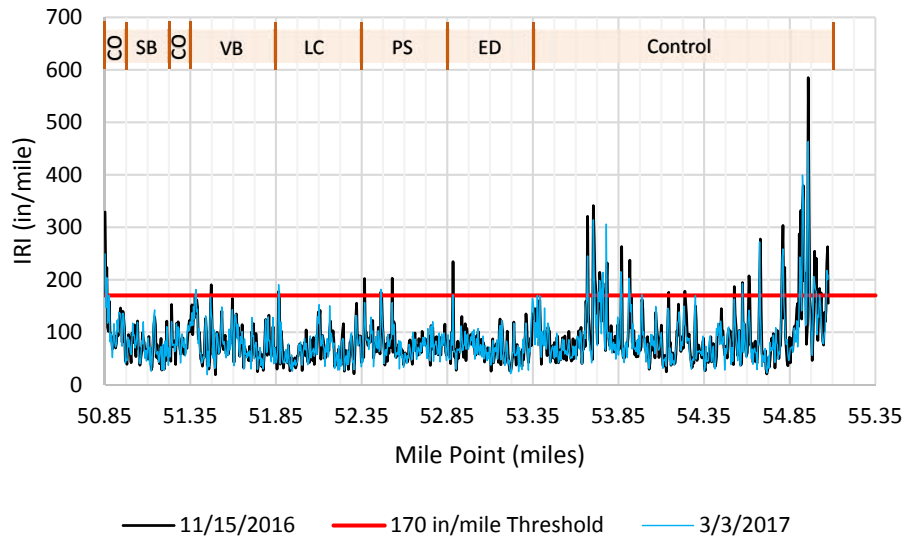


Figure 92: North Bound Lane-Outside Wheel Path

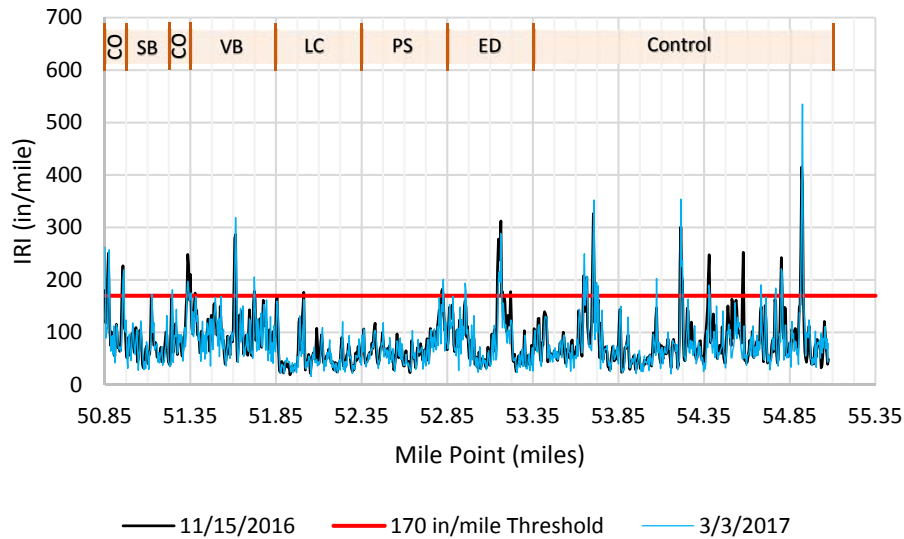


Figure 93: South Bound Lane – Outside Wheel Path

In addition, the average IRI value of both lanes in each test section were found for all four IRI surveys. The average IRI values are shown in chronological order for each test section in Figure 94. From this graph, it is easy to see that the IRI was greatly reduced post construction and since then has remained constant.

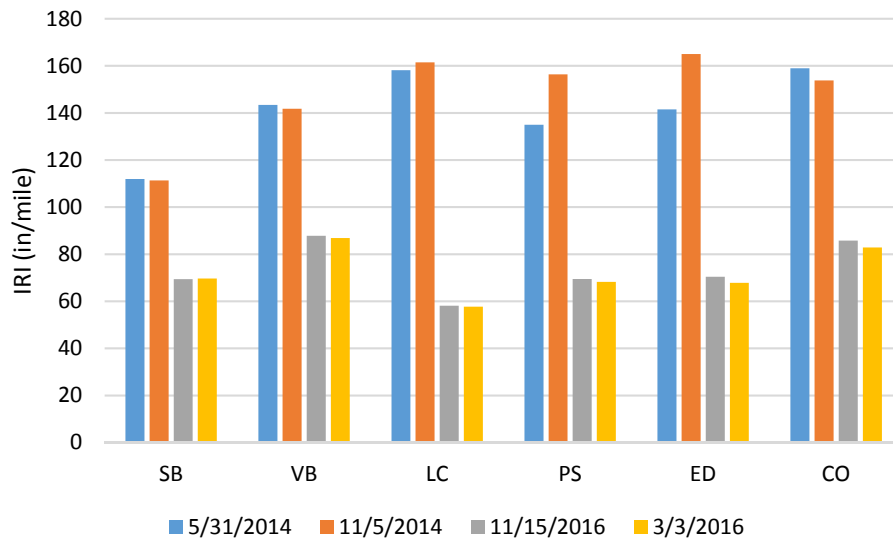


Figure 94: Average IRI Values over Time

7.3.2 Weather Data

To help understand trends in the sensor data, the temperature and rainfall data collected from the weather station are provided. Daily average, max, and minimum temperatures are shown in Figure 95. The daily rainfall accumulation is shown in Figure 96. It should be noted that the first substantial rainfall event was recorded on November 29, 2016. Since that day, over 28 inches of rain has fallen at AL-5.

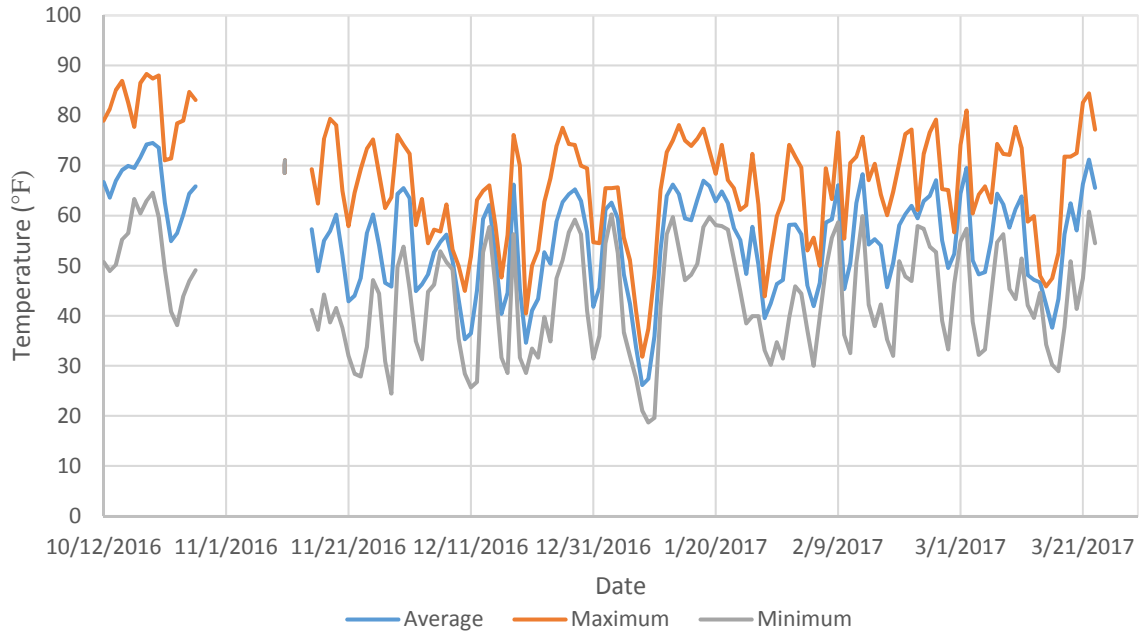


Figure 95: Temperature Data at AL-5

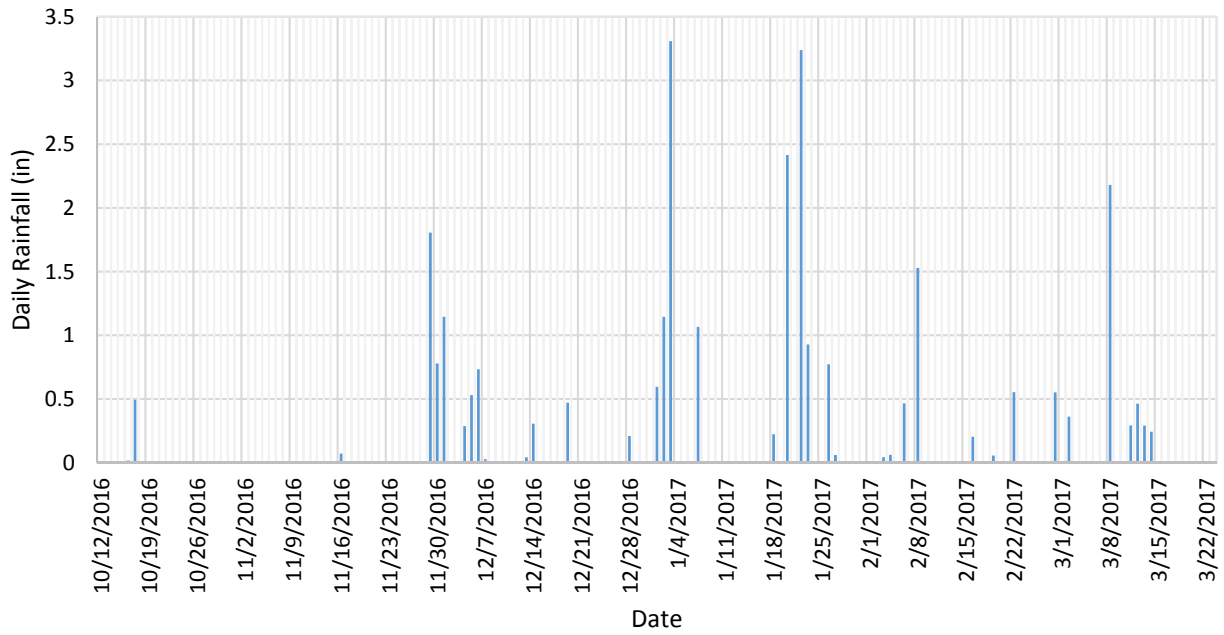


Figure 96: Rainfall Data at AL-5

7.3.3 Control

Based on visual inspection and IRI data, no distress has been observed in the control section at the time of publication. This confirms trends in the strain gauge data shown in Figure 97. To date, changes in strain can be attributed to temperature fluctuations as no appreciable plastic deformation has occurred. As more time passes and the subgrade goes through cycles of shrinking and swelling, it is expected that plastic deformations of the pavement will be reflected on strain gauge trends.

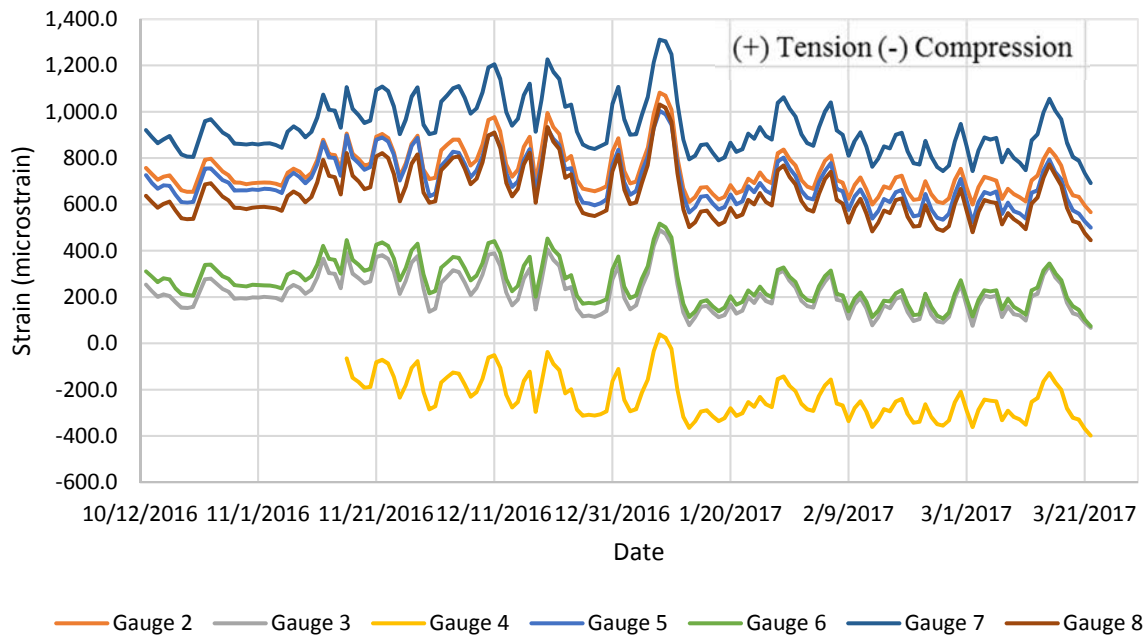


Figure 97: Strain with Time - Control

The moisture contents at the control section has responded as expected. The trends of the eight moisture sensors are shown in Figure 98. Up until the first substantial rain event, the moisture content recorded by all the sensors showed either decreasing or constant moisture contents. It should be noted that any noise in the first two weeks is most likely attributed to the sensor equalizing with the surrounding moisture content after the initial installation. Also, the

shoulder sensor at 7.5 feet was installed in a clump of disturbed soil rather than inserted into the side of the borehole. While the sensor is measuring a reasonable moisture content, it appears that it is not capable of measuring small fluctuations in moisture contents.

Following the first substantial rainfall event on November 29, 2016, the shoulder sensor at a depth of 2.5 feet immediately spiked. The road sensor at a depth of 2.5 feet also increased following the rainfall event but did so at a slower rate. This lag can be attributed to the rain having to permeate down through cracks in the pavement and migrate in from the shoulders. Although it appears that these shallow sensors have stabilized they continue to show small fluctuations with rainfall events.

The 5 feet deep shoulder sensor and the 7.5 feet deep road sensor both continued to show a drying trend even after the numerous rainfall events and does not show as much sensitivity to rainfall events. This could be due to tree roots absorbing the moisture and effectively stopping the downward moving wetting front.

Finally the 10 feet deep sensors in both the road and shoulder have remained stable since installation. In addition, these two sensors are reading much lower moisture contents. This is most likely due to the sensors being installed in the underlying chalk layer. It is likely that the chalk has remained saturated and the sensors are located beneath the water table.

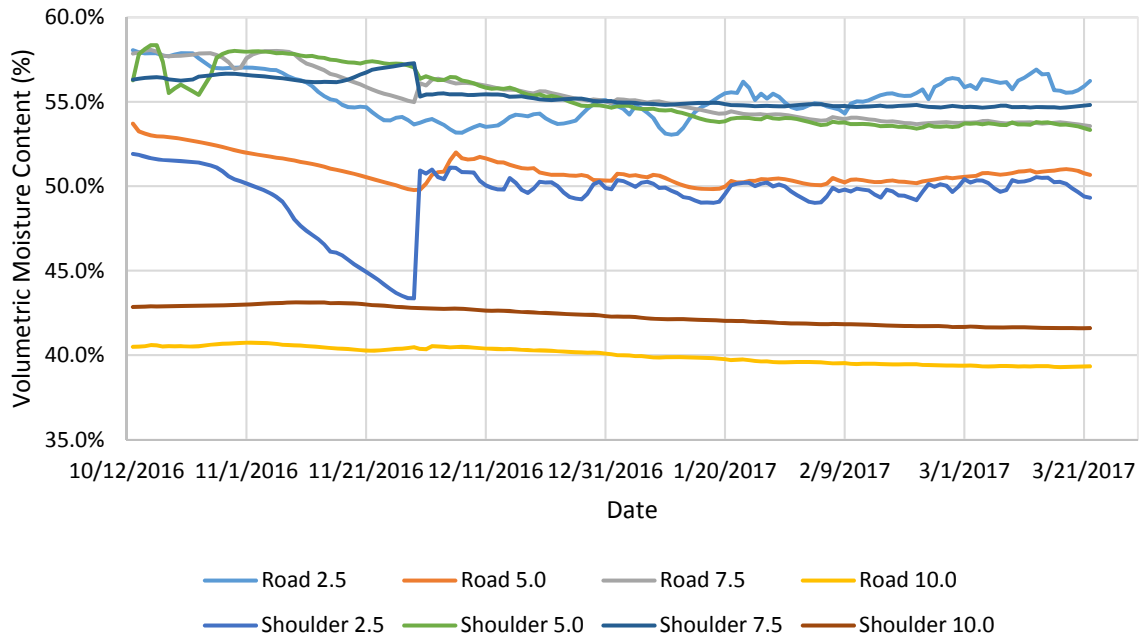
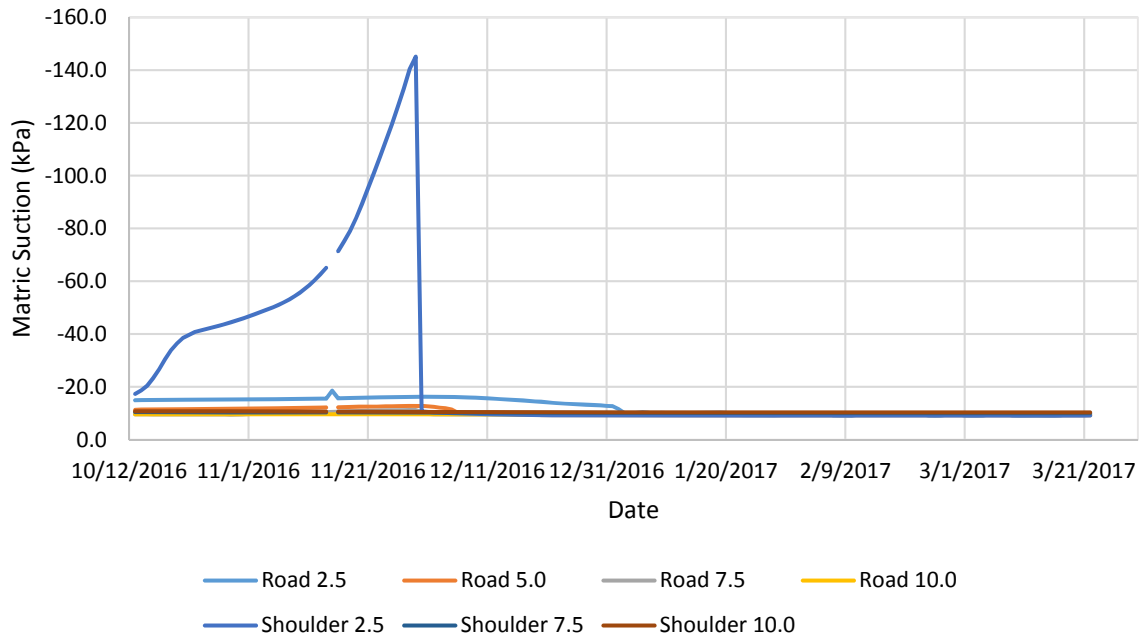


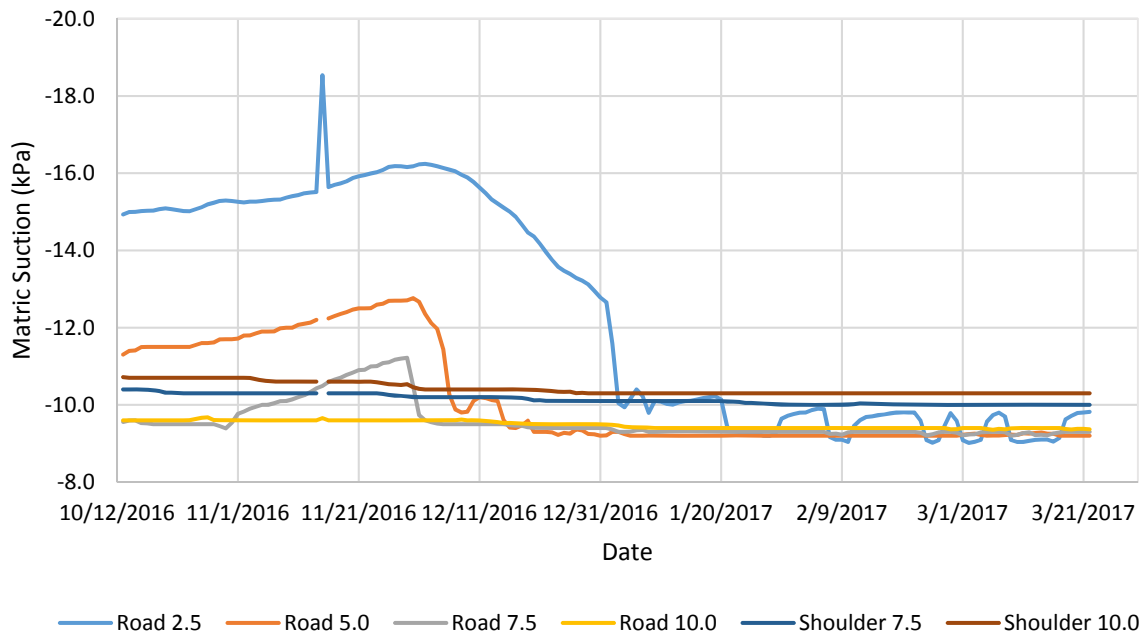
Figure 98: Moisture Content with Time – Control

The suction sensors in the control section have also responded as expected and the data with respect to time is shown in Figure 99. Up until the first substantial rainfall event, the shallow suction sensors recorded increasing levels of matric suction. A max suction of 145 kPa was recorded in the 2.5 feet deep shoulder sensor prior to the rainfall event. The shallow road sensor also shows the suction diminishing at a lower rate due to the lag in the moisture content as discussed above.

The deeper suction sensors showed little activity and remained near the sensor air entry value of approximately 9 kPa. This indicates that the soil is saturated and below the air entry value of the soil. After the rainfall events all the sensors have leveled off at the air entry value of the sensor.



(A)



(B)

Figure 99: Matric Suction with Time – Control (A&B shown with different scales for clarity)

Pore pressure data in the control section has also responded as expected and is shown in Figure 100. Pore pressures in all the sensors continued to decrease up until the first rainfall event. The sensors at a depth of approximately 6.5 feet reported a pore pressure of 0 or less prior to the rainfall, indicating that the water table fell below this depth. Following the rainfall, the pore pressures in all the sensors spiked and steady positive pore pressures have been reported ever since. Each small spike in the data is associated with a rainfall event. Since the first rainfall event, the pore pressures have remained roughly constant correlating to a water table depth of approximately 3 feet deep under the road and 2 feet deep under the shoulder.

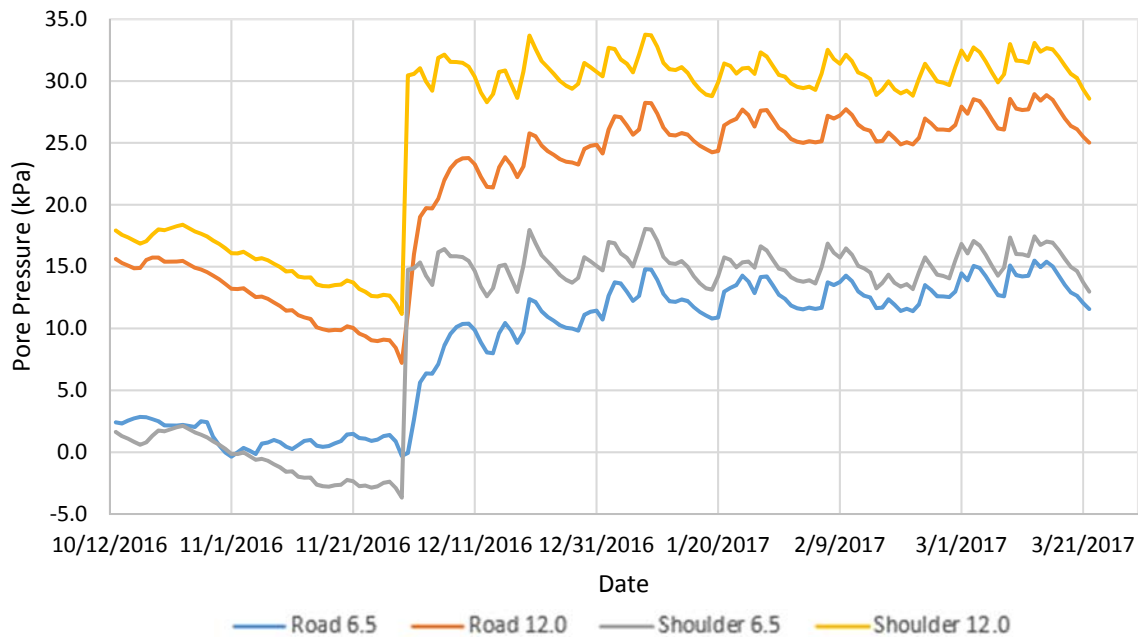


Figure 100: Pore Pressure with Time - Control

7.3.4 Sand Blanket – Test Section 1

Strain gauges in the sand blanket Test Section have also not shown any plastic deformations to date. The trends are shown in Figure 101.

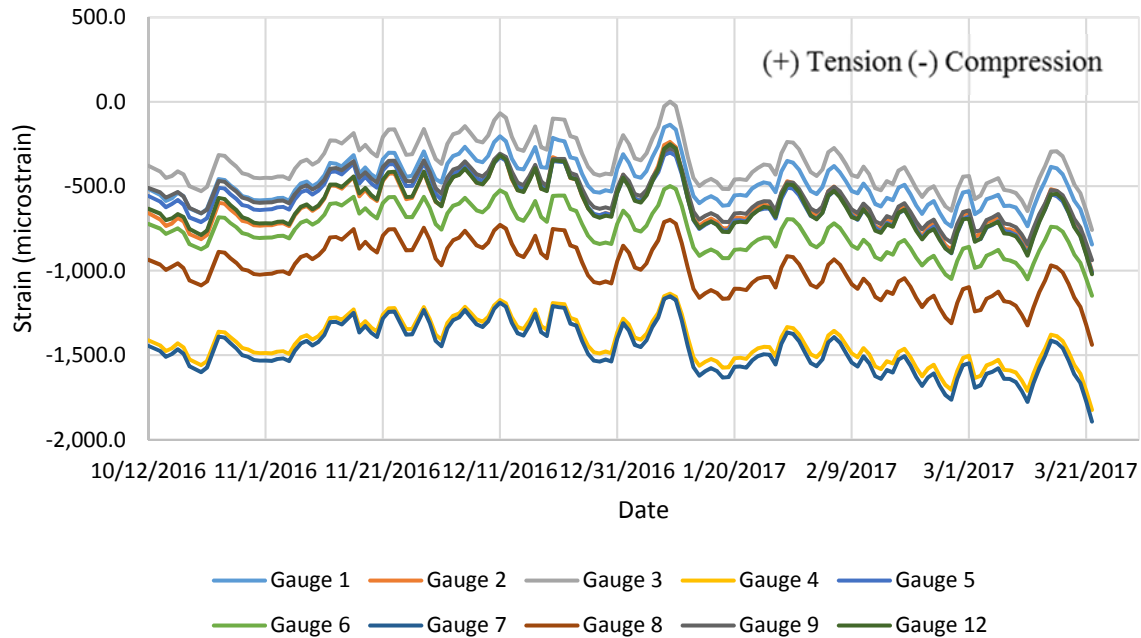


Figure 101: Strain with Time – Sand Blanket

Moisture content trends in the sand blanket Test Section are shown in Figure 102 and are similar to the control section with some exceptions. The 2.5 feet and 5 feet deep sensors beneath the road showed a drying trend even through the first rainfall events. This suggests the sand blanket is helping drain the water permeating through the pavement away from the subgrade. The 7.5 and 10 feet deep road sensors show a drying phase through the first rainfall event and then slowly increases and stabilizes to a moisture content similar to the shoulder. This suggests that the water is migrating from the shoulder into the subgrade beneath the road. The shoulder sensors in this section follow the same trends as the control section as expected. The same stable and low moisture content is recorded in the 10 feet deep shoulder sensor.

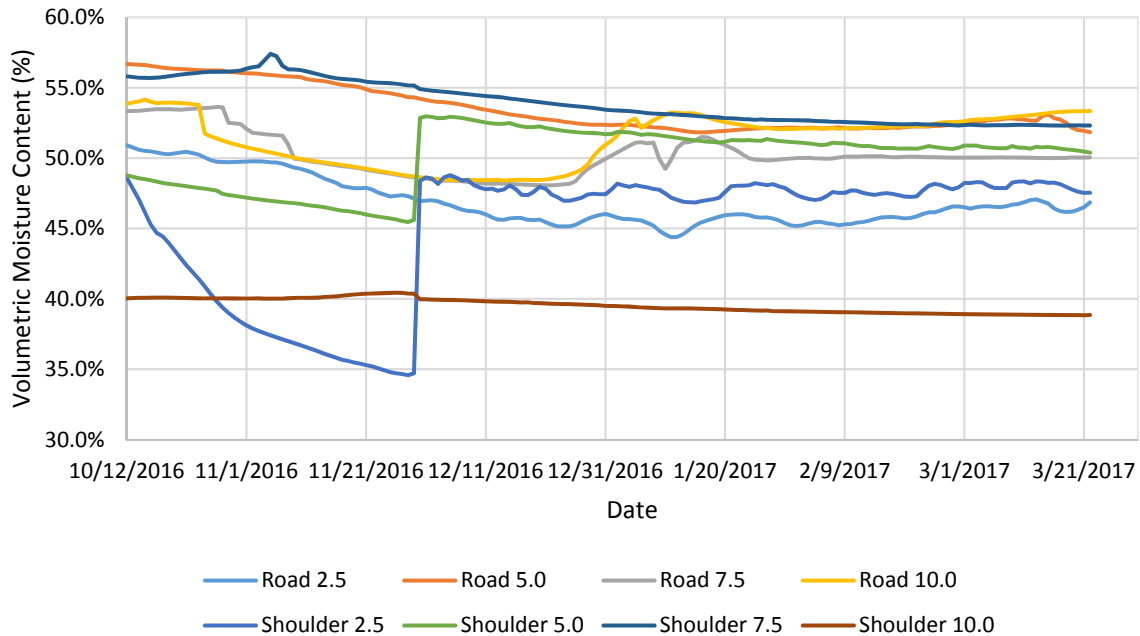


Figure 102: Moisture Content with Time – Sand Blanket

The trends of matric suction in the sand blanket Test Section are shown in Figure 103. Unlike the control section, a high suction value was not recorded in any of the sensors. However, it appears that the sensors are reading accurately as the suctions in each sensor respond appropriately to the changing moisture contents. Like the control section, all the sensors have approached the air entry value of the sensor indicating that the soil is saturated.

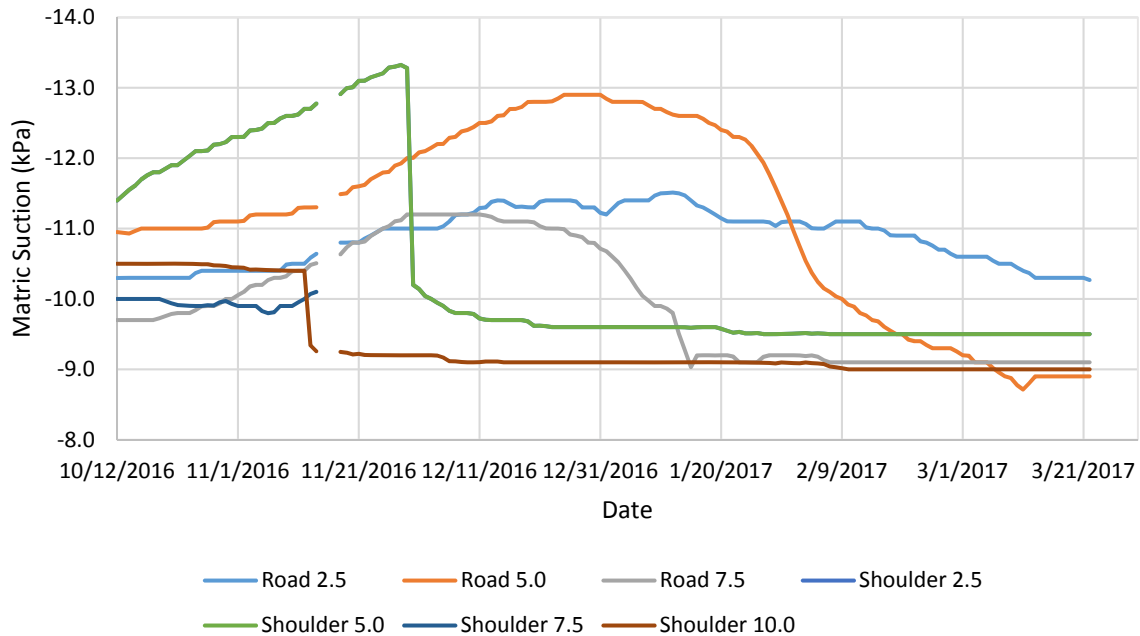


Figure 103: Matric Suction with Time – Sand Blanket

The pore pressures recorded at the sand blanket test section are shown in Figure 104. The trends are very similar to that of the control section. However, following first rainfall event the pore pressure transducers beneath the road did not sharply react to the rainfall like the shoulder sensors. This again suggests that the sand blanket is helping to drain the water infiltrating from the pavement away from the subgrade. At the time of publication, the water table is approximately 4.5 feet below the road and 2.5 feet below the shoulder.

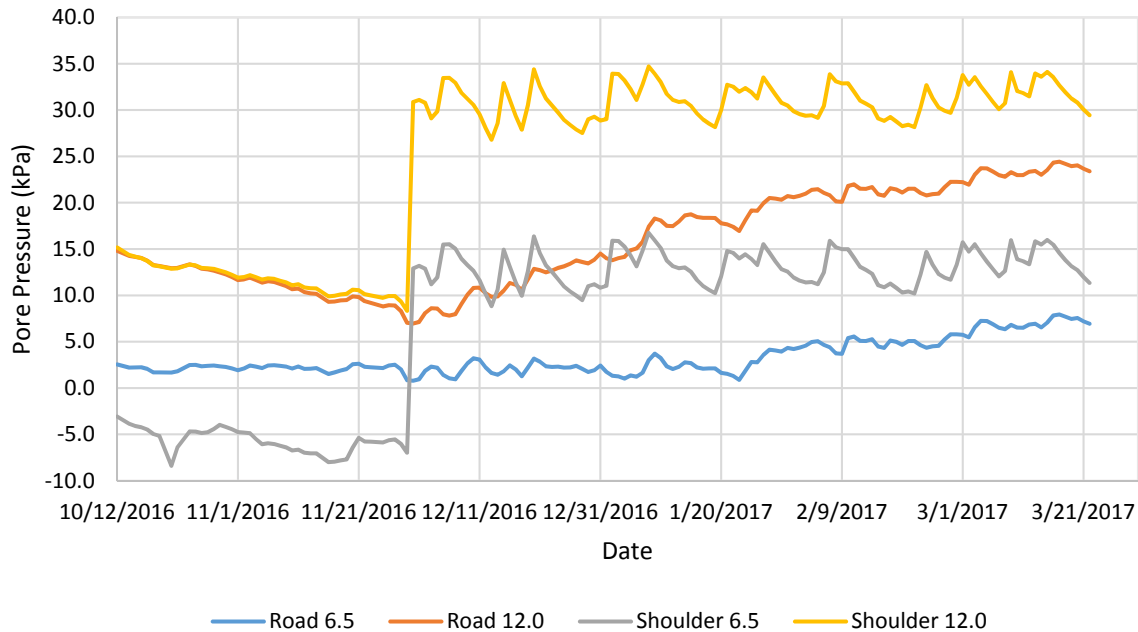


Figure 104: Pore Pressure with Time – Sand Blanket

7.3.5 Vertical Barriers – Test Section 2

The strain data from the vertical barrier Test section is shown in Figure 105. The strain gauges oriented in the longitudinal direction, gauges 2 and 8, show similar trends as the other sections. That is, no plastic deformation has occurred and the strain has remained fairly constant aside from daily temperature effects.

The gauges oriented in the transverse direction appear to have shown some plastic deformation as they have not stayed near their baseline reading. Initially, the strain gauges showed a positive trend as the gauges were placed in increasing tension. The strain continued to increase up until the first large rainfall event. Following that, the strain gauges have followed a negative training indicating that the strain gauges are being placed in compression. This could be the first indication of the shrink-swell nature of the subgrade. As the soil continued to dry and shrink, tension developed. As the moisture content rose following the rainfall events, the soil then began to swell placing the gauges in compression. However, more wetting and drying

cycles will need to be recorded to confirm this as the amount of strain recorded to date is very small.

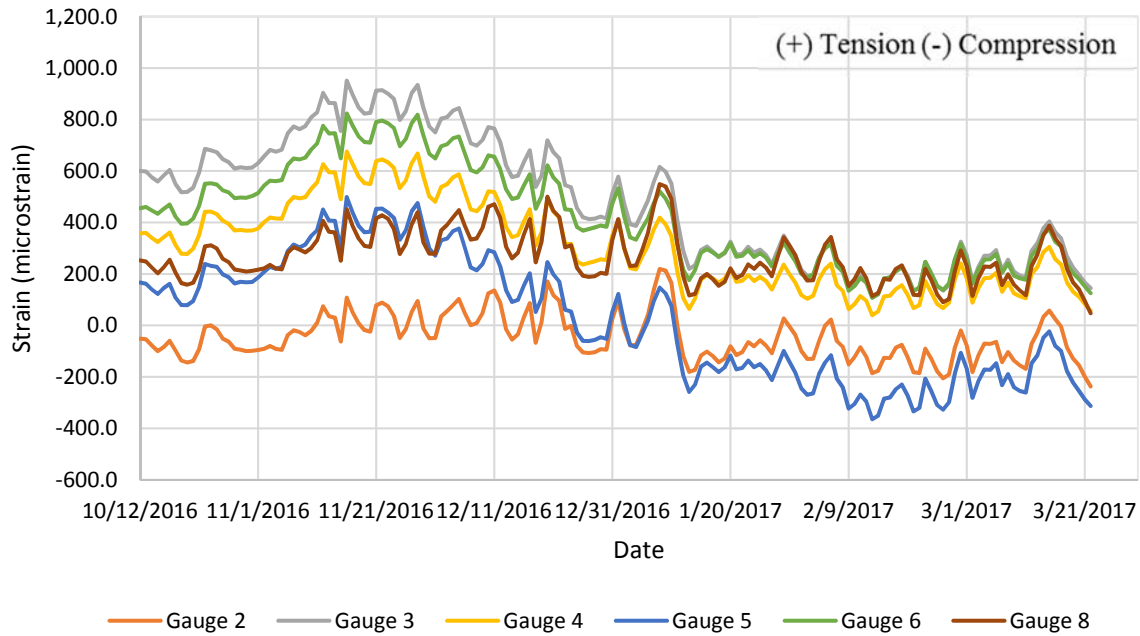


Figure 105: Strain with Time – Vertical Barriers

The moisture content trends for the vertical barrier Test Section are shown in Figure 106. Ideally, the moisture content beneath the pavement should remain fairly constant due to the vertical barriers. While this is true to some extent, the trends show a gradual increase in moisture content following the first rainfall in all the sensors below the road. The 10 feet deep sensors in the road and shoulder appear to be in the chalk layer beneath the clay and have remained at a stable water content. The 2.5 and 5 feet deep sensors in the shoulder follow similar trends as the other sections with sharp increases in the water content following the first rainfall event.

The 7.5 feet deep shoulder sensor shows an interesting trend as it is much dryer than any sensor throughout the project prior to the first rainfall event. Following the first rainfall, it seems that the soil quickly dries back out until another rainfall event. One possible explanation for this

is the sensor was placed in a sandy pocket which drains quickly. As the water table moves above and below the pocket in the month following the first rainfall event, the moisture content increases and decreases. Since the end of January, the moisture content of this sensor has stabilized indicating that the soil is most likely saturated and beneath the water table.

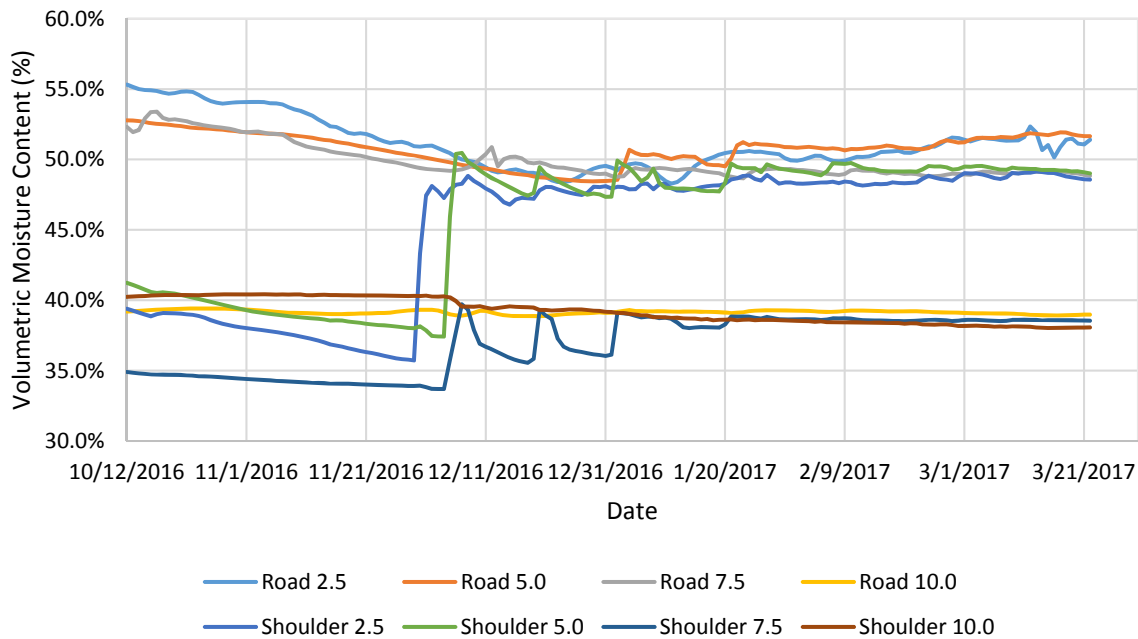
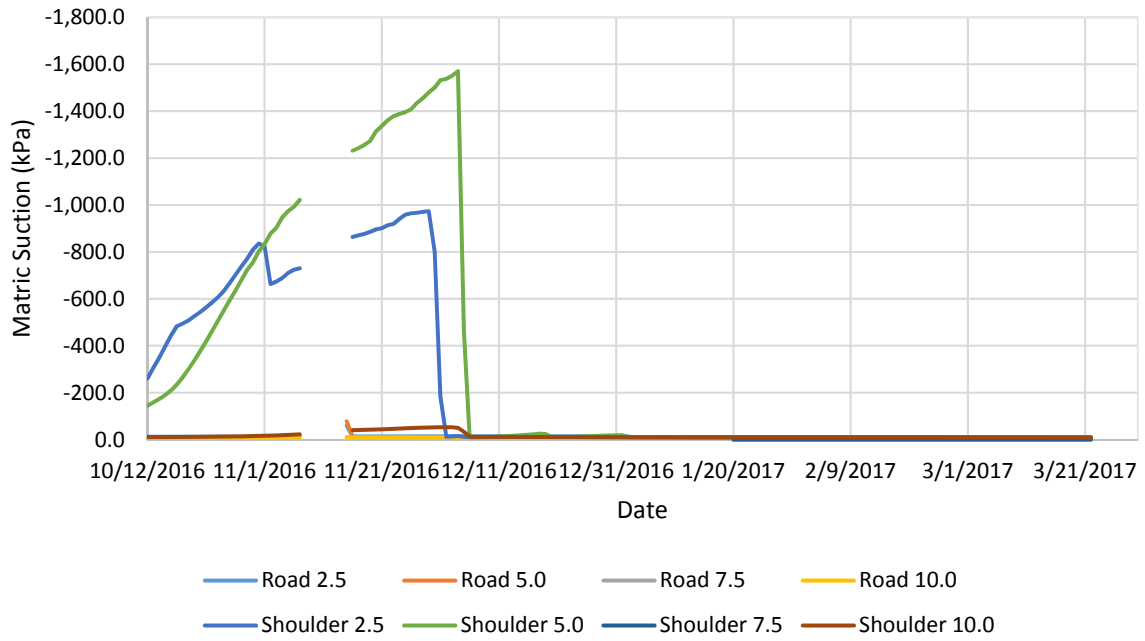
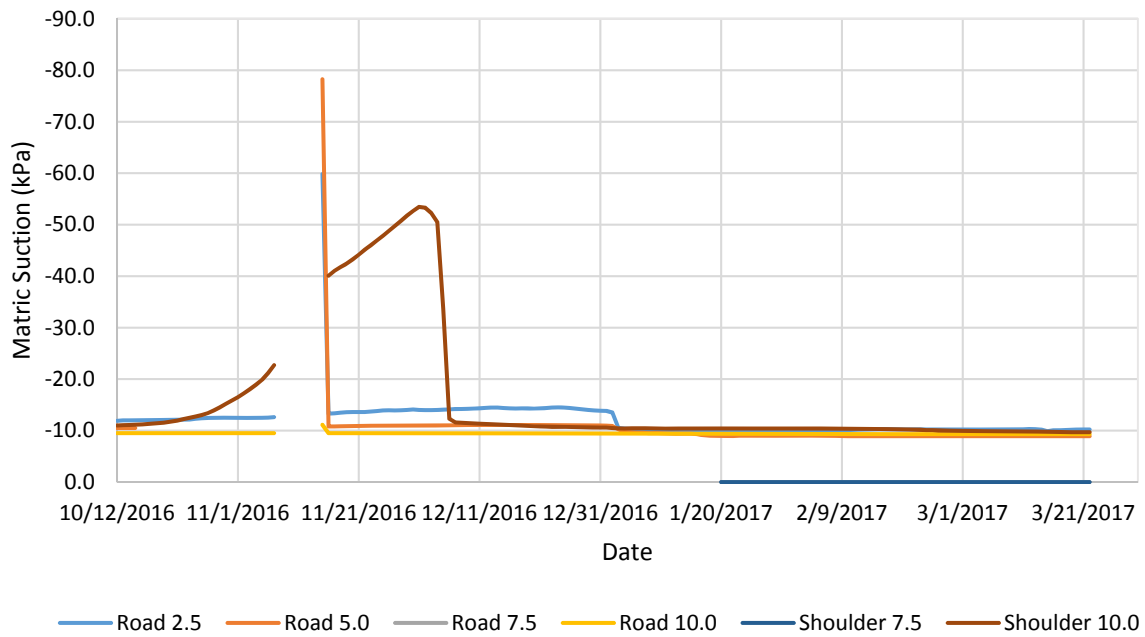


Figure 106: Moisture Content with Time – Vertical Barriers

The trends in matric suction for the vertical barrier Test Section are shown in Figure 107. Substantially larger amounts of suction was recorded in this section than that of the control. Interestingly, the shoulder sensor at 5 feet shows a higher suction value than that of the 2.5 feet deep sensor. It would be expected that the 2.5 feet deep shoulder sensor would record the highest amounts of suction due to evapotranspiration. This could be explained by a deep root system which is inducing large amounts of suction. As with the other sections, following the first rainfall, the suction sensors are all reading approximately 9 kPa.



(A)



(B)

Figure 107: Matric Suction with Time – Vertical Barriers (A&B shown with different scales for clarity)

Pore pressure data for the vertical barrier test section is shown in Figure 108. The trends indicate that the water table was below 12 feet in the shoulder prior to the rainfall event. Since then the same general trend of increasing pore pressures with rainfall events has been recorded. Unlike the other sections, the changes in pore pressures after each rainfall event are much more drastic in the shoulder. This could possibly indicate that there is preferential flow down the shoulder bore hole to the pore pressure transducers. At the time of publication, water table depths were approximately 3 feet deep below the road and 1 feet deep below the shoulder.

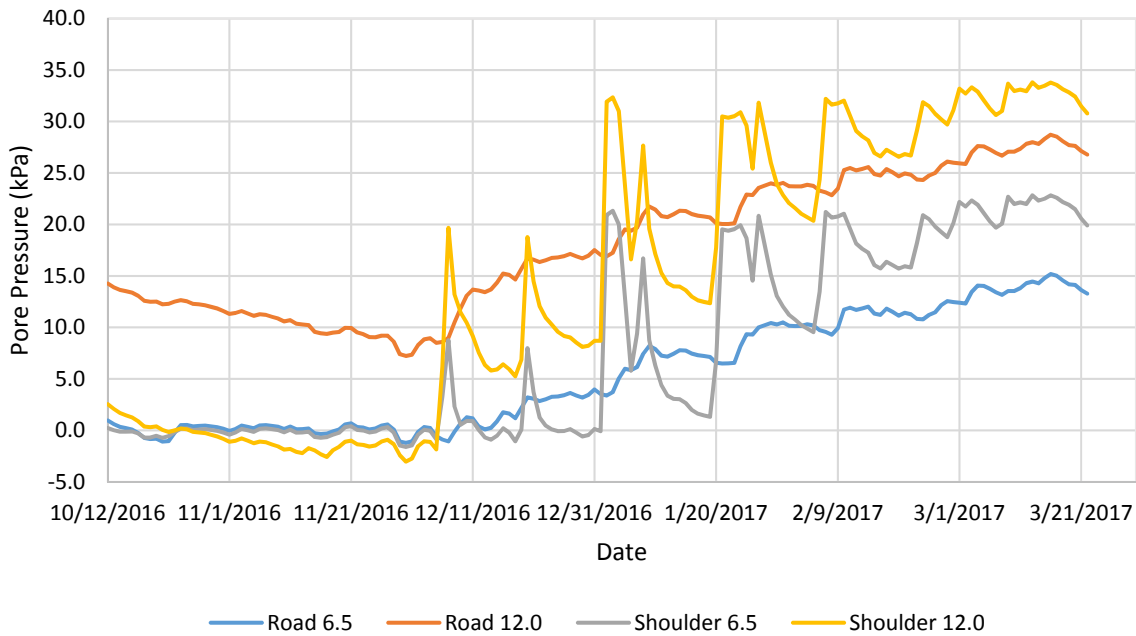


Figure 108: Pore Pressure with Time – Vertical Barriers

7.3.6 Lime Columns – Test Section 3

The strain gauge data for the lime columns test section is shown in Figure 109. To date no plastic deformation has been recorded in any of the strain gauges.

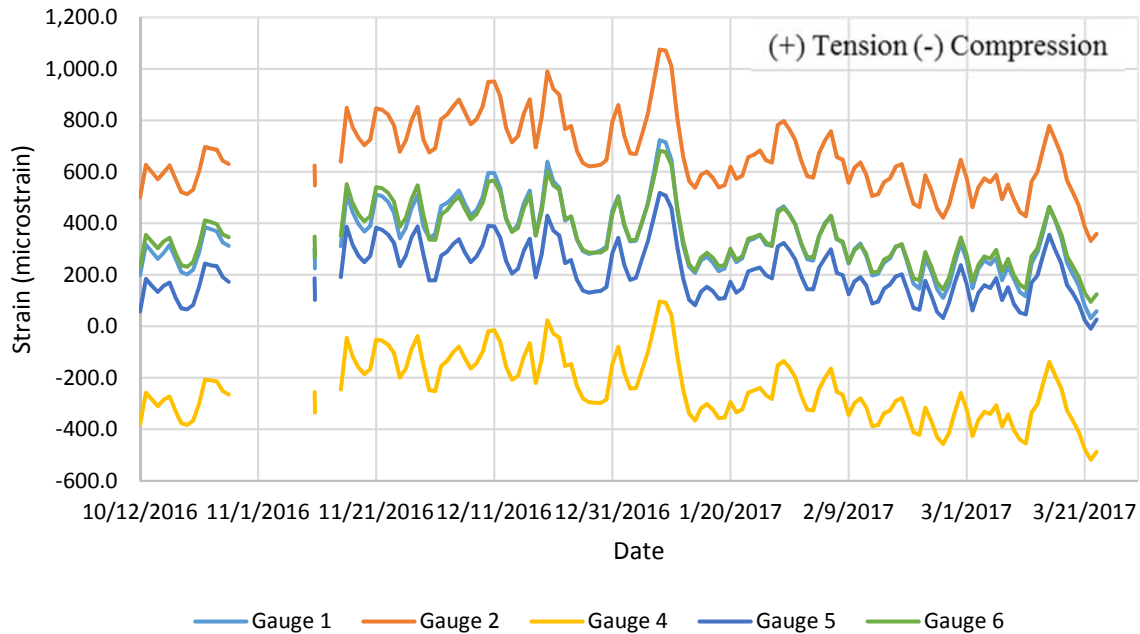


Figure 109: Strain with Time – Lime Columns

The moisture content data for the lime column test section is shown in Figure 110. Unlike the other sections, there is no spike following the first rainfall event. Rather, all the sensors show that the soil continued to dry. The two 10 feet deep sensors have remained at a constant moisture content and appear to be in the chalk layer as well as they are reading lower moisture contents similar to the other test sections. After some time all the sensors appear to have stabilized at a fairly constant moisture content. This could indicate that the lime has successfully reacted with the clay and reduced the water carrying capacity of the soil. While more cycles of wetting and drying will be needed to confirm this, this shows promising results for lime columns.

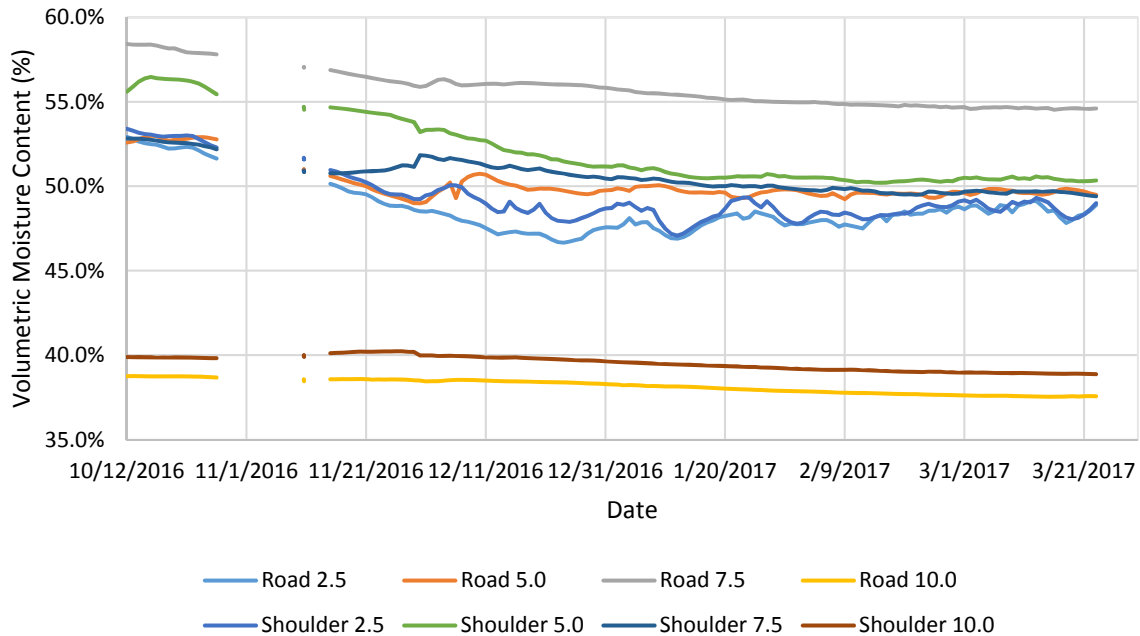


Figure 110: Moisture Content with Time – Lime Columns

Matric suction trends for the lime column test section are shown in Figure 111. Large amounts of suction were not recorded in this section. This is somewhat expected as this section of the road does not have trees near the road. Following the first rainfall, the sensors are all reading near 9.0 kPa indicating that the soil is most likely saturated.

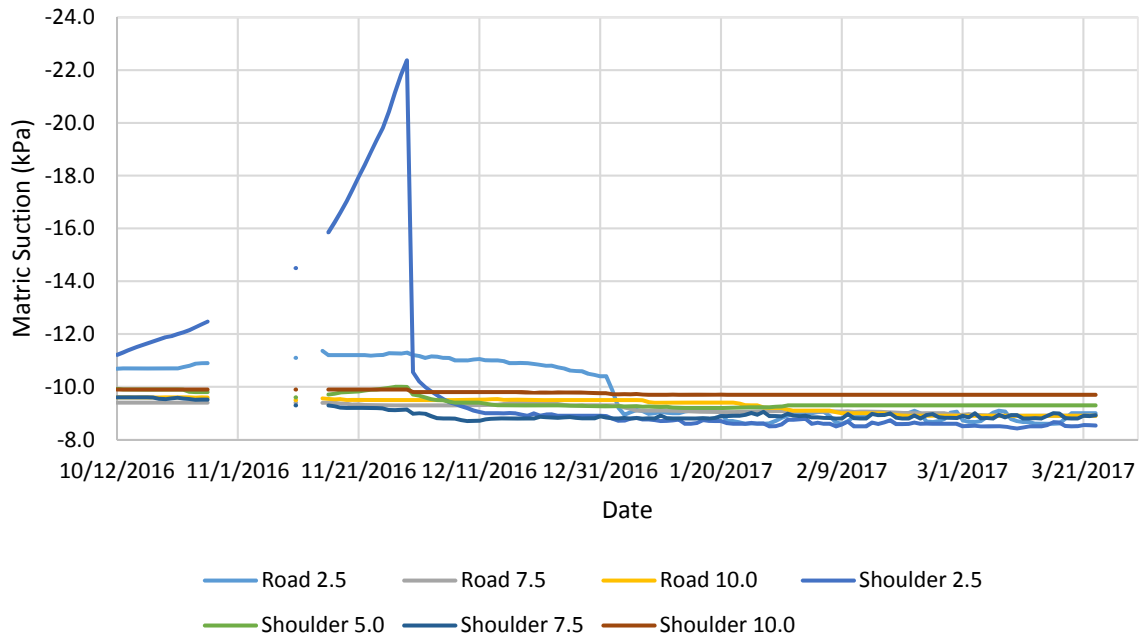


Figure 111: Matric Suction with Time – Lime Columns

Pore pressure data from the lime column test section is shown in Figure 112. The trends in the data are very similar to the control section. At the time of publication, the water table was approximately 3.5 feet below the road and 2.25 feet below the shoulder.

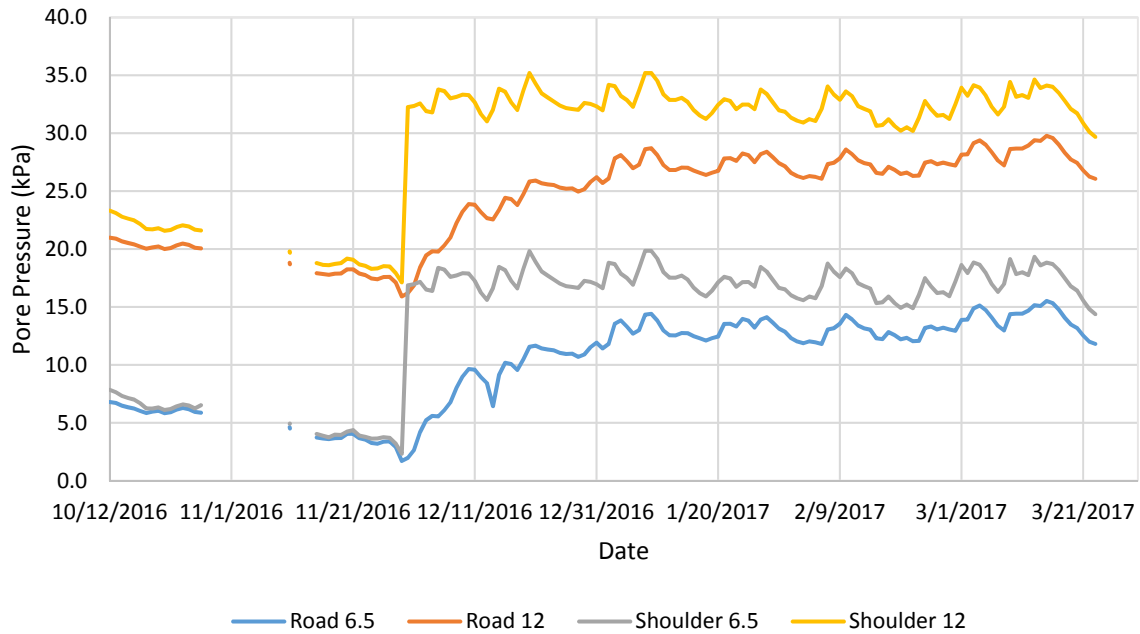


Figure 112: Pore Pressure with Time – Lime Columns

7.3.7 Paved Shoulders – Test Section 4

The strain gauge data for the paved shoulders test section is shown in Figure 113. To date no plastic deformation has been recorded in any of the strain gauges.

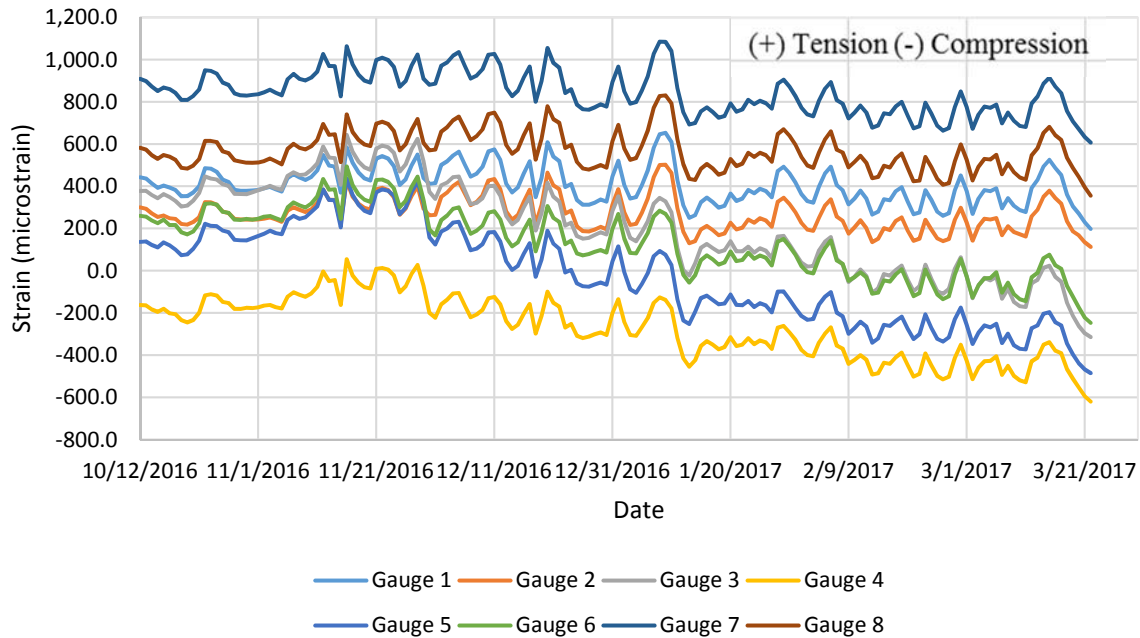


Figure 113: Strain with Time – Paved Shoulders

The moisture content data for the paved shoulders Test Section is shown in Figure 114. As hoped, the moisture contents below the road have remained fairly constant and continued to dry following the first rainfall event. The opposite is shown in the shoulder sensors which fluctuate accordingly due to rainfall events. This shows that the path for water to reach the subgrade has been increased due to the addition of paved shoulders. While more time will be needed to fully evaluate this finding, it appears that the paved shoulders have helped to maintain a relatively constant moisture content beneath the road.

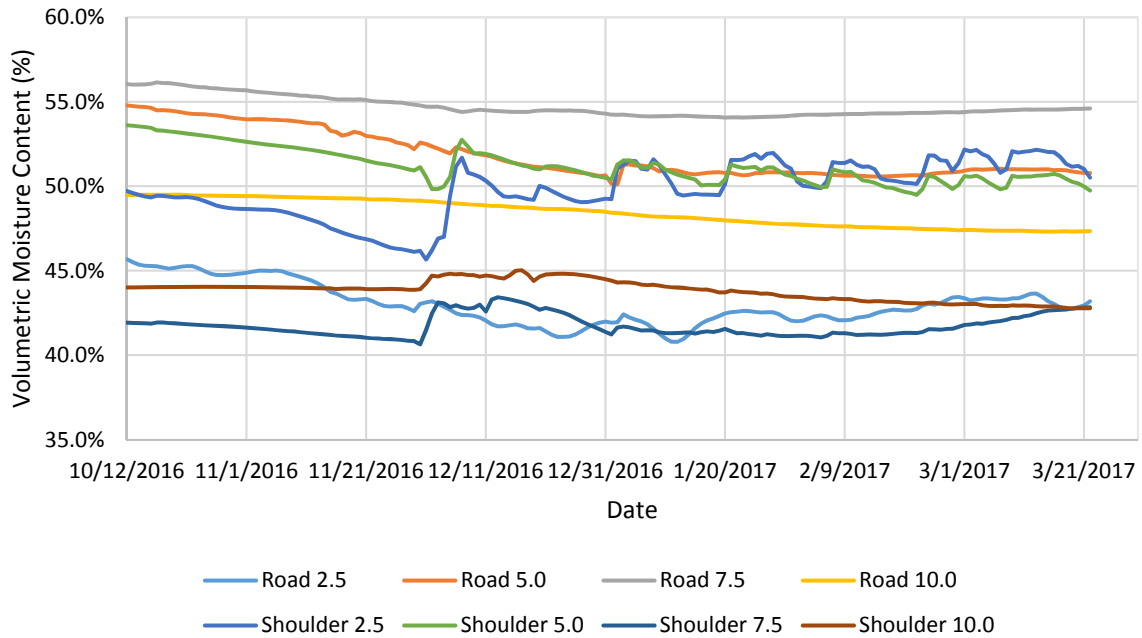
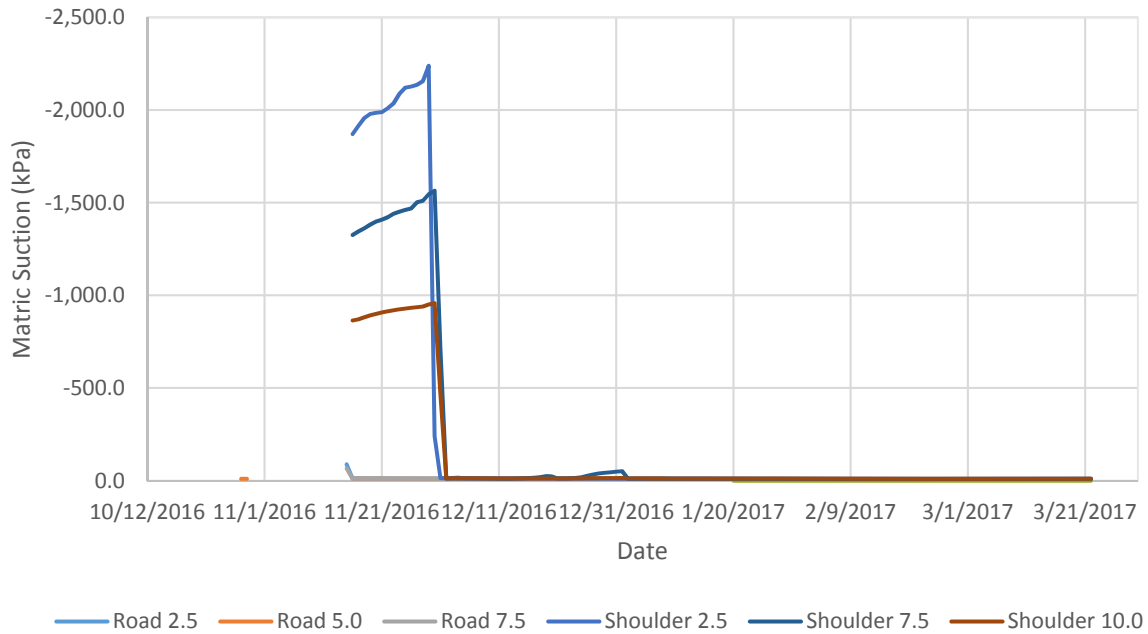
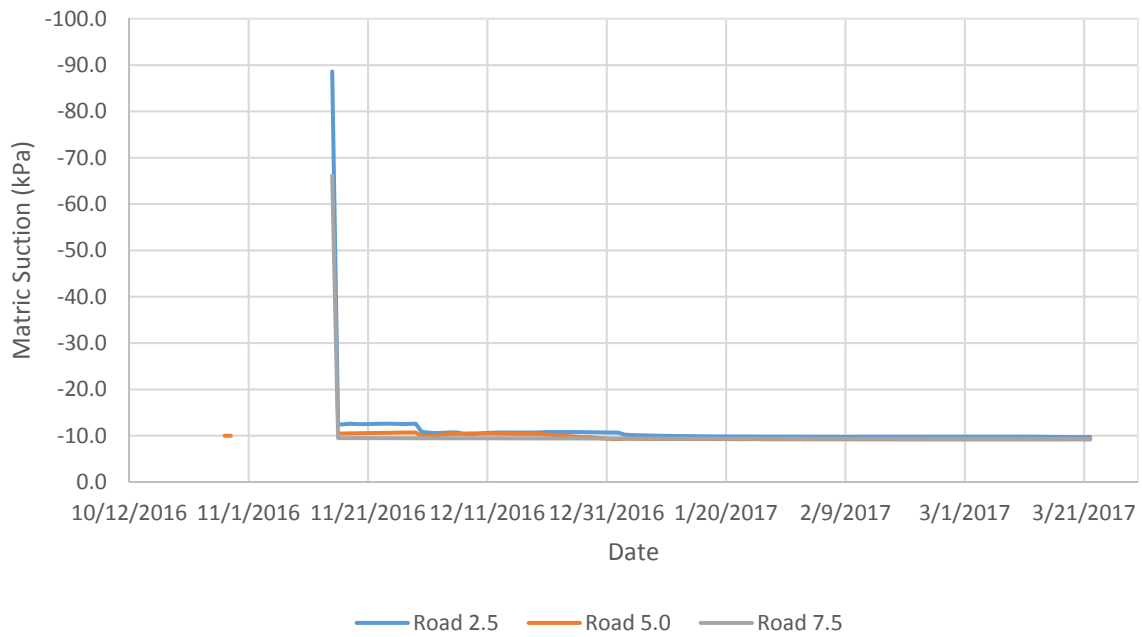


Figure 114: Moisture Content with Time – Paved Shoulders

Matric suction trends for the lime column test section are shown in Figure 115. The same trends shown in other sections is seen here as well. Following the first rainfall, the sensors are all reading values near 9.0 kPa.



(A)



(B)

Figure 115: Matric Suction with Time – Paved Shoulders (A&B shown with different scales for clarity)

The data from the pore pressure sensors in the paved shoulder Test Section are shown in Figure 116. The pore pressures beneath the road exhibit similar trends to that of the control. Following the first rainfall event, the pore pressures have gradually risen. The pore pressures beneath the shoulder however show large fluctuations in pore pressures. The reason for these large fluctuations is unclear but suggests that the water table fluctuates up and down very quickly in this area. Borings indicate that the underlying chalk layer is much shallower in this area at depths of 6 to 7 feet deep. This could be one possible explanation for the quick changes in pore pressures. At the time of publication the water table depth below both the road and shoulder was approximately 3.5 feet deep.

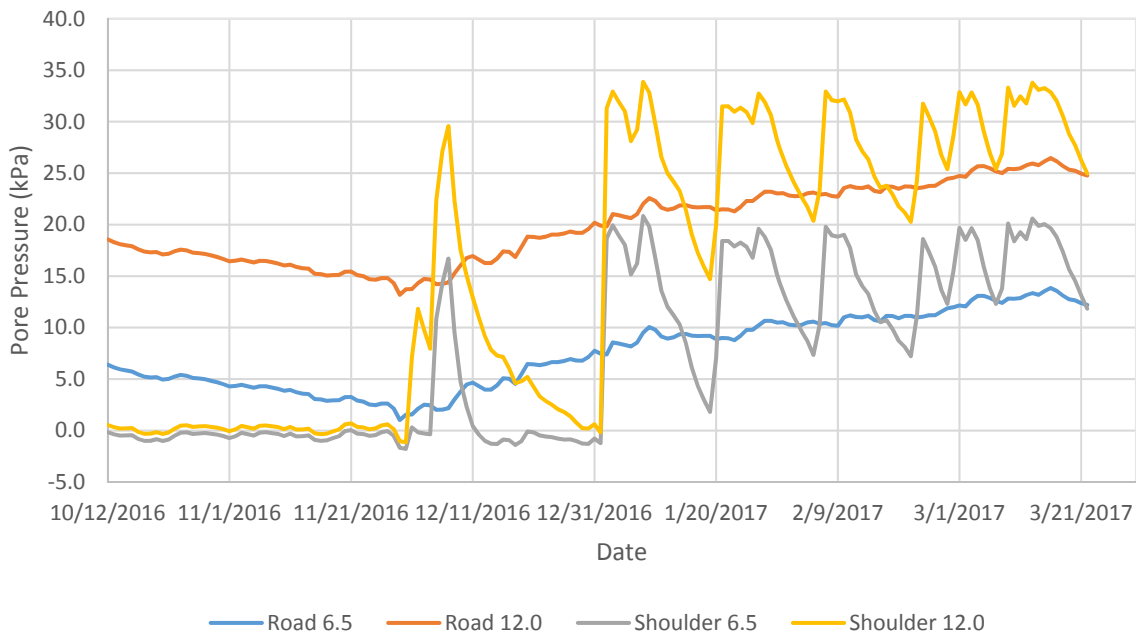


Figure 116: Pore Pressure with Time – Paved Shoulders

7.3.8 Edge Drains – Test Section 6

The strain gauge data for the edge drains test section is shown in Figure 117. To date no plastic deformation has been recorded in any of the strain gauges.

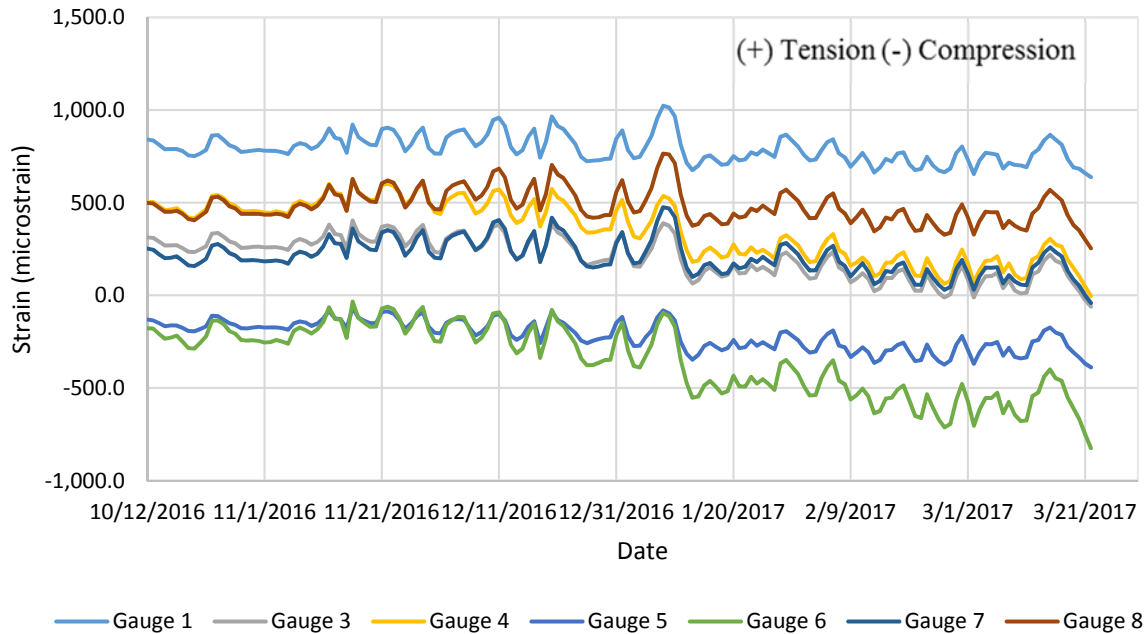


Figure 117: Strain with Time – Edge Drains

The moisture content data for the edge drains Test Section is shown in Figure 118. The trends indicate that the moisture contents below the road have continued to dry until reaching a fairly constant moisture content in late December. This indicates that the edge drains are helping to drain any water infiltrating the pavement away from the subgrade.

In the subgrade, the shallow 2.5 feet deep sensor shows some erratic readings. Following the first rainfall, an increase in the moisture content was recorded as expected. However, following the first initial spike, the moisture content continued to decrease to an all-time dry level even though it continued to rain over this time. Following another heavy rainfall event in early January, the moisture content spiked back to a more realistic value and has remained fairly constant since. Unlike the moisture content trends in the other test sections, the remaining shoulder sensors did not react to the first rainfall event but rather continued to dry. It is unclear why these shoulder sensors responded in this manner.

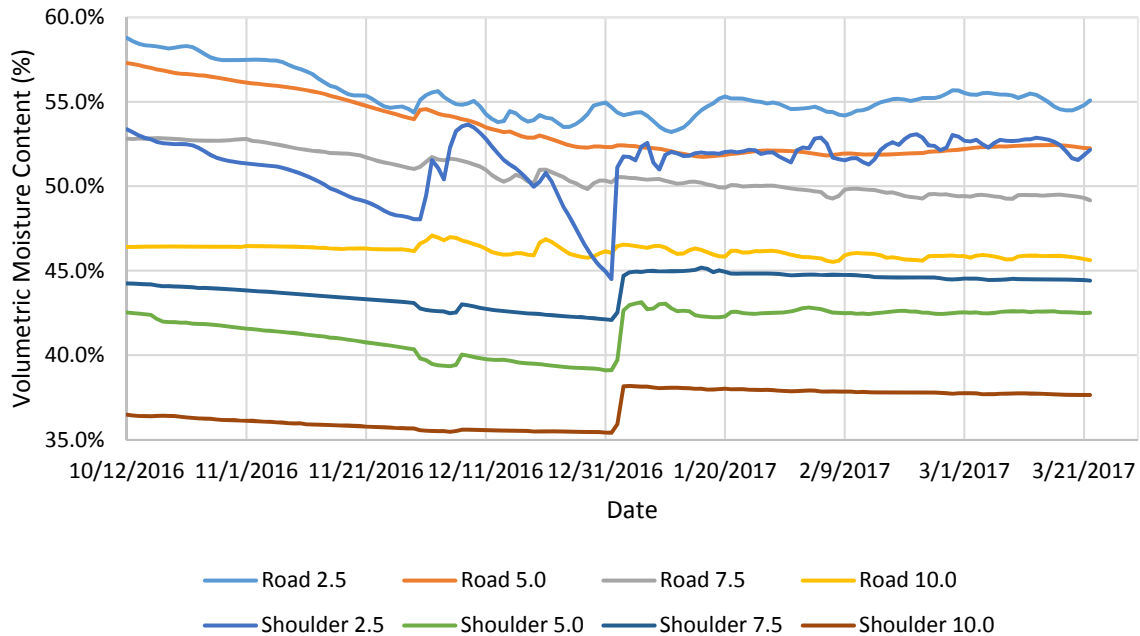
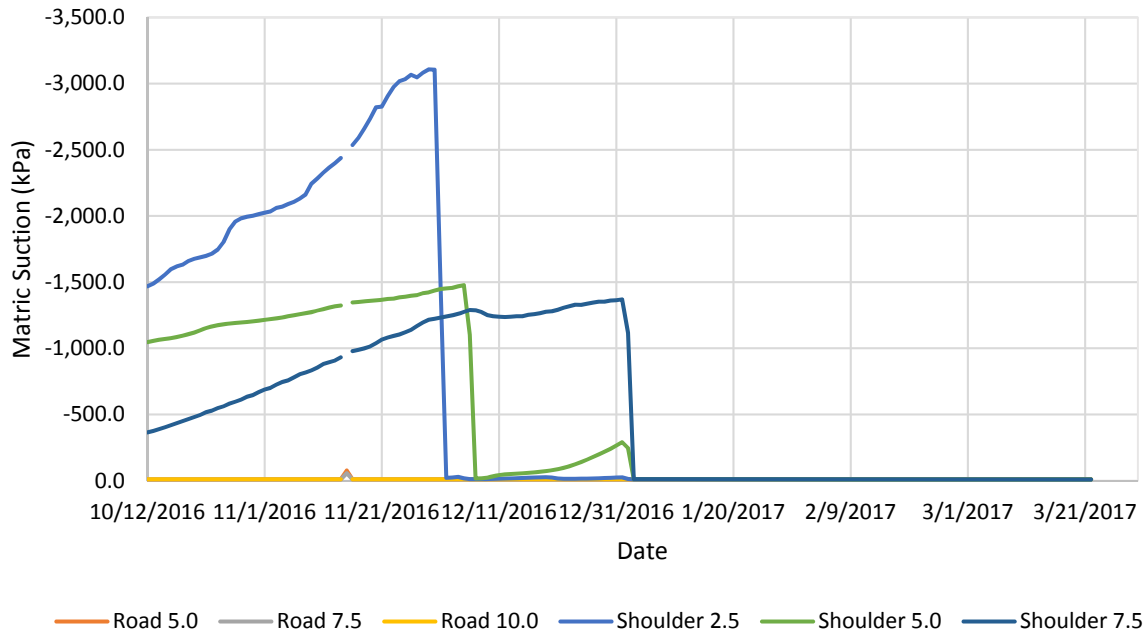
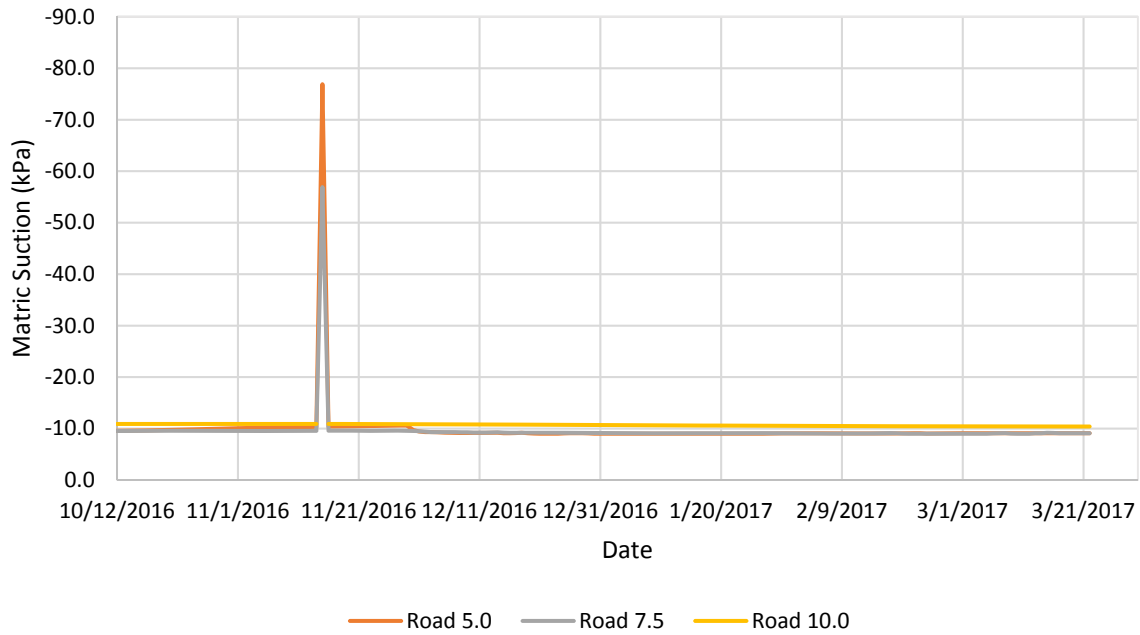


Figure 118: Moisture Content with Time – Edge Drains

The matric suction data for the Edge Drain test section is shown in Figure 119. This section recorded the highest values of suction but still followed the same trends as the other sections. Following the first rainfall the 2.5 and 5 feet deep shoulder sensors appear to have become saturated as the suction values quickly dropped off to a value of 9 kPa. Interestingly, the suction remained fairly constant at a depth of 7.5 feet in the shoulder until the large rainfall event in early January. Since then, all the sensors have remained saturated and reading suction values of 9 kPa. This anomaly in the 7.5 feet deep sensor is most likely associated with the shallow chalk layer in this area of the project.



(A)



(B)

Figure 119: Matric Suction with Time – Edge Drains (A&B shown with different scales for clarity)

Pore pressure data for the edge drains Test Section is shown in Figure 120. Similarly to the paved shoulder tests section, large fluctuations in pore pressures is shown in the shoulder. Also, unlike any of the other sections, the spike in pore pressure in the shoulder did not occur until the second large rainfall event in early January. This is especially peculiar because the sensors beneath the road responded to the first rainfall event. It is unclear why the trend in the shoulder is different. More cycles of wetting and drying will need to be collected in order to see if this happens again.

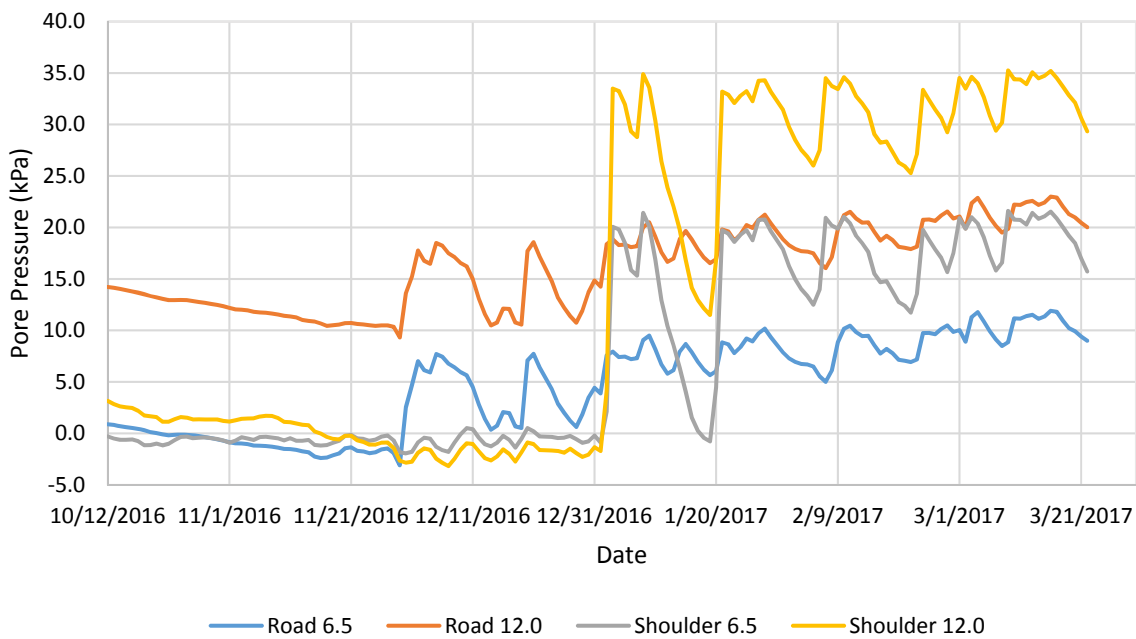


Figure 120: Pore Pressure with Time – Edge Drains

7.3.9 Trees

These two sensor holes were installed roughly 10 feet apart in the shoulder in line with a large tree. This was done in an attempt to measure how far out the tree influenced the soil properties. The moisture content data for the sensors installed by a large tree are shown in Figure 121. Similarly to the edge drain shoulder moisture sensors the moisture content continued to dry through the first rainfall event and did not spike until the early January rainfall

event. This suggests that the first rainfall event may have been localized at the southern end of the project. Another explanation could be that due to the long drought before the first rainfall, the trees sucked up any rainfall before the soil could absorb it.

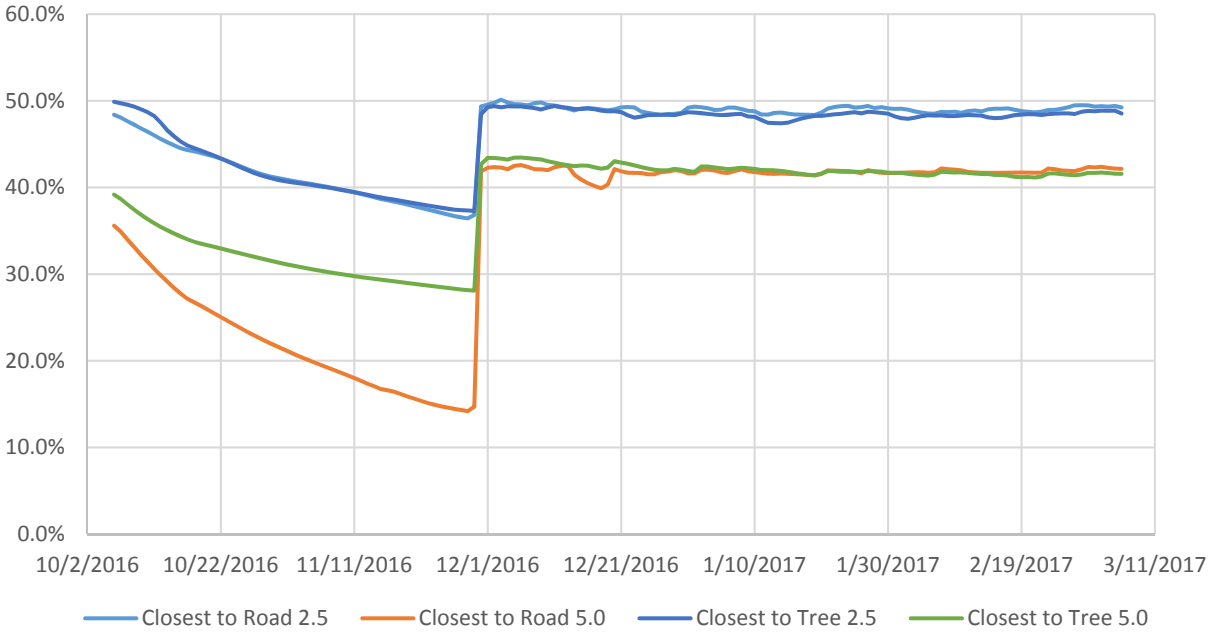


Figure 121: Moisture Content with Time – Trees

The matric suction data for the two sensor holes by the large tree are shown in Figure 122. Unfortunately for an unknown reason, the sensor closest to the road at a depth of 5 feet never recorded any values and appears to be dead. Also, the sensor closest to the tree at a depth 2.5 feet initially started reading values but since October 27, it has died and no longer is recording any values. This makes it difficult to compare suction values between the two holes and determine any influence of the tree.

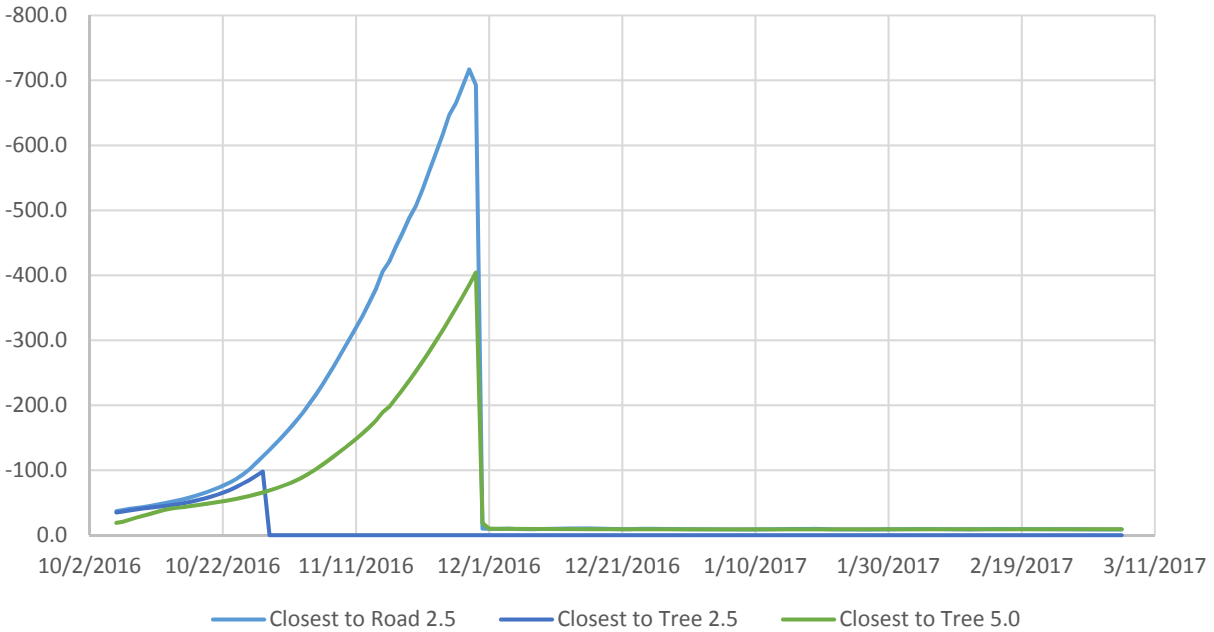


Figure 122: Matric Suction with Time – Trees

7.3.10 Summary of Sensor Data

To date the vertical barrier Test Section is the only section showing substantial changes in the asphalt strain gauges. In this section, the strain gauges oriented in the transverse direction show some signs of plastic deformations. In all other sections, daily temperature fluctuations can be observed in the strain gauges but no plastic deformations have been observed. From the findings of the site visit and the IRI surveys it is believed that these readings are accurate.

The moisture sensors, suction sensors, and piezometers are all behaving as expected. Elevated moisture contents have been observed corresponding to the various rainfall events in all sections. The matric suction has also reacted accordingly throughout the project. Following the rainfall, the piezometers recorded increased pore water pressures as expected throughout the project as well.

7.4 Website

To allow for easy continued live monitoring of the instrumentation installed at AL-5, Campbell Scientific software was used to download the daily readings of the sensors automatically each day. This data was saved as a tab delimited text file. An individual text file was created for each test section which included the daily minimum, maximum, and average reading of every sensor in that section. The data connection feature of Microsoft Excel was then utilized to import the text files. Once in excel, graphs of moisture content, soil suction, and pore pressures with depth were plotted for each test section. Also, temporal graphs of moisture content, soil suction, pore pressure, and strain were plotted. A user interface was then created to easily access this data and publish it to a website daily. An image of the home screen and an example of one of the test section pages is shown in Figure 123 and Figure 124, respectively. At the time of publication, the temporary website address is <http://eng.auburn.edu/users/dtj0008/>. A permanent address will be provided in subsequent papers.

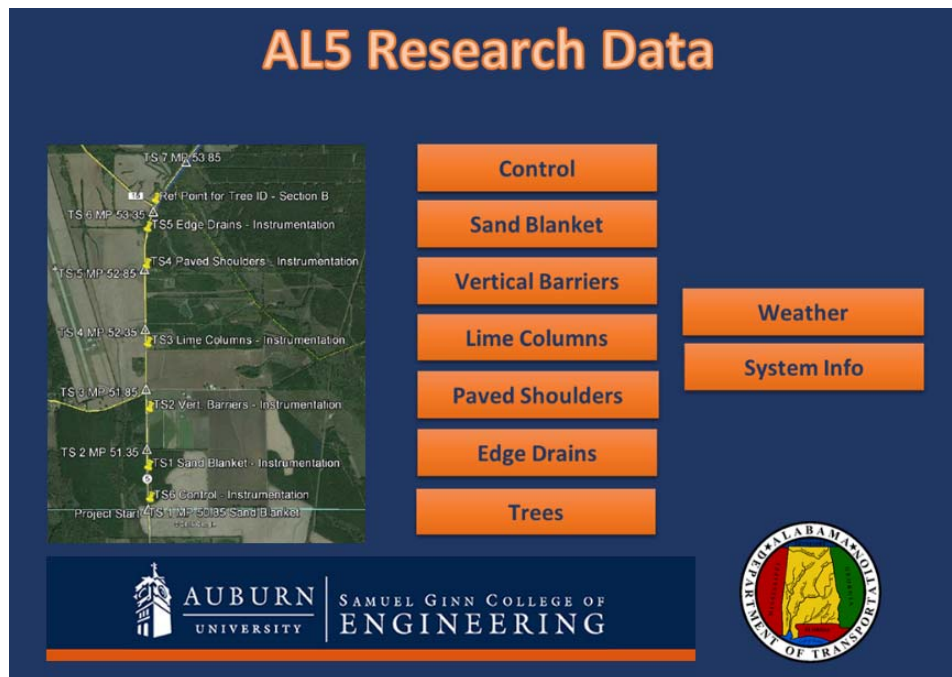


Figure 123: AL-5 Website Home Screen



Figure 124: Website Page – Lime Columns

CHAPTER 8: SUMMARY, CONCLUSIONS, & RECCOMENDATIONS

8.1 Summary

As a farm-to-market road, AL-5 is an important route for the delivery of goods from rural areas. Built directly on an expansive clay soil subgrade, AL-5 experiences rapid deterioration of the riding surface with seasonal moisture fluctuations. In total, six remediation strategies were implemented at AL-5 in an effort to increase the interval of resurfacing required to maintain a safe riding surface. The first objective of this investigation was to develop a method to monitor the fluctuating moisture contents using a nuclear moisture probe. The second objective of this investigation was to document the construction process of each of the remediation strategies. In addition, a user-friendly website was to be created to monitor the array of sensors installed at AL-5.

8.2 Conclusions

In conclusion, the objectives of this investigation were successfully completed as follows:

- The construction of the remediation strategies was well documented by providing detail drawings and construction photos in Chapter 5. In addition, challenges faced during the construction of each remediation strategy were discussed.
- An efficient method of installing access holes for monitoring moisture contents using a nuclear moisture gauge was developed as discussed in Chapter 6. In total 14 access holes were installed at the AL-5 site and base line readings were taken at each hole.

- A website was created to automatically retrieve data from the field and upload it to a user-friendly website. This website allows for quick and easy monitoring of the sensors installed at AL-5.

From baseline readings, it appears that the installation method of the access holes was successful. Relative moisture fluctuations and the depth of the active zone will be determined with continued monitoring of the access holes. Further readings with the hydroprobe will allow for a more accurate calibration by relating the data to the moisture sensors in adjacent holes.

So far, the riding surface throughout the project has remained smooth. Apart from the vertical barrier test section, no longitudinal cracks have formed throughout the project. At the time of publication, based on visual inspections, IRI surveys, and strain gauge data, the pavement sections are performing well with the exception of the vertical barriers.

8.3 Recommendations

Based on observations during construction, some recommendations on construction techniques are provided. First, to prevent the depressions at the location of the lime columns, it is recommended that the asphalt cap on the lime column be compacted with greater effort. Also, it is recommended that the granular backfill used in the vertical barrier test section be better compacted in lifts to prevent rutting in the shoulder of the pavement. Finally, it is recommended that care be taken when folding the vertical barrier on the pavement prior to paving. Specifically, folds and wrinkles in the fabric should be minimized to prevent any raveling or spalling of the pavement surface.

It is recommended that the readings be taken monthly with the hydroprobe for several years. This will allow for the seasonal moisture fluctuations to be captured and the depth of the active zone to be determined. It is also recommended to install additional access holes at nearby

roads exhibiting similar shrink-swell distress. This could allow for damage at AL-5 to be correlated to other roads. Should additional holes be installed, field calibrations should be conducted. Also, a calibration curve should be created by correlating hydroprobe readings to moisture sensor readings. In addition, the sensors installed should continue to be monitored so that the effectiveness of each test section can be determined. Finally, IRI surveys should continue to be taken periodically to monitor the progression of pavement distress throughout the project.

REFERENCES

- Abeelee, W.V. (1978). "The Influence of Access Hole parameters on Neutron Moisture Probe Readings." Department of Energy, Los Alamos Scientific Laboratory.
- Aitchison, G. D. (1961). "Relationship of Moisture and Effective Stress Functions in Unsaturated Soils." *Pore Pressure and Suction in Soils Conf.* London, England. (47-52). British Nat. Soc. of Int. Soc. Soil Mech. Found Eng.
- Alabama Department of Transportation (2015). "Research Project for Soil Stabilization on SR-5 from the Dallas County Line to 0.15 Miles North of E. Goley Road (MP 54.850)." Plans of Proposed Project Number 990305-535-005-401.
- Alabama Department of Transportation (2016). "Alabama Traffic Data." Retrieved Oct. 13, 2016 from <https://aldotgis.dot.state.al.us/atd/default.aspx>.
- Alabama Road Builders Associations (2017). "Edwin N. Rodgers." Retrieved Mar. 3, 2017 from <https://www.alrba.org/hall-of-fame/edwin-n-rodgers/>.
- Bishop, A. W. (1959). "The Principle of Effective Stress." *Teknisk Ukeblad*, 106(39): 859-863.
- Bishop, C.W. and Porro, I. (1997). "Comparison of Neutron Moisture Gauges and a Neutron Tool for Use in Monitoring Wells." *Ground Water*, 35(3): 394-399.
- Chen, D. H., Scullion, T., Hong, F., & Lee, J. (2012). Pavement Swelling and Heaving at State Highway 6. *Journal of Performance of Constructed Facilities*, 26(3): 335-344.
- Cronney, D., Coleman, J.D., & Black, W.P.M. (1958). "Movement and Distribution of Water in

- Soil in Relation to Highway Design and Performance.” *Water and Its Conduction in Soils*. Highway Res. Board Special Report no. 40 (226-252). Washington, DC.
- Evans, R. P., & Mcmanus, K. J. (1999). Construction of Vertical Moisture Barriers to Reduce Expansive Soil Subgrade Movement. *Transportation Research Record*(1652), 108-112.
- Flackenstein, J. L., & Allen, L. D. (2007). Evaluation of Pavement Edge Drains and Their Effect on Pavement Performance. *Transportation Research Record*(1519), 28-35.
- Fredlund, D.G. (1973). “Volume Change Behavior of Unsaturated Soils.” Ph.D. Dissertation, Univ. of Alberta, Edmonton, Alta., Canada.
- Fredlund, D. G., and Morgenstern, N. R. (1977). "Stress State Variables for Unsaturated Soils." *ASCE Journal of Geotechnical Engineering Division GT5*, 103: 447-466.
- Fredlund, D. G., and Rahardjo, H. (1993). *Soil Mechanics for Unsaturated Soils*, John Wiley & Sons, Inc., New York.
- Fredlund, D.G., Rahardjo, H., & Fredlund, M.D. (2012). *Unsaturated Soil Mechanics in Engineering Practice*. John Wiley & Sons, Inc., Hoboken, NJ.
- Google Inc. (2015). Google Earth (Version 7.1.2.2041) [Software]
- Harris, M. C. (1998). *Soil Survey of Perry County, Alabama*. Washington, D.C.: United States Department of Agriculture (USDA).
- Hayward Baker. (2010). *Hayward Baker Geotechnical Construction*. Retrieved February 19, 2015, from Injection Systems:
<http://www.haywardbaker.com/WhatWeDo/Techniques/GroundImprovement/InjectionSystems/default.aspx>
- Herman, J.M. (2015). “Damage to Pavements from Expansive Clays: A Review of Behavior and Remediation Techniques.” MCE Research Paper. Auburn University.

- IAEA (1970). *Neutron Moisture Gages*. International Atomic Energy Agency. Technical Reports Series No. 112. Vienna, Austria.
- IAEA (2002). *Soil and Water Management & Crop Nutrition Section*. International Atomic Energy Agency. Training Course Series No. 16. Vienna, Austria.
- Jackson, D.T. (2016). "Insitu Measurement of Pavement Distress and Causal Mechanisms in Expansive Soil along Alabama Highway 5." MS Thesis, Auburn University.
- Jennings, J.E. (1961). "A Revised Effective Stress Law for Use in the Prediction of the Behavior of Unsaturated Soils." *Pore Pressure and Suction in Soils Conf.* London, England. (26-30). British Nat. Soc. of Int. Soc. Soil Mech. Found Eng.
- Jones, D.E. (1981). "Perspectives on Needs for an Availability of Scientific and Technical Information." Dept. Housing and Urban Development. 1st meeting of Committee on Emergency Management, Commission on Sociotechnical Systems, National Research Council.
- Kramer, J.H., Everett, L.G., Eccles, L.A. (1990). "Effects of Well Construction Materials on Neutron Probe Readings with Implications for Vadose Zone Monitoring Strategies." *Ground Water Management*, 2: 1303-1317 (4th NOAC).
- Li, J. and Ren, G. (2010) "Monitoring In-Situ Soil Moisture Variations of Expansive Clay using Neutron Probes." *GeoShanghai International Conference*, Deep Foundations and Geotechnical In Situ Testing.
- Little, D. N. (1995). *Handbook for Stabilization of Pavement Subgrades and Base Courses with Lime*.
- Little, D. N., & Nair, S. (2009). *Recommended Practice for Stabilization of Sulfate Rich Subgrade Soils*. Texas Transportation Institute, Texas A&M University.

Lytton, R., Aubeny, C., Bulut, R. (2005) *Design Procedure for Pavements on Expansive Soils*.

Texas Transportation Institute, Texas A&M Universtiy.

Lu, N., and Likos, W. J. (2004). *Unsaturadted Soil Mechanics*, John Wiley & Sons, Inc.,

Hoboken, NJ.

Madhyannapu, R. S. (2007). *Deep Mixing Technology for Mitigation of Swell-Shrink Behavior of Expansive Soils of Moderate to Deep Active Depths*. Dissertation, The University of

Texas at Arlington.

Madhyannapu, R. S., Puppala, A. J., Bhadriraju, V., & Nazarian, S. (2009). Deep Soil Mixing (DSM) Treatment of Expansive Soils. *2009 US-China Workshop on Ground*

Improvement Technologies. ASCE.

Madhyannapu, R. S., Puppala, A. J., Nazarian, S., & Yuan, D. (2010, January 1). Quality

Assessment and Quality Control of Deep Soil Mixing Construction for Stabilization Expansive Subsoils. *Journal of Geotechnical and Geoenvironmental Engineering*,

136(1): 119-128.

Mitchell, J. K. (1986). The Twentieth Terzaghi Lecture. *Journal of Geotechnical*

Engineering(112), 255-289.

McQueen, I. S., and Miller, R. F. (1974). "Approximating Soil Moisture Characteristics from

Limited Data: Empirical Evidence and Tentative Model." *Water Resources Research*, *10*(3): 521-527.

Nelson, J. D., and Miller, D. J. (1992). *Expansive Soils: Problems and Practice in Foundation and Pavement Engineering*, John Wiley & Sons, Inc., New York.

Management in Intensive Agriculture.” *Sensors*, 9: 2809-2835.

- Petry, T. M., & Little, D. N. (2002, December 1). Review of Stabilization of Clays and Expansive Soils in Pavements and Lightly Loaded Structures - History, Practice, and Future. *Journal of Materials in Civil Engineering*, 14(6), 447-460.
- Picornell, M., & Lytton, R. L. (1986). Behavior and Design of Vertical Moisture Barriers. *Transportation Research Record*(1137), 71-81.
- Sayers, M. W., and Karamihas, S. M. (1998). *The Little Book of Profiling*, The University of Michigan, Michigan.
- Snethen, D. R. (1979). *Technical Guidelines for Expansive Soils in Highway Subgrades*. Washington, D.C.: Federal Highway Administration.
- Stallings, E.G. (2016). "Investigation of Pavement and Subgrade Distress at Alabama Highway 5." MS Thesis, Auburn University.
- Steinberg, M. L. (1980). Deep Vertical Fabric Moisture Seals. *Fourth International Conference on Expansive Soils* (383-400). Denver, CO: ASCE.
- Steinburg, M. L. (1985). "Controlling Expansive Soil Destructiveness by Deep Vertical Geomembranes on Four Highways." *Transportation Research Record*, 1032: 48-53.
- Steinberg, M. L. (1989). *Further Monitoring of Twelve Geomembrane Sites in Texas*. Austin, Texas: Texas State Department of Highways and Public Transportation.
- Steinberg, M. L. (1992). Vertical Moisture Barrier Update. *Transportation Research Record*, 1362: 111-117.
- Steinberg, M. L. (1998). *Geomembranes and the Control of Expansive Soils in Construction*. The McGraw-Hill Companies, Inc.
- Troxler Inc. (2006) "Manual of Operation and Instruction, Model 4300 Depth Moisture Gauge." Troxler Electronic Laboratories Inc., Research Triangle Park, North Carolina.

Zornberg, J. G., and Gupta, R. (2009). "Reinforcement of pavements over expansive clay subgrades." *Proc., 17th International Conference on Soil Mechanics and Geotechnical Engineering: The Academia and Practice of Geotechnical Engineering*, 765-768.

APPENDIX A: BORING LOGS



BORING NUMBER B-1A

PAGE 1 OF 1

CLIENT Auburn University
PROJECT NAME AL-5 Research Project
PROJECT NUMBER 99-305-635-005-401
PROJECT LOCATION AL 5, Perry County
DATE STARTED 11/19/13 **COMPLETED** 11/19/13
GROUND ELEVATION 182 ft **HOLE SIZE** 4"
DRILLING CONTRACTOR ALDOT
GROUND WATER LEVELS:
DRILLING METHOD CME 55, Auto-Hammer, SFA w/ SPT
AT TIME OF DRILLING None Encountered
LOGGED BY _____ **CHECKED BY** _____
AT END OF DRILLING None Encountered
NOTES _____ **AFTER DRILLING** None Encountered

ELEVATION (ft)	DEPTH (ft)	GRAPHIC LOG	MATERIAL DESCRIPTION	SAMPLE TYPE NUMBER	RECOVERY % SHELBY TUBE	BLOW COUNTS (N VALUE)	DRY UNIT WT. (pcf)	MOISTURE CONTENT (%)	ATTERBERG LIMITS			FINES CONTENT (%)
									LIQUID LIMIT	PLASTIC LIMIT	PLASTICITY INDEX	
0			Asphalt									
180			FAT CLAY (CH), gray, stiff, moist	ST	100				70	24	46	
5			FAT CLAY (CH), gray, medium, moist	ST	100				88	30	58	
175			FAT CLAY (CH), yellow-brown, gray, stiff, moist	ST	100				110	27	83	
10				ST	100				79	29	50	
170				ST	100				103	29	74	
15			FAT CLAY (CH), yellow-brown, hard	SS	100	8-13-18 (31)						
165			FAT CLAY (CH), light gray, hard (CHALK)	SS	100	9-16-26 (42)						
20			Boring was terminated at 19.5 feet.									
160												
25												
155												
30												
150												
35												



BORING NUMBER B-1.5A

CLIENT Auburn University **PROJECT NAME** AL-5 Research Project
PROJECT NUMBER 99-305-635-005-401 **PROJECT LOCATION** AL 5, Perry County
DATE STARTED 11/20/13 **COMPLETED** 11/20/13 **GROUND ELEVATION** 180 ft **HOLE SIZE** 4"
DRILLING CONTRACTOR ALDOT **GROUND WATER LEVELS:**
DRILLING METHOD CME 55, Auto-Hammer, SFA w/ SPT **AT TIME OF DRILLING** None Encountered
LOGGED BY _____ **CHECKED BY** _____ **AT END OF DRILLING** None Encountered
NOTES _____ **AFTER DRILLING** None Encountered

ELEVATION (ft)	DEPTH (ft)	GRAPHIC LOG	MATERIAL DESCRIPTION	SAMPLE TYPE NUMBER	RECOVERY % SHELBY TUBE	BLOW COUNTS (N VALUE)	DRY UNIT WT. (pcf)	MOISTURE CONTENT (%)	ATTERBERG LIMITS			FINES CONTENT (%)
									LIQUID LIMIT	PLASTIC LIMIT	PLASTICITY INDEX	
180	0		Asphalt									
			FAT CLAY (CH) (A-7-6), gray, brown, medium, moist, Layer 1	ST	100				97	29	68	
175	5			ST	100		84.0	37.0	66	24	42	98
				ST	50							
				ST	100				91	25	66	
170	10		FAT CLAY (CH), yellow-brown, stiff, moist, Layer 1	ST	75		87.5	32.9	85	24	61	98
				ST	0							
165	15		FAT CLAY (CH), light gray, hard (CHALK), Layer 2	SS	100	9-13-23 (36)						
			Boring was terminated at 16.7 feet.									
160	20											
155	25											
150	30											
145	35											



BORING NUMBER B-2A

CLIENT Auburn University **PROJECT NAME** AL-5 Research Project
PROJECT NUMBER 99-305-635-005-401 **PROJECT LOCATION** AL 5, Perry County
DATE STARTED 11/19/13 **COMPLETED** 11/20/13 **GROUND ELEVATION** 180 ft **HOLE SIZE** 4"
DRILLING CONTRACTOR ALDOT **GROUND WATER LEVELS:**
DRILLING METHOD CME 55, Auto-Hammer, SFA w/ SPT **AT TIME OF DRILLING** None Encountered
LOGGED BY _____ **CHECKED BY** _____ **AT END OF DRILLING** None Encountered
NOTES _____ **AFTER DRILLING** None Encountered

ELEVATION (ft)	DEPTH (ft)	GRAPHIC LOG	MATERIAL DESCRIPTION	SAMPLE TYPE NUMBER	RECOVERY % SHELBY TUBE	BLOW COUNTS (N VALUE)	DRY UNIT WT. (pcf)	MOISTURE CONTENT (%)	ATTERBERG LIMITS			FINES CONTENT (%)
									LIQUID LIMIT	PLASTIC LIMIT	PLASTICITY INDEX	
180	0		Asphalt									
175	5		FAT CLAY (CH), gray, moist	ST	100				83	31	52	
				ST	33				73	25	48	
				ST	100				86	27	59	
170	10		FAT CLAY (CH), white, yellow-brown, moist	ST	100				95	27	68	
			FAT CLAY (CH), gray, brown, moist	ST	90							
165	15		FAT CLAY (CH), yellow-brown, gray, very stiff moist, (CHALK)	SS	100	8-12-15 (27)						
160	20		FAT CLAY (CH), gray, hard (CHALK)	SS	100	17-26-28 (54)						
			Boring was terminated at 20.0 feet.									
155	25											
150	30											
145	35											



BORING NUMBER B-2.5A

CLIENT Auburn University **PROJECT NAME** AL-5 Research Project
PROJECT NUMBER 99-305-635-005-401 **PROJECT LOCATION** AL 5, Perry County
DATE STARTED 11/20/13 **COMPLETED** 11/20/13 **GROUND ELEVATION** 191 ft **HOLE SIZE** 4"
DRILLING CONTRACTOR ALDOT **GROUND WATER LEVELS:**
DRILLING METHOD CME 55, Auto-Hammer, SFA w/ SPT **AT TIME OF DRILLING** None Encountered
LOGGED BY _____ **CHECKED BY** _____ **AT END OF DRILLING** None Encountered
NOTES _____ **AFTER DRILLING** None Encountered

ELEVATION (ft)	DEPTH (ft)	GRAPHIC LOG	MATERIAL DESCRIPTION	SAMPLE TYPE NUMBER	RECOVERY % SHELBY TUBE	BLOW COUNTS (N VALUE)	DRY UNIT WT. (pcf)	MOISTURE CONTENT (%)	ATTERBERG LIMITS			FINES CONTENT (%)
									LIQUID LIMIT	PLASTIC LIMIT	PLASTICITY INDEX	
190	0		Asphalt									
			FAT CLAY (CH) (A-7-6), gray, stiff, moist, Layer 1	ST	100				70	24	46	
	5		FAT CLAY (CH), yellow-brown, stiff, moist, Layer 1	ST	75		90.1	31.9	84	26	58	93
185			FAT CLAY (CH), yellow-brown, stiff, moist, Layer 1	ST	40				79	32	47	
	10		FAT CLAY (CH), yellow-brown, very stiff (CHALK), Layer 2	SS	100	9-12-14 (26)	92.4	29.2				98
			Boring was terminated at 11.0 feet.									
	15											
175												
	20											
170												
	25											
165												
	30											
160												
	35											



BORING NUMBER B-3A

CLIENT Auburn University	PROJECT NAME AL-5 Research Project
PROJECT NUMBER 99-305-635-005-401	PROJECT LOCATION AL 5, Perry County
DATE STARTED 11/19/13	COMPLETED 11/19/13
DRILLING CONTRACTOR ALDOT	GROUND ELEVATION 190 ft
DRILLING METHOD CME 55, Auto-Hammer, SFA w/ SPT	HOLE SIZE 4"
LOGGED BY	CHECKED BY
NOTES	GROUND WATER LEVELS:
	AT TIME OF DRILLING None Encountered
	AT END OF DRILLING None Encountered
	AFTER DRILLING None Encountered

ELEVATION (ft)	DEPTH (ft)	GRAPHIC LOG	MATERIAL DESCRIPTION	SAMPLE TYPE NUMBER	RECOVERY % SHELBY TUBE	BLOW COUNTS (N VALUE)	DRY UNIT WT. (pcf)	MOISTURE CONTENT (%)	ATTERBERG LIMITS			FINES CONTENT (%)
									LIQUID LIMIT	PLASTIC LIMIT	PLASTICITY INDEX	
190	0		Asphalt									
			FAT CLAY (CH), gray	ST	100				93	26	67	
185	5			ST	100				65	24	41	
				ST	100							
				ST	100				74	25	49	
180	10		FAT CLAY (CH), yellow-brown, gray (CHALK)	ST	100							
			FAT CLAY (CH), yellow-brown, gray, very stiff moist, (CHALK)	ST	100							
				SS	100	8-11-13 (24)						
175	15		Boring was terminated at 14.0 feet.									
170	20											
165	25											
160	30											
155	35											



BORING NUMBER B-3.5A

CLIENT Auburn University
PROJECT NAME AL-5 Research Project
PROJECT NUMBER 99-305-635-005-401
PROJECT LOCATION AL 5, Perry County
DATE STARTED 11/19/13 **COMPLETED** 11/19/13
GROUND ELEVATION 200 ft **HOLE SIZE** 4"
DRILLING CONTRACTOR ALDOT
GROUND WATER LEVELS:
DRILLING METHOD CME 55, Auto-Hammer, SFA w/ SPT
AT TIME OF DRILLING None Encountered
LOGGED BY _____ **CHECKED BY** _____
AT END OF DRILLING None Encountered
NOTES _____ **AFTER DRILLING** None Encountered

ELEVATION (ft)	DEPTH (ft)	GRAPHIC LOG	MATERIAL DESCRIPTION	SAMPLE TYPE NUMBER	RECOVERY % SHELBY TUBE	BLOW COUNTS (N VALUE)	DRY UNIT WT. (pcf)	MOISTURE CONTENT (%)	ATTERBERG LIMITS			FINES CONTENT (%)
									LIQUID LIMIT	PLASTIC LIMIT	PLASTICITY INDEX	
200	0		Asphalt									
			FAT CLAY (CH) (A-7-6), brown, stiff, moist, Layer 1	ST	100		82.5	38.6	68	28	40	99
195	5		FAT CLAY (CH), gray, stiff, moist, Layer 1	ST	70				87	28	59	
			FAT CLAY (CH), yellow-brown, gray, stiff, Layer 1	ST	100				84	27	57	
			FAT CLAY (CH), yellow-brown, stiff moist, (CHALK), Layer 2	ST	65		77.7	41.5				97
190	10		FAT CLAY (CH), yellow-brown, very stiff (CHALK), Layer 2	ST	50							
			FAT CLAY (CH), yellow-brown, very stiff (CHALK), Layer 2	SS	100	5-11-15 (26)						
			Boring was terminated at 12.8 feet.									
185	15											
180	20											
175	25											
170	30											
165	35											



BORING NUMBER B-4A

CLIENT Auburn University
PROJECT NAME AL-5 Research Project
PROJECT NUMBER 99-305-635-005-401
PROJECT LOCATION AL 5, Perry County
DATE STARTED 11/19/13 **COMPLETED** 11/19/13
GROUND ELEVATION 199 ft **HOLE SIZE** 4"
DRILLING CONTRACTOR ALDOT
GROUND WATER LEVELS:
DRILLING METHOD CME 55, Auto-Hammer, SFA w/ SPT
AT TIME OF DRILLING None Encountered
LOGGED BY _____ **CHECKED BY** _____
AT END OF DRILLING None Encountered
NOTES _____ **AFTER DRILLING** None Encountered

ELEVATION (ft)	DEPTH (ft)	GRAPHIC LOG	MATERIAL DESCRIPTION	SAMPLE TYPE NUMBER	RECOVERY % SHELBY TUBE	BLOW COUNTS (N VALUE)	DRY UNIT WT. (pcf)	MOISTURE CONTENT (%)	ATTERBERG LIMITS			FINES CONTENT (%)
									LIQUID LIMIT	PLASTIC LIMIT	PLASTICITY INDEX	
0	0		Asphalt									
			CLAYEY SAND with GRAVEL (SC), stiff, moist									
			FAT CLAY (CH), gray, moist									
195	5			ST	(100)				72	25	47	
				ST	(100)							
			FAT CLAY (CH), yellow-brown, gray, moist									
190	10		FAT CLAY (CH), yellow-brown, gray, very stiff moist, (CHALK)	SS	(100)	5-8-12 (20)			93	23	70	
			Boring was terminated at 9.1 feet.									
185	15											
180	20											
175	25											
170	30											
165	35											



BORING NUMBER B-4.5A

CLIENT Auburn University
PROJECT NAME AL-5 Research Project
PROJECT NUMBER 99-305-635-005-401
PROJECT LOCATION AL 5, Perry County
DATE STARTED 11/19/13 **COMPLETED** 11/19/13
GROUND ELEVATION 206 ft **HOLE SIZE** 4"
DRILLING CONTRACTOR ALDOT
GROUND WATER LEVELS:
DRILLING METHOD CME 55, Auto-Hammer, SFA w/ SPT
AT TIME OF DRILLING None Encountered
LOGGED BY _____ **CHECKED BY** _____
AT END OF DRILLING None Encountered
NOTES _____ **AFTER DRILLING** None Encountered

ELEVATION (ft)	DEPTH (ft)	GRAPHIC LOG	MATERIAL DESCRIPTION	SAMPLE TYPE NUMBER	RECOVERY % SHELBY TUBE	BLOW COUNTS (N VALUE)	DRY UNIT WT. (pcf)	MOISTURE CONTENT (%)	ATTERBERG LIMITS			FINES CONTENT (%)	
									LIQUID LIMIT	PLASTIC LIMIT	PLASTICITY INDEX		
205	0		Asphalt										
			FAT CLAY (CH) (A-7-6), brown, gray, medium, moist, Layer 1	ST	100		81.5	38.8	68	28	40	97	
	5		FAT CLAY (CH), brown, gray, stiff, moist, Layer 1	ST	100								
200			FAT CLAY (CH), yellow-brown, stiff (CHALK), Layer 2	ST	50					97	28	69	
			Boring was terminated at 9.2 feet.	ST	0		84.4	33.3					96
195	10												
	15												
190													
	20												
185													
	25												
180													
	30												
175													
	35												



BORING NUMBER B-5A

CLIENT Auburn University **PROJECT NAME** AL-5 Research Project
PROJECT NUMBER 99-305-635-005-401 **PROJECT LOCATION** AL 5, Perry County
DATE STARTED 11/19/13 **COMPLETED** 11/19/13 **GROUND ELEVATION** 211 ft **HOLE SIZE** 4"
DRILLING CONTRACTOR ALDOT **GROUND WATER LEVELS:**
DRILLING METHOD CME 55, Auto-Hammer, SFA w/ SPT **AT TIME OF DRILLING** None Encountered
LOGGED BY _____ **CHECKED BY** _____ **AT END OF DRILLING** None Encountered
NOTES _____ **AFTER DRILLING** None Encountered

ELEVATION (ft)	DEPTH (ft)	GRAPHIC LOG	MATERIAL DESCRIPTION	SAMPLE TYPE NUMBER	RECOVERY % SHELBY TUBE	BLOW COUNTS (N VALUE)	DRY UNIT WT. (pcf)	MOISTURE CONTENT (%)	ATTERBERG LIMITS			FINES CONTENT (%)
									LIQUID LIMIT	PLASTIC LIMIT	PLASTICITY INDEX	
210	0		Asphalt									
			CLAYEY SAND with GRAVEL (SC), stiff, moist									
			FAT CLAY (CH), gray, moist	ST	100				50	24	26	
	5			ST	100							
205				ST	100							
			FAT CLAY (CH), yellow-brown, gray, moist	ST	100				91	23	68	
200	10		FAT CLAY (CH), yellow-brown, gray, very stiff moist, (CHALK)	SS	100	10-9-12 (21)						
			Boring was terminated at 10.7 feet.									
	15											
195												
	20											
190												
	25											
185												
	30											
180												
	35											



BORING NUMBER B-5.5A

CLIENT Auburn University **PROJECT NAME** AL-5 Research Project
PROJECT NUMBER 99-305-635-005-401 **PROJECT LOCATION** AL 5, Perry County
DATE STARTED 11/19/13 **COMPLETED** 11/19/13 **GROUND ELEVATION** 210 ft **HOLE SIZE** 4"
DRILLING CONTRACTOR ALDOT **GROUND WATER LEVELS:**
DRILLING METHOD CME 55, Auto-Hammer, SFA w/ SPT **AT TIME OF DRILLING** None Encountered
LOGGED BY _____ **CHECKED BY** _____ **AT END OF DRILLING** None Encountered
NOTES _____ **AFTER DRILLING** None Encountered

ELEVATION (ft)	DEPTH (ft)	GRAPHIC LOG	MATERIAL DESCRIPTION	SAMPLE TYPE NUMBER	RECOVERY % SHELBY TUBE	BLOW COUNTS (N VALUE)	DRY UNIT WT. (pcf)	MOISTURE CONTENT (%)	ATTERBERG LIMITS			FINES CONTENT (%)	
									LIQUID LIMIT	PLASTIC LIMIT	PLASTICITY INDEX		
210	0		Asphalt										
			FAT CLAY (CH) (A-7-6), yellow-brown, gray, medium, moist, Layer 1	ST	100		81.0	39.6	86	26	60	96	
					ST	100							
205	5			FAT CLAY (CH), gray, yellow-brown, stiff, moist, Layer 1	ST	100							
				FAT CLAY (CH) (A-7-6), yellow-brown, stiff (CHALK), Layer 2	ST	100		87.7	33.3	88	27	61	96
200	10					ST	100						
				FAT CLAY (CH), yellow-brown, hard (CHALK), Layer 2	SS	100	7-13-18 (31)						
195	15		Boring was terminated at 14.1 feet.										
190	20												
185	25												
180	30												
175	35												



BORING NUMBER B-6A

CLIENT Auburn University **PROJECT NAME** AL-5 Research Project
PROJECT NUMBER 99-305-635-005-401 **PROJECT LOCATION** AL 5, Perry County
DATE STARTED 11/19/13 **COMPLETED** 11/19/13 **GROUND ELEVATION** 194 ft **HOLE SIZE** 4"
DRILLING CONTRACTOR ALDOT **GROUND WATER LEVELS:**
DRILLING METHOD CME 55, Auto-Hammer, SFA w/ SPT **AT TIME OF DRILLING** None Encountered
LOGGED BY _____ **CHECKED BY** _____ **AT END OF DRILLING** None Encountered
NOTES _____ **AFTER DRILLING** None Encountered

ELEVATION (ft)	DEPTH (ft)	GRAPHIC LOG	MATERIAL DESCRIPTION	SAMPLE TYPE NUMBER	RECOVERY % SHELBY TUBE	BLOW COUNTS (N VALUE)	DRY UNIT WT. (pcf)	MOISTURE CONTENT (%)	ATTERBERG LIMITS			FINES CONTENT (%)
									LIQUID LIMIT	PLASTIC LIMIT	PLASTICITY INDEX	
0			Asphalt									
			CLAYEY SAND with GRAVEL (SC), stiff, moist									
			FAT CLAY (CH), gray, moist	ST	100				97	24	73	
190	5		FAT CLAY (CH), brown, moist	ST	100							
			FAT CLAY (CH), brown, gray, moist	ST	100							
185	10		FAT CLAY (CH), gray, yellow-brown moist, (CHALK)	ST	100				80	30	50	
			FAT CLAY (CH), gray, yellow-brown, very stiff moist, (CHALK)	SS	100	9-11-13 (24)						
			Boring was terminated at 12.2 feet.									
180	15											
175	20											
170	25											
165	30											
160	35											



BORING NUMBER B-6.5A

CLIENT Auburn University **PROJECT NAME** AL-5 Research Project
PROJECT NUMBER 99-305-635-005-401 **PROJECT LOCATION** AL 5, Perry County
DATE STARTED 11/20/13 **COMPLETED** 11/20/13 **GROUND ELEVATION** 181 ft **HOLE SIZE** 4"
DRILLING CONTRACTOR ALDOT **GROUND WATER LEVELS:**
DRILLING METHOD CME 55, Auto-Hammer, SFA w/ SPT **AT TIME OF DRILLING** None Encountered
LOGGED BY _____ **CHECKED BY** _____ **AT END OF DRILLING** None Encountered
NOTES _____ **AFTER DRILLING** None Encountered

ELEVATION (ft)	DEPTH (ft)	GRAPHIC LOG	MATERIAL DESCRIPTION	SAMPLE TYPE NUMBER	RECOVERY % SHELBY TUBE	BLOW COUNTS (N VALUE)	DRY UNIT WT. (pcf)	MOISTURE CONTENT (%)	ATTERBERG LIMITS			FINES CONTENT (%)
									LIQUID LIMIT	PLASTIC LIMIT	PLASTICITY INDEX	
180	0	Asphalt										
		CLAYEY SAND with GRAVEL (SC), stiff, moist		ST	100							
	5	SANDY FAT CLAY (CH) (A-7-6), gray, moist, Layer 1		ST	100		90.2	28.2	71	24	47	60
	175	SANDY FAT CLAY (CH), gray, brown, moist, Layer 1		ST	100				57	18	39	
		FAT CLAY with SAND (CH), gray, brown, very stiff moist, (CHALK)		ST	100				50	15	35	
	10			SS	100	8-10-13 (23)						45
	170	Boring was terminated at 10.3 feet.										
	15											
	165											
	20											
	160											
	25											
	155											
	30											
	150											
	35											



BORING NUMBER B-7A

CLIENT Auburn University **PROJECT NAME** AL-5 Research Project
PROJECT NUMBER 99-305-635-005-401 **PROJECT LOCATION** AL 5, Perry County
DATE STARTED 11/20/13 **COMPLETED** 11/20/13 **GROUND ELEVATION** 181 ft **HOLE SIZE** 4"
DRILLING CONTRACTOR ALDOT **GROUND WATER LEVELS:**
DRILLING METHOD CME 55, Auto-Hammer, SFA w/ SPT **AT TIME OF DRILLING** None Encountered
LOGGED BY _____ **CHECKED BY** _____ **AT END OF DRILLING** None Encountered
NOTES _____ **AFTER DRILLING** None Encountered

ELEVATION (ft)	DEPTH (ft)	GRAPHIC LOG	MATERIAL DESCRIPTION	SAMPLE TYPE NUMBER	RECOVERY % SHELBY TUBE	BLOW COUNTS (N VALUE)	DRY UNIT WT. (pcf)	MOISTURE CONTENT (%)	ATTERBERG LIMITS			FINES CONTENT (%)
									LIQUID LIMIT	PLASTIC LIMIT	PLASTICITY INDEX	
180	0		Asphalt									
			CLAYEY SAND (SC), yellow-brown, red, loose, moist	ST	100							
	5		FAT CLAY (CH), gray, brown, medium, moist	ST	100				57	17	40	
175				ST	100				58	20	38	
	10			ST	45				63	21	42	
170				ST	100							
	15		FAT CLAY (CH), yellow-brown, gray, stiff, moist	ST	40							
165				ST	100							
	20		FAT CLAY (CH), yellow-brown, very stiff (CHALK)	SS	100	6-9-13 (22)						
	20		Boring was terminated at 18.8 feet.									
160												
	25											
155												
	30											
150												
	35											



BORING NUMBER B-7.5A

CLIENT Auburn University **PROJECT NAME** AL-5 Research Project
PROJECT NUMBER 99-305-635-005-401 **PROJECT LOCATION** AL 5, Perry County
DATE STARTED 11/20/13 **COMPLETED** 11/20/13 **GROUND ELEVATION** 191 ft **HOLE SIZE** 4"
DRILLING CONTRACTOR ALDOT **GROUND WATER LEVELS:**
DRILLING METHOD CME 55, Auto-Hammer, SFA w/ SPT **AT TIME OF DRILLING** None Encountered
LOGGED BY _____ **CHECKED BY** _____ **AT END OF DRILLING** None Encountered
NOTES _____ **AFTER DRILLING** None Encountered

ELEVATION (ft)	DEPTH (ft)	GRAPHIC LOG	MATERIAL DESCRIPTION	SAMPLE TYPE NUMBER	RECOVERY % SHELBY TUBE	BLOW COUNTS (N VALUE)	DRY UNIT WT. (pcf)	MOISTURE CONTENT (%)	ATTERBERG LIMITS			FINES CONTENT (%)
									LIQUID LIMIT	PLASTIC LIMIT	PLASTICITY INDEX	
190	0		Asphalt									
			CLAYEY SAND with GRAVEL (SC), brown, moist									
			FAT CLAY with SAND (CH) (A-7-6), gray, brown, moist, Layer 1	ST	100							
	5			ST	100							
185				ST	100		93.9	29.2	67	18	49	81
			FAT CLAY with SAND (CH) (A-7-6), brown, moist, Layer 2	ST	100		95.4	27.8	60	18	42	78
180	10			ST	0							
			Boring was terminated at 11.0 feet.									
	15											
175												
	20											
170												
	25											
165												
	30											
160												
	35											



BORING NUMBER B-8A

PAGE 1 OF 1

CLIENT Auburn University **PROJECT NAME** AL-5 Research Project
PROJECT NUMBER 99-305-635-005-401 **PROJECT LOCATION** AL 5, Perry County
DATE STARTED 11/20/13 **COMPLETED** 11/20/13 **GROUND ELEVATION** 197 ft **HOLE SIZE** 4"
DRILLING CONTRACTOR ALDOT **GROUND WATER LEVELS:**
DRILLING METHOD CME 55, Auto-Hammer, SFA w/ SPT **AT TIME OF DRILLING** None Encountered
LOGGED BY _____ **CHECKED BY** _____ **AT END OF DRILLING** None Encountered
NOTES _____ **AFTER DRILLING** None Encountered

ELEVATION (ft)	DEPTH (ft)	GRAPHIC LOG	MATERIAL DESCRIPTION	SAMPLE TYPE NUMBER	RECOVERY % SHELBY TUBE	BLOW COUNTS (N VALUE)	DRY UNIT WT. (pcf)	MOISTURE CONTENT (%)	ATTERBERG LIMITS			FINES CONTENT (%)
									LIQUID LIMIT	PLASTIC LIMIT	PLASTICITY INDEX	
0			Asphalt									
195			CLAYEY SAND with GRAVEL (SC), brown, moist	ST	100							
			FAT CLAY (CH), brown, moist	ST	100							
5			FAT CLAY (CH), gray, brown, moist	ST	100							
190				ST	100				64	16	48	
				ST	100				50	16	34	
10			CLAYEY SAND (SC), brown, moist	SS	171							
185				ST	0							
				ST	100							
15			FAT CLAY (CH), gray, yellow-brown moist, (CHALK)	SS	100	5-19-20 (39)						
			FAT CLAY (CH), gray, yellow-brown, hard moist, (CHALK)									
180			Boring was terminated at 16.0 feet.									
20												
175												
25												
170												
30												
165												
35												



BORING NUMBER B-8.5A

CLIENT Auburn University **PROJECT NAME** AL-5 Research Project
PROJECT NUMBER 99-305-635-005-401 **PROJECT LOCATION** AL 5, Perry County
DATE STARTED 11/20/13 **COMPLETED** 11/20/13 **GROUND ELEVATION** 200 ft **HOLE SIZE** 4"
DRILLING CONTRACTOR ALDOT **GROUND WATER LEVELS:**
DRILLING METHOD CME 55, Auto-Hammer, SFA w/ SPT **AT TIME OF DRILLING** None Encountered
LOGGED BY _____ **CHECKED BY** _____ **AT END OF DRILLING** None Encountered
NOTES _____ **AFTER DRILLING** None Encountered

ELEVATION (ft)	DEPTH (ft)	GRAPHIC LOG	MATERIAL DESCRIPTION	SAMPLE TYPE NUMBER	RECOVERY % SHELBY TUBE	BLOW COUNTS (N VALUE)	DRY UNIT WT. (pcf)	MOISTURE CONTENT (%)	ATTERBERG LIMITS			FINES CONTENT (%)
									LIQUID LIMIT	PLASTIC LIMIT	PLASTICITY INDEX	
200	0		Asphalt									
			CLAYEY SAND with GRAVEL (SC), brown, moist	ST	100							90
			FAT CLAY (CH), brown, moist									
			FAT CLAY (CH), gray, yellow-brown, moist	ST	100							78
			FAT CLAY (CH), gray, yellow-brown moist, (CHALK)									
195	5			ST	100							
				ST	100							
			FAT CLAY (CH), gray, yellow-brown, very stiff moist, (CHALK)	SS	100	5-7-11 (18)						
190	10		Boring was terminated at 9.6 feet.									
185	15											
180	20											
175	25											
170	30											
165	35											



BORING NUMBER B-9A

CLIENT Auburn University
PROJECT NAME AL-5 Research Project
PROJECT NUMBER 99-305-635-005-401
PROJECT LOCATION AL 5, Perry County
DATE STARTED 11/20/13 **COMPLETED** 11/20/13
GROUND ELEVATION 198 ft **HOLE SIZE** 4"
DRILLING CONTRACTOR ALDOT
GROUND WATER LEVELS:
DRILLING METHOD CME 55, Auto-Hammer, SFA w/ SPT
AT TIME OF DRILLING None Encountered
LOGGED BY _____ **CHECKED BY** _____
AT END OF DRILLING None Encountered
NOTES _____ **AFTER DRILLING** None Encountered

ELEVATION (ft)	DEPTH (ft)	GRAPHIC LOG	MATERIAL DESCRIPTION	SAMPLE TYPE NUMBER	RECOVERY % SHELBY TUBE	BLOW COUNTS (N VALUE)	DRY UNIT WT. (pcf)	MOISTURE CONTENT (%)	ATTERBERG LIMITS			FINES CONTENT (%)
									LIQUID LIMIT	PLASTIC LIMIT	PLASTICITY INDEX	
0			Asphalt, hard									
195			FAT CLAY (CH), brown, moist	ST	100							
5				ST	100							
190			FAT CLAY (CH), yellow-brown, gray, very stiff moist, (CHALK)	SS	100	5-10-13 (23)						
10			Boring was terminated at 8.7 feet.									
185												
15												
180												
20												
175												
25												
170												
30												
165												
35												

APPENDIX B: TECHNICAL DATA SHEET FOR MOISTURE BARRIER

99-305-535-005-401 PERLY CO SRS
(221A001 & 221A002)

PERMALON®
PLY X-210 G

RI® REEF INDUSTRIES, INC.

TECHNICAL DATA SHEET

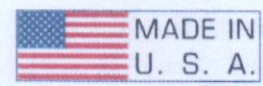
PHYSICAL PROPERTIES AND TYPICAL VALUES

PROPERTY	ASTM TEST METHOD	U.S. VALUE	METRIC VALUE
Weight	D-5261	117 LB/1000 FT ²	57.1 KG/100 M ²
Thickness	D-5199	48 MIL	1.2 MM
Load @ Yield	D-882	50 LBF	222 N
Load @ Break	D-882	65 LBF	289 N
		1350 PSI	9.3 MPA
Elongation @ Break	D-882	575 %	575 %
Tongue Tear	D-5735	50 LBF	222 N
Trapezoidal Tear	D-4533	94 LBF	418 N
PPT Resistance	D-2582	75 LBF	334 N
Dart Impact Strength	D-1709	5.0 LBS	2.3 KG
Puncture Strength	D-4833	97 LBS	431 N
Permeability	E-96	.0143 Grain/Hr•Ft ² •In.Hg	

FEATURES AND BENEFITS

- Cross-laminated polyethylene with a geotextile fabric reinforcement layer that resists punctures and tears.
- UV stabilized to withstand prolonged exposure to sunlight.
- Ply X-210 is not prone to environmental stress-cracking (ESC) so it can endure repeated thermal expansion & contraction cycles.

OUR CUSTOMERS DON'T JUST *cover their business,*
➔ THEY PROTECT IT



REEF INDUSTRIES, INC.
9209 Airmeda Genoa Rd. • Houston, Texas 77075
P: 713.507.4251 • F: 713.507.4295
E-mail: ri@reefindustries.com • www.reefindustries.com

TOLLFREE 1.800.231.6074

The information provided herein is based upon data believed to be reliable. All testing is performed in accordance with ASTM standards and procedures. All values are typical and nominal and do not represent either minimum or maximum performance of the product. Although the information is accurate to the best of our knowledge and belief, no representation of warranty or guarantee is made as to the suitability or completeness of such information. Likewise, no representation of warranty or guarantee, expressed or implied, or merchantability, fitness or otherwise, is made as to product application for a particular use.

APPENDIX C: TROXLER 4301 CALIBRATION SHEET

Model: 4301A Serial: 69849 Calib. date: Feb 02, 2017
 Source: AM-241/Be Serial: 57-1805 Print date: Feb 02, 2017

Neutron Depth Moisture Gauge

**41.4 x 39.4 mm Aluminum Access Tube (STD) **

On 4300 series depth moisture gauges, kg/M3 = mm/M3, and % Vol. = cm/M3

Calibration count rate data

Reference standard count = 835

Standard	Moisture (kg/M3)	Counts/Min.	Count Ratio
1	0	27	0.032
2	392	807	0.966
3	568	1150	1.377
4	711	1440	1.725
5	747	1560	1.868
6	894	1821	2.181

Linear Regression Analysis (kg/M3)

Actual	Calculated	Difference
0	3	- 3.1
392	390	2.2
568	560	8.1
711	704	7.4
747	763	-16.1
894	893	1.5

Fit correlation = 0.99961
 Intercept (A0) = 0.02492

Std. error of est. = 0.02407
 Slope (A1) = 0.00242

Precision for normal (one minute) measurement time

Moisture (kg/M3)	0.0	200.0	400.0	600.0	800.0	1000.0
Precision	0.6	2.6	3.6	4.3	5.0	5.6

Test Values

404 kg/M3 40.4% Vol. 25.2 PCF
 404 mm/M3 40.4 cm/M3 4.8 in/ft

APPENDIX D: WEBSITE MACRO CODES

```
Private Sub ToggleButton1_Click()  
If Cells(1, 1) = True Then  
    Application.OnTime TimeValue("11:20:00"), "Publish"  
End If  
End Sub
```

```
Sub Publish()  
Workbooks.Open Filename:= _  
    "C:\Users\dtj0008\Desktop\AL5 Website Excel File 2.xlsx", Origin:=xlWindows  
ActiveWorkbook.RefreshAll  
ActiveWorkbook.Save  
End Sub
```